Universidade de Brasília - Instituto de Geociências (UnB/IG)

Programa de Pós-graduação em Geologia

Mineralogia Quantitativa de Alta Definição e sua Aplicação em Qualidade dos Reservatórios da Formação Barra Velha Superior, Bacia de Santos

Maria Moutinho Masella Machado de Mendonça

Dissertação de Mestrado Nº 510

Orientadora: Prof. Drª. Paola Ferreira Barbosa

Brasília, 2023

Universidade de Brasília - Instituto de Geociências (UnB/IG)

Programa de Pós-graduação em Geologia

Maria Moutinho Masella Machado de Mendonça

Mineralogia Quantitativa de Alta Definição e sua Aplicação em Qualidade dos Reservatórios da Formação Barra Velha Superior, Bacia de Santos

Dissertação apresentada ao Programa de Pós-Graduação em Geologia do Instituto de Geociências da Universidade de Brasília, como requisito parcial obrigatório para a obtenção do título de Mestre em Geologia.

Área de concentração

Mineralogia e Petrologia

Orientadora

Prof. Drª. Paola Ferreira Barbosa

Comissão Examinadora

Prof. Dr. Alessandro Batezelli (Unicamp)
Prof. Drª. Lucieth Cruz Vieira (IG/UnB)

Brasília, Julho de 2023

Ficha catalográfica

"Cambia, todo cambia."

Mercedes Sosa

AGRADECIMENTOS

Agradeço a minha orientadora, Paola Ferreira Barbosa, por ter me orientado e guiado neste projeto. Agradeço a Carlos Jorge Abreu, pelas aulas sobre o tema que ele conhece tanto e pela oportunidade de integrar um projeto tão importante para a ciência e para o nosso país. Agradeço, assim, a toda equipe da UnB que participou deste projeto dos carbonatos da Bacia de Santos.

O presente trabalho foi realizado com apoio da Coordenação de Aperfeiçoamento de Pessoal de Nível Superior - Brasil (CAPES) – Código de financiamento 001. Agradeço ao Instituto de Geociências da Universidade de Brasília, aos seus servidores, professores e aos colegas pelo acolhimento nesta minha volta à instituição.

À Equinor, agradeço a concessão da bolsa durante o mestrado e todo apoio financeiro dado para desenvolver o nosso trabalho. À UFRJ, agradeço por disponibilizar os testemunhos junto à ANP, que nos forneceu tantos dados.

Agradeço a todos que encontrei no caminho, os que encontrei mato adentro e foram copilotos nesta jornada, e aos dessa nova aventura catalana, que proporcionaram finalizar este trabalho com muita dedicação. Agradeço aos amigos novos feitos no mestrado: Lucas, Geovana, Fabiana, João, Brunno, Renato, Steffanie e aos do cafezinho da sala ao lado. E principalmente, a Aline e a Ana Valéria pela companhia no RU de todo dia e também nas noites na sala 297.

Às amizades já sedimentadas: Raquel, Laeticia, Matheus, Regina, Victor, Kristy, Gustavo, Raíra, Julianna daqui e Juliana de lá, agradeço a amizade. A Fernando, agradeço por ser abrigo. E agradeço imensamente a Victor por me mostrar outros tons da mineralogia.

Assim como os carbonatos, tudo muda. Muda o superficial e também o profundo. Com essas palavras, dedico este trabalho à minha força e base, minha mãe, Margarida, e ao meu bom abrigo, meu pai, Miguel, sem os quais eu não teria chegado tão longe. Aos que estão a um oceano de distância, Bernardo, Gabriel, João, Guilherme e minha irmã, Anna. Ao meu irmão, Miguel, que cantou essa música para mim em meus primeiros dias desta jornada acadêmica. A Dante Tisin. À minha nova família estendida, e àquele que me faz seguir, André.

RESUMO

As facies da Formação Barra Velha são conhecidas pela sua complexidade. A ausência de análogos recentes de seu ambiente deposicional e as condições de deposição ainda são motivo de controvérsia. O principal objetivo deste trabalho é analisar a mineralogia de um poço da seção Pré-sal do Campo de Sapinhoá para compreender o comportamento dos componentes por meio do empilhamento vertical das fácies.

As fácies foram classificadas com base nas características mineralógicas e texturas sedimentares e separadas em duas categorias: *in situ* e retrabalhadas. As fácies *in situ* são compostas por *spherulitestones*, *shrubstones* e *mudstones*. As fácies retrabalhadas foram classificadas em wackstones, packstones e grainstones. Os dados consistem em descrições de um testemunho 200 metros e na análise de 100 lâminas delgadas distribuídas ao longo deste testemunho.

A integração entre microscopia óptica e mineralogia quantitativa, somada à descrição macroscópica, dados de registro de poços e dados sísmicos fornecidos pela ANP, proporcionou uma compreensão abrangente das escalas microscópicas (mm) e macroscópicas (m) dos ciclos de empilhamento definidos pelas fácies *in situ* e retrabalhadas, que são distribuídas proporcionalmente ao longo dos reservatórios estudados.

Os principais minerais quantificados por QEMSCAN foram dolomita, calcita e quartzo, resultado de processos deposicionais e pós-deposicionais. Em média, as amostras ao longo dos núcleos mostraram 40% de dolomita, 40% de calcita e 20% de quartzo. Minerais acessórios corroboram com a possibilidade de que o hidrotermalismo afetou os carbonatos assim como a diagênese. Barita, pirita, fluorita e minerais ricos em sódio atuam como minerais-guia destes processos.

Embora os processos de diagênese e hidrotermalismo tenham afetado a porosidade e permeabilidade do reservatório, a granulometria das fácies foi essencial para definir a qualidade do reservatório. Fácies suportadas por grãos grossos, como *shrubs* e grainstones, mostraram maior porosidade e permeabilidade absoluta. Em contraste, fácies de grãos finos, como mudstone e packstone, permaneceram não-reservatórias e com baixa permeabilidade, mesmo após a substituição de seus componentes primários.

Palavras-chave: Formação Barra Velha; diagênese; hidrotermalismo; fácies sedimentares; QEMSCAN;

ABSTRACT

The facies from the Barra Velha Formation are known for their complexity. The lack of recent analogs of the depositional setting of these carbonates and the depositional conditions remains controversial. The main objective of this work is to analyze the mineralogy of a well from the carbonates of the Pre-salt section of the Sapinhoá Field to understand the components' behavior through the vertical stacking of facies.

The facies were classified and quantified based on mineralogy features and sedimentary textures. The data consists of 200m core descriptions and 100 thin sections distributed throughout this well core.

The facies were classified into two categories: in situ and reworked. The *in situ* facies are composed of spherulitestones, shrubstones, and mudstones. The reworked facies were classified into wackstones, packstones and grainstones.

Integration between petrographic data from optical microscopy and quantitative mineralogy, added to the description of cores, well-logging data, and seismic data provided by the ANP, provided a broad understanding of the microscopic (millimetric) to the macroscopic (metric) scale cycles stacking, defined by in situ and reworked facies, which are proportionally distributed along the studied pools.

The main minerals quantified via QEMSCAN were dolomite, calcite and quartz, the result of depositional and post-depositional processes. On average, the samples along the cores showed 40% dolomite, 40% calcite and 20% quartz. Accessory minerals support the possibility of hydrothermalism affected the carbonates as well as diagenesis. Barite, pyrite, fluorite, and Na-bearing minerals corroborate as guides-minerals.

Although the processes of diagenesis and hydrothermalism affected the reservoir's porosity and permeability, the facies' granulometry was essential for defining the quality of the reservoir. Coarse-grained supported facies such as shrubs and grainstones showed greater porosity and absolute permeability. In contrast, fine-grained facies such as mudstone and packstone remained non-reservoir and poor reservoirs, respectively, even after their primary components were replaced.

Keywords: Barra Velha Formation; Diagenesis; hydrothermalism; Sedimentary facies; QEMSCAN

LISTA DE FIGURAS

INDEX FIGURES

SUMÁRIO

CAPÍTULO 1

INTRODUÇÃO

1   INTRODUÇÃO

1.1   Caracterização do Problema

Desde a descoberta do pré-sal, o desenvolvimento da exploração em águas ultra profundas nos depósitos carbonáticos das bacias da margem continental brasileira tem sido alvo de diversos estudos por universidades e empresas, tanto nacionais quanto estrangeiras, devido às grandes reservas de óleo e gás encontradas desde 2006.

Os carbonatos aptianos das bacias da margem continental concentram grandes volumes de hidrocarbonetos. Na Bacia de Santos, esses depósitos estão predominantemente na Formação Barra Velha (BVF). A caracterização das fácies que compõem essa formação e suas alterações diagenéticas são importantes para a previsibilidade da exploração de petróleo.

Apesar da mineralogia das fácies sedimentares *in situ, mudstones, shrubstones* e *spherulitestones*, típicas da BVF, ser simples, ela se torna mais complexa pelo fato de ter sido eventualmente camuflada pela atividade dos processos que interferem na química do ambiente de sua formação e pelas alterações diagenéticas e hidrotermais. Porém, parte desse "problema" tem sido melhor entendido com a aplicação de técnicas de identificação mineralógica quantitativa, que é a metodologia de estudo nesta dissertação.

A caracterização estratigráfica das fácies constitui ainda um desafio, pois os ciclos deposicionais dos carbonatos da Formação Barra Velha não são completamente entendidos.

Fontes recentes como Wright e Barnett (2015), Pietzsch *et al.* (2018) e Gomes *et al.* (2020) entendem que os sedimentos da Formação Barra Velha formaram-se em lagos rasos, suscetíveis a variações externas como clima, pH, salinidade e evaporação.

1.2   Objetivo

O objetivo central deste trabalho é caracterizar as fácies carbonáticas, a sua composição primária e as alterações diagenéticas e hidrotermais ocorridas na Formação Barra Velha Superior da Bacia de Santos. Este objetivo foi alcançado a partir da aplicação de técnicas analíticas que correlacionam estruturas, texturas e mineralogia modal. Já os objetivos específicos foram:

   i.   Fazer uma retrospectiva do arcabouço estratigráfico e história diagenética da Formação Barra Velha;

   ii.   Identificar e caracterizar a textura e estruturas das fácies sedimentares que ocorrem no poço por meio de microscopia eletrônica automatizada;

   iii. Analisar o grande volume de dados quantitativos acerca dos minerais que compõem as fácies classificadas, complementando com um banco de dados de 100 amostras que servirá como base para pesquisas posteriores.

   iv.   Relacionar dados observados em escala microscópica a dados em escala macroscópica e petrofísica.

1.3   Área de Estudo

A Bacia de Santos se localiza na margem sudeste continental brasileira e abrange cerca de 350.000 km², desde o litoral do estado do Rio de Janeiro até o estado de Santa Catarina. Encontra-se limitada a norte pelo Alto de Cabo Frio, que a separa da Bacia de Campos, e a sul pela falha de Florianópolis, que a separa da Bacia de Pelotas (Moreira *et al.*, 2007; Contreras *et al.*, 2010). A área de estudo encontra-se em um alto estrutural na porção central da Bacia (Figura1).
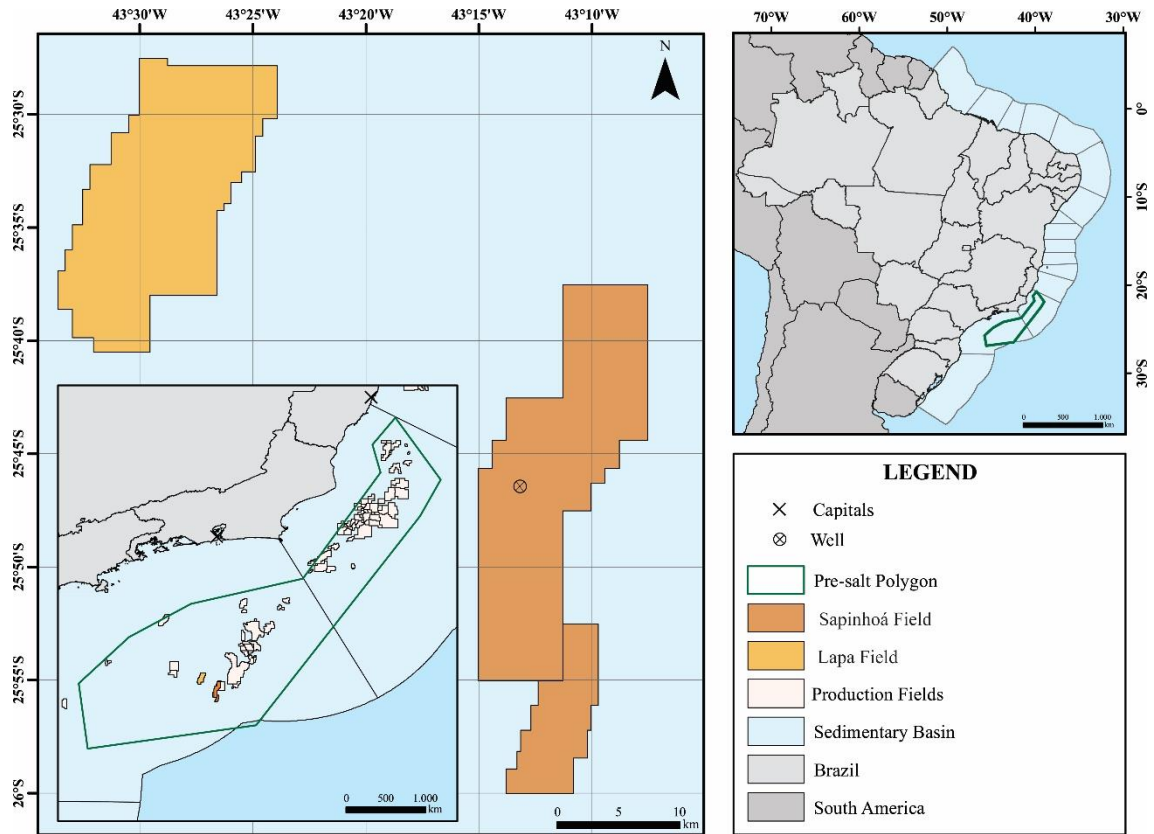
Figura 1 - Mapa de localização da área em estudo, onde o polígono em verde representa a área do pré-sal; em branco, estão destacados os campos de produção; em laranja o campo a ser estudado.

CAPÍTULO 2

ESTADO DA ARTE

2   ESTADO DA ARTE

2.1   Referencial Teórico

Na década de 1970, foram feitos os primeiros investimentos exploratórios na Bacia de Santos, e junto a dados sísmicos, após os primeiros poços pioneiros perfurados, foram descobertos os campos do "pós-sal". O potencial da Bacia de Santos começou a tomar novos rumos a partir dos levantamentos geofísicos em poços de exploração no campo de Tupi (Morais *et al.*, 2013). Entre os anos de 1997 e 2007, foram anunciadas grandes reservas presentes no sistema petrolífero selado por uma camada de cerca de 2 km de espessura de sal, a qual foi denominada como "pré-sal".

Desde a descoberta do pré-sal, o cenário exploratório brasileiro mudou intensamente. As grandes acumulações de hidrocarbonetos propiciaram o aumento da produção no setor energético no país, tornando-se o reservatório mais produtivo da história da exploração petróleo da América do Sul (Karner e Gambôa, 2007; Barnett *et al.*, 2018).

Atualmente, o campo de Sapinhoá, que é objeto deste estudo, produz cerca de 187 mil barris por dia de petróleo e 9,5 milhões de metros cúbicos por dia de gás natural, sendo o terceiro maior produtor do país (ANP, 2021).

A exploração desses reservatórios trouxe desafios. Os carbonatos, que funcionam como rochas reservatório de hidrocarbonetos apresentam alta variabilidade nos padrões de suas fábricas, o que dificulta a caracterização dessas rochas e obstaculiza o planejamento da exploração de óleo e gás nestes reservatórios (Wright e Barnett, 2015).

A falta de análogos recentes ao modelo de deposição do pré-sal dificulta a compreensão acerca das condições climáticas, químicas e sedimentares que formaram as rochas reservatório do pré-sal. Conhecer desde a microscopia e aspectos texturais, as microestruturas e as fácies se torna essencial para compreender o comportamento destes grandes reservatórios em escalas maiores.

O ambiente deposicional dessas rochas ainda é bastante discutido devido aos processos deposicionais que afetaram esses carbonatos. Ainda não existe um consenso acerca de fatores como a variabilidade do pH, da química da água, da entrada de sedimentos terrígenos, a interferência de microrganismos e sua relação com a matriz rica em magnésio e as origens das estruturas de *shrubs* e esferulitos calcíticos (De Carvalho

e Fernandes, 2021).

A mineralogia original dos carbonatos do pré-sal na Bacia de Campos e Santos não é muito complexa, porém os registros de diversos processos diagenéticos a tornou mais complexa devido à diversidade das fases minerais de gerados. Diversas alterações diagenéticas afetaram as estruturas originais de laminitos (*mudstones), shrubs* e esferulitos, e originaram novas fases minerais, tornando o sistema carbonático do pré-sal mais complexo. (Herlinger, Zambonato e Re Ros, 2017; Lima e de Ros, 2019; Almeida Carvalho *et al.*, 2022).

As fases minerais originais da BVF seriam constituídas a partir de um substrato silicoso rico em magnésio e estruturas de calcita (*shrubs* e esferulitos) precipitadas nesse meio. Estes elementos passaram por retrabalhamento. Um exemplo disso é a dolomita, que é um constituinte diagenético e substitui a calcita original das estruras, além de se apresentar em diferentes formas, formando um mosaico pervasivo que preenche poros, assim como romboedros comumente denominados de dolomita em sela (*saddle*) e em forma de micro cristais comumente associados a fraturas (Lima e De Ros, 2019; Almeida Carvalho *et al.*, 2022).

Quartzo e variedades de sílica são frequentes modificadores de estruturas, devido à silicificação pervasiva que afeta a fábrica carbonática da Formação Barra Velha, podendo ser encontrados como sílica microcristalina preenchendo os microporos. Cristais subédricos microcristalinos de quartzo formam um mosaico que preenche os poros e fraturas. Sílica com estrutura radial fibrosa substitui cristais de quartzo e de calcita. A substituição dos minerais pela sílica pode ser muito intensa, gerando porções de *chert* ao longo da sequência (Lima e De Ros, 2019; Almeida Carvalho *et al.*, 2022).

A dolomitização ocorre devido ao aumento da razão Mg/Ca disponível no ambiente, pela entrada de água do mar no sistema, além da baixa atividade de CO_3^{2-}. O processo de substituição pode ser parcial ou total dos componentes originais durante a eodiagênese ou na mesodiagênese (Lima e De Ros, 2019, Gomes *et al.*, 2020).

A silicificação é um processo de alteração que costuma ocorrer como a dolomitização, durante a eodiagênese ou na diagênese tardia, e ocorre devido a mudanças químicas do ambiente. A dedolomitização é a substituição de calcita por dolomita, que pode ocorrer devido ao contato do carbonato com água meteórica, ou seja, este processo ocorre mais próximo à superfície (Lima e De Ros; De Carvalho e Fernandes, 2021).

Estudos registram minerais acessórios preenchendo como sulfetos (pirita, calcopirita, galena, esfalerita), zeólita, barita, dawnsonita, criolita, magnesita. De acordo com Lima e De Ros (2019), que estudaram os carbonatos da Formação Macabu na Bacia de Campos, análoga a BVF da Bacia de Sandos, a presença dessas fases nos carbonatos estaria associada à presença de fluidos hidrotermais que percolaram por sistemas de falhas e fraturas. Esses autores mencionam o processo como fonte de dolomitização, de silicificação e de precipitação de diferentes fases minerais em várias intensidades, alterando os constituintes originais e porosidade por meio de dissolução e precipitando minerais ao longo do campo.

A hipótese abiótica surgiu da escassez de evidências microbianas (Wright e Barnett, 2015). De acordo com essa hipótese, as crostas calcíticas, compostas por *shrubs*, e esferulitos do pré-sal teriam se formado devido à evaporação da água dos lagos, diminuindo a lâmina d'água entre a superfície e o meio composto por um gel de argila magnesiana (Lima e De Ros, 2019).

Há uma vertente que considera que a precipitação pode ter sido um processo induzido bióticamente (Mercedes-Martín *et al.*, 2022). Experimentos avaliaram os efeitos da salinidade e concentrações de ácidos orgânicos no crescimento de calcita em soluções alcalinas. Mercedes-Martín *et al.* (2022) concluíram, em um experimento feito em laboratório que simulava as condições hidroquímicas dos lagos alcalinos, que o pH variava devido à influência da taxa de evaporação, como mencionam os autores Farias *et al.* (2019); Lima e De Ros *et al.* (2019) e Wright e Barnett (2015). Notou-se que não é possível afirmar, segundo Mercedes-Martín *et al.* (2022), que existam relações causais entre a flutuação da salinidade e o grau de evaporação durante a formação de esferulitos calcíticos ou arbustiformes (*shrubs)*. Porém esses autores mencionam que a presença de ácido orgânico e agregados de calcita, como *shrubs,* favoreceu a precipitação de calcita radial em esferulitos.

A tectônica influencia não só a morfologia do relevo do ambiente deposicional dos carbonatos geradores de hidrocarboneto, mas também as feições estruturais. Essas feições, por sua vez, estão correlacionadas à variação de condições químicas devido à presença de fontes hidrotermais. As condições do ambiente deposicional são controladas pelas mudanças climáticas que alteram a entrada da água. Assim, o balanço da alcalinidade se dá pela mudança da taxa de precipitação e evaporação (Gomes *et al.*, 2020).

2.1.1   Classificação de Fácies

A classificação das rochas carbonáticas tem como base a fábrica, textura, os tipos de partículas, poros, composição e diagênese (Tucker e Wright, 1990). A primeira classificação criada para rochas carbonáticas foi de Grabau em 1904. Até os dias de hoje, os dois sistemas mais usados para classificação de rochas carbonáticas são os de Folk (1959, 1962) e o de Dunham (1962). O primeiro combina os elementos que formam as partículas com o arcabouço. O segundo é baseado nas texturas que compõem o arcabouço. A classificação de Folk detalha a proporção de grãos formados a partir do retrabalhamento de componentes depositados dentro na bacia.

CALCÁRIOS ALÓCTONES							CALCÁRIOS AUTÓCTONES		
Componentes originais não-ligados organicamente durante a deposição (<10% grão >2 mm)				Textura deposicional não-reconhecível	Componentes originais não-ligados organicamente durante a deposição >10% grãos >2 mm		Componentes originais ligados organicamente durante a deposição		
Contém Matriz (Partículas tamanho argila/silte fino)			Sem matriz, grão-suportado				Organismos que atuam como obstáculos	Organismos que encrustam e ligam	Organismos que constroem um arcabouço rígido
Suportado por matriz		O arcabouço é grão-suportado com matriz			Suportado pela matriz	Suportado por componentes maiores que 2 mm			
Menos de 10% de grãos	Mais de 10% de grãos								
Mudstone	*Wackestone*	*Packstone*	*Grainstone*	*Crystalline*	*Floatstone*	*Rudstone*	*Bafflestone*	*Bindstone*	*Framestone*

Figura 2 - Classificação de carbonatos de Dunham (1962) retirado de Terra *et al.* (2010)

Dunham (1962) classifica as rochas carbonáticas de acordo com os seguintes aspectos: presença de matriz, partículas mais finas que 20 µm e grãos. Assim as rochas seriam divididas naquelas suportadas por matriz, os *mudstones,* que contém menos de 10% de clastos; ou suportadas por clastos, os *grainstones,* que são rochas grão-suportadas com menos de 10% de matriz, podendo apresentar a porosidade aberta e ser preenchida por cimento. As rochas nomeadas como *wackestones* são matriz-suportadas, compostas por mais de 10% de clastos. Os *packstones* são rochas grão-suportadas que possuem matriz fina entre os grãos. Dunham (1962) ainda sugere o *boundstone* para rochas unidas durante a formação, principalmente por estruturas construídas. Embry e Klovan (1971) adaptaram a classificação de Dunham e a subdividiram em autóctone e alóctone, além de ampliarem os termos de influência orgânica e os termos de rochas com influência detrítica. Neste trabalho, focaremos na descrição de Dunham (1962) como mostra a Figura 2, associada à mais recente de Gomes *et al.* (2020), descrita a seguir.

A compreensão acerca da fábrica carbonática e estruturas que formam as rochas carbonáticas da FBV evoluiu bastante ao longo dos últimos anos.

Diversos autores descreveram as fácies do pré-sal e tentaram classificá-las de acordo com os sistemas pré-existentes, aplicando-as às particularidades do local. Carminatti, Dias e Wolff (2009) associaram aos carbonatos do pré-sal, uma origem biótica, classificaram suas fácies e definiram, a partir de seções sísmicas, duas unidades principais: os microbialitos limpos, situados no topo da sequência, e microbialitos ricos em argila, dispostos na base.

Terra *et al.* (2010) introduziram uma nova nomenclatura e propuseram uma classificação levando em consideração as rochas carbonáticas das bacias brasileiras, visando os campos do pré-sal e a produção de petróleo. As fácies detalhadas compreendem tipos de estromatólitos, esferulitos, laminitos e fácies de retrabalhamento.

Terra *et al.* (2010) dividiram as rochas carbonáticas em quatro grupos: elementos não ligados durante a formação (*mudstone*, *wackestone*, *packstone*, *grainstone*, *floatstone*, *rudstone*, bioacumulado e brecha); elementos ligados durante a formação ou *in situ (boundstone*, estromatólitos, trombolito, dendrolito, leiolito, esferulitito, travertino e tufa); elementos ligados ou não durante a formação, formados por laminação (laminitos); e elementos com textura deposicional das quais não era possível reconhecer sua textura original (calcário cristalino e dolomito).

A classificação de Terra *et al.* (2010) sugere grande influência biótica na sua origem destas rochas. Por este motivo, os carbonatos do pré-sal seriam denominados comumente como microbialitos. Segundo os autores, os estromatólitos são depósitos de estrutura laminar que apresentam estruturas de crescimento e ramificações voltadas para o topo. Na maioria das vezes, possuem origem microbial, gerados a partir de bactérias e cianobactérias. Os esferulitos são partículas *in situ* de calcita com forma esféricas e sub esféricas, que não apresentam núcleo. Os laminitos são rochas carbonáticas de granulação fina que formam finas lâminas e podem ter origem microbial ou não. As fácies de retrabalhamento seguem o critério de Dunham (1962) e são compostas principalmente por *grainstones* e *packstones*, suportadas por grãos, porém também apresentam *wackestones* e *mudstones,* suportadas pela matriz (Terra *et al.*, 2010).

Wright e Barnett (2015) propõem uma classificação alternativa, pois são raros os registros microbiais preservados na Formação Barra Velha. Os autores sugerem sucessões de ciclotemas que variam de centímetros a metros, que se repetem ao longo

de toda a formação (Figura 3). Essas sucessões são formadas por três fácies principais:

Fácies 1 - composta por estruturas em forma de leque, *shrubs, in situ* formados por precipitação em condições de baixo teor de Mg/Ca. Trata-se da mesma fácies retratada por Terra *et al.* (2010) como estromatólito;

Fácies 2 - composta por estruturas de calcita radial em esferulitos formadas por precipitação e um gel de silicato magnesiano, associadas à estevensita;

Fácies 3 - composta majoritariamente por laminações finas de carbonato e argila magnesiana em *mudstones* e *packstones*, associados a restos de peixes e ostracodes silicificados que indicam a incursão de água no ambiente.
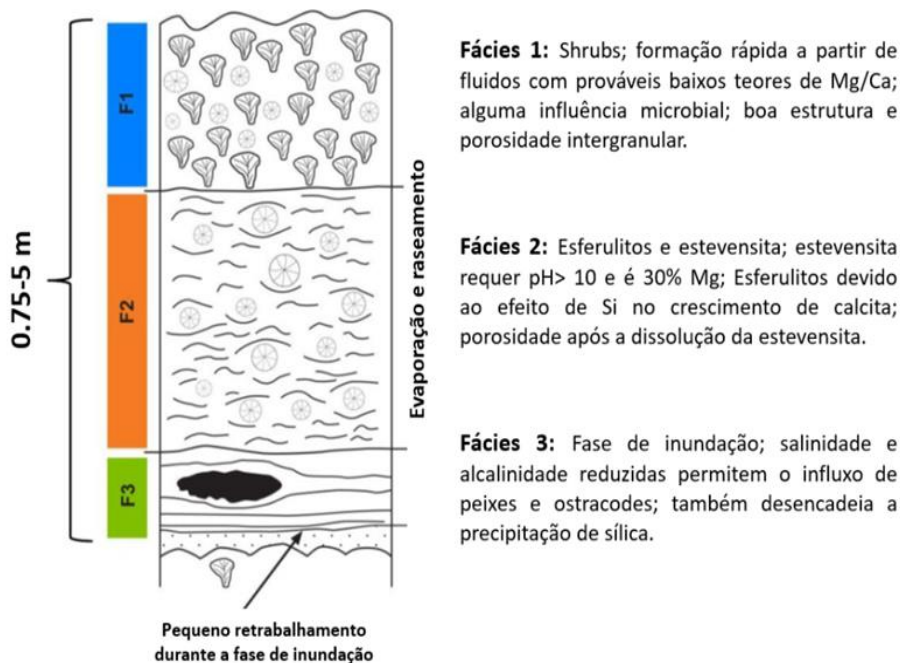

Figura 3 - Ciclotema proposto por Wright e Barnett evidenciando as três fácies *in situ* da Fm. Barra Velha. Retirado de Wright e Barnett (2015).

Wright e Barnett (2015) propõem que os *shrubs* se assemelham aos travertinos modernos de origem abiótica. Os autores consideram que as texturas refletem a rápida precipitação em meio a soluções saturadas. Cada ciclotema teria início com a fácies 3, de inundação, e seguiria para a fácies 1, de ressecamento. Os argilominerais magnesianos ocorrem associados a ambientes de água alcalina (Tosca e Materson, 2014). Para Wright e Barnett (2015), a mudança significativa entre as fácies 3 e 2 ocorre associada à mudança de pH, gerando a precipitação de argilominerais magnesianos em forma de gel. Então, os esferulitos cresceriam em meio a géis de estevensita.

Herlinger, Zambonato e De Ros (2017) e Lima e De Ros (2019) classificam os esferulitos da Formação Macabu, da Bacia de Campos, correlata à Formação Barra

Velha, da Bacia de Santos, como sendo constituintes diagenéticos que substituem os argilominerais magnesianos. Lima e De Ros (2019) complementam que, conforme a energia do ambiente aumentou, os esferulitos se desenvolveram em meio à argila magnesiana, deslocando-a e por vezes substituindo-a ao atingir o limite entre a interface substrato-água. À medida que a taxa de precipitação aumentava, gerava feições de leque que cresciam em direção ao topo, denominadas pelos autores como calcita fascicular. Estas feições, mencionadas por Wright e Barnett (2015) como *shrubs*, ao alcançarem um espaço de acomodação maior, formam crostas de calcita.

Lima e De Ros (2019) e Barnett e Wright (2015) acreditam que a calcita fascicular (*shrub*) tem origem abiótica, com possível influência microbial, e sugerem que os efeitos diagenéticos, como a silicificação e a dolomitização, podem camuflar a composição original das fácies (Figura 4).

Gomes *et al.* (2020) sugeriram um novo método de classificação de fácies que será parcialmente utilizado no presente trabalho. Existem três componentes principais formados *in situ*: laminitos compostos por calcita microcristalina e minerais argilosos, esferulitos de calcita e *shrubs* de calcita. Além dessas, são observadas fácies de retrabalhamento que coincidem com a classificação de Dunham (1962) (*wackestone, packstone, grainstone*). Neste cenário, Gomes *et al.* (2020) sugerem também ampliar o termo laminito a fim de detalhar os componentes dominantes no membro final, como mostra o diagrama a seguir.
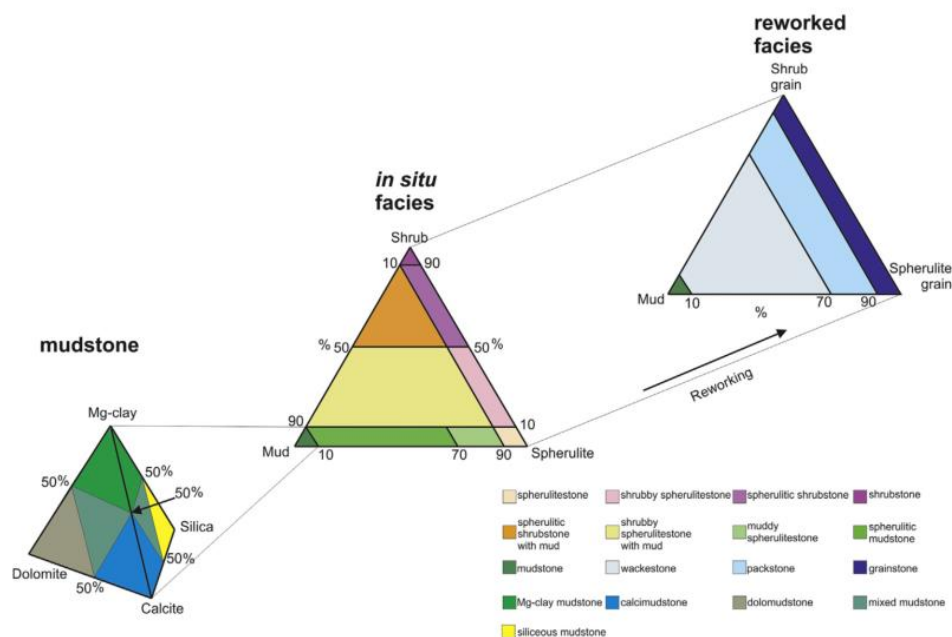

Figura 4 - Classificação de fácies *in situ* e reatarabalhada sugerida por Gomes. Retirada de Gomes (2020).

2.2   Contexto Geológico

A Bacia de Santos se encontra na porção sul do Segmento Central do Oceano Atlântico e está inserida no contexto das bacias da margem continental brasileira, que tiveram origem a partir da ruptura da porção oeste do paleocontinente Gondwana durante o Mesozoico (Moulin, 2013). A Bacia de Santos é definida como uma bacia de margem passiva por Farias *et al.* (1992).

O processo de rifteamento América do Sul-África ocorreu de forma diácrona ao longo do território. As estruturas observadas no oceano Atlântico Sul sugerem que a deformação se deu de maneira polifásica (Lavier e Manatschal, 2006), ou seja, ao longo de um eixo com direção preferencial NNE, que parte desde a costa argentina até a Bacia de Sergipe-Alagoas, e outro eixo para WNW-ENE na margem equatorial brasileira (Chang *et al.*, 1992).

A fragmentação do bloco afro-brasileiro teve início ao sul, durante o Eocretáceo, no Neocomiano (Guardado *et al.*, 2000 e Thiede e Vasconcelos, 2010). Na margem equatorial, o processo tectônico extensivo teve início posteriormente, entre o Aptiano e o Albiano. Esse processo extensivo resultou na formação do proto-oceano Atlântico Sul, na separação das placas sul-americana e africana.

Um intenso magmatismo precedeu a ruptura do Gondwana durante o Aptiano. Os derrames têm sua origem associada à anomalia termal Tristão da Cunha e formaram a província ígnea Paraná-Etendeka, que conectava a costa brasileira à costa oeste africana (White e Mckenzie, 1989).

Chang *et al.* (1992) atribuem às anomalias térmicas um papel secundário no processo de rifteamento, porém Kusznir e Ziegler (1992) mencionam a condução de calor durante o rifteamento como fator que eleva o gradiente geotérmico, podendo levar à maturação das rochas geradoras de hidrocarbonetos no estágio pré-rifte e sin-rifte.

O regime tectônico predominante na Bacia de Santos é o de transtração sinistral (MILANI *et al.*, 2007). Uma ampla zona de cisalhamento conecta as Bacias de Santos e Campos. A Bacia de Santos é marcada por falhas normais orientadas, em sua maioria, na direção NE-SW, paralelas à costa. Além dessas estruturas, rotacionamento e falhamento de blocos com grábens formaram grandes depocentros de sedimento (Chang *et al* 1992; Milani *et al.*, 2007).

Uma feição estrutural importante para compreender a geometria das deposições na Bacia de Santos é o platô de São Paulo, que atinge a cota batimétrica de 2800 m. O Alto Externo da Bacia de Santos se encontra na porção central do platô. É uma estrutura alongada disposta na direção NE-SW com um soerguimento gerado durante o rifteamento formado por derrames basálticos. De acordo com Carminatti, Dias e Wolff (2009), é uma área na qual houve menor estiramento da crosta continental e é onde se encontra maior acúmulo das rochas reservatório de hidrocarbonetos do Barremiano e Aptiano (Rigoti, 2015).

De acordo com Buckley *et al.* (2015), a bacia registra seis principais fases do desenvolvimento tectônico: embasamento cristalino, fase sin-rifte inferior, fase sin-rifte superior, fase *sag*, sequência evaporítica e fase drifte. Essa definição vai de encontro à proposta por Moreira *et al.* (2007), que sugeriram que o desenvolvimento da Bacia de Santos pode ser dividido em 3 fases de evolução tectônica: 1) Fase inicial de rifte; 2) Fase transicional pós-rifte; e 3) Fase de deriva continental ou drifte (Moreira *et al.*, 2007 e Chang *et al.*, 2008), como mostra a figura 5.

Na fase rifte, que ocorreu do Hauteriviano ao Aptiano, os esforços extensionais culminaram na fragmentação do paleocontinente Gondwana. As bacias de rifte da margem brasileira se formaram de modo diácrono, ou seja, as idades das unidades estratigráficas variam lateralmente. Deste modo, o afinamento da crosta e a expansão do proto oceano Atlântico Sul estão relacionados às anomalias termais diferentes das localizadas ao norte. Ao sul, o *hotspot* Tristão da Cunha gerou magmatismo intenso e deu origem à cadeia Rio Grande-Walvis, contato entre a margem leste brasileira com a costa leste africana. Nesta fase, houve extensos derrames de basalto nas porções em que a litosfera se encontrava menos espessa, que deram origem ao embasamento econômico da Bacia de Santos (Moreira *et al.*, 2007 e Karner *et al.*,1999). O tectonismo ativo gerou falhas normais orientadas, em sua maioria, na direção NE-SW, paralelas à costa. Além dessas estruturas, o rotacionamento e o falhamento de blocos com grábens formaram grandes depocentros de sedimento (Milani *et al.*, 2007). Esta seção é formada pelas formações Camboriú, Piçarras e Itapema.

De acordo com Moreira *et al.* (2007), a fase pós-rifte ocorreu entre o Aptiano e o início do Albiano. Esta seção é marcada pela discordância Intra-Alagoas, que marca a transição entre as fases tectônicas. Neste momento, houve relativa calmaria tectônica característica da fase *sag*, na qual ocorreu subsidência termal da crosta continental e

aumento gradual de incursões marinhas contínuas. Esses autores ainda sugerem que a deposição dos evaporitos durante essa fase foi induzida pela barreira gerada pela Dorsal de São Paulo, que impediu a circulação de água, criando a condição de um ambiente semiárido a árido. Sob estas condições, a influência das falhas normais diminuiu e predominou mais uma vez a subsidência termal, marcando uma segunda bacia com geometria *sag* que selou as seções rifte e *sag* anteriores. A bacia é marcada por feições de halocinese, os diápiros de sal (Mohriak *et al.*, 2004). Esta seção abrange as Formações Barra Velha e Ariri (Milani *et al.*, 2007).

Na fase drifte descrita por Moreira *et al.* (2007), ocorreu a individualização das placas sulamericana e africana. Os sedimentos dessa fase começaram a ser depositados no Albiano, o que perdura até o recente, marcando a transição da crosta continental para crosta oceânica (Mohriak *et al.*, 2003). Esta fase é representada por sedimentos de água rasa seguidos de sedimentos depositados em águas profundas devido ao aumento da batimetria, impactada pela variação eustática e pela tectônica do sal. Esta seção engloba os grupos Camburi, Frade e Itamambuca (Moreira *et al.*, 2007).
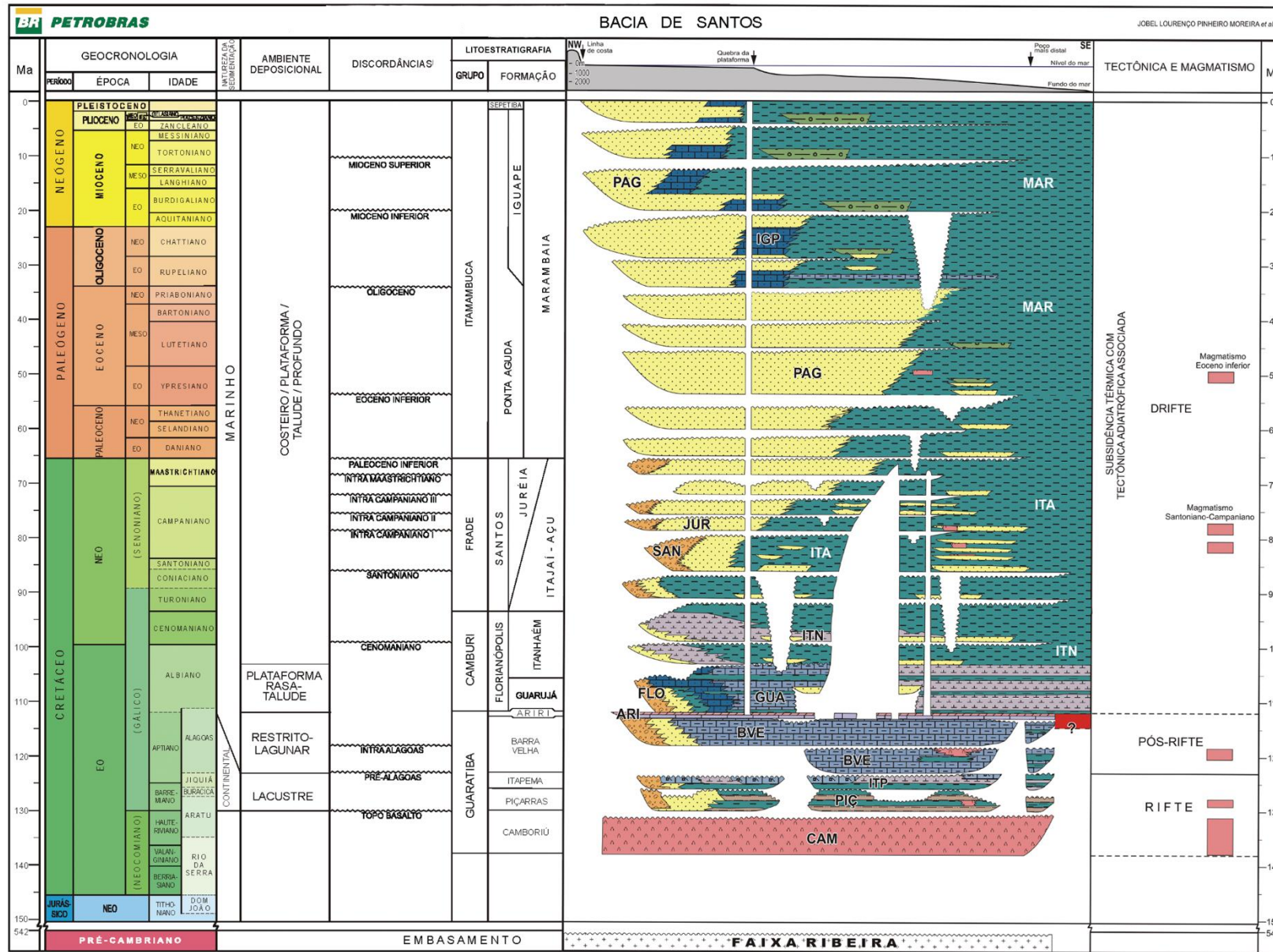
Figura 5 - Carta estratigráfica do Cretáceo para a Bacia de Santos. Linhas onduladas indicam discordâncias regionais. Evolução da bacia omitindo a fase de deriva. Imagem descrita e retirada de Moreira *et al.*

CAPÍTULO 3

MATERIAIS E MÉTODOS

3 MATERIAIS E MÉTODOS

Essa dissertação faz parte da porção microscópica de um projeto da UnB em parceria com a Equinor. Dados de sísmica 3D, petrofísica e a difração de raio-X (XRD) também foram adquiridos da ANP para compor este trabalho, que abrange de uma escala microscópica até uma mega escala, em upscaling.

Informações de sísmica 3D foram processadas e interpretadas por Cesar Atsushi Ushirobira na qual foi feita a localização espacial do poço.

A fim de entender e caracterizar as fácies presentes nos reservatórios da Formação Barra Velha Superior (BVF), foram realizadas as seguintes etapas para esse trabalho: análises macroscópicas e microscópicas por meio de microscópios ótico e eletrônico de varredura, em que foram definidas relações petrográficas e faciológicas.

O testemunho de cerca de 200 metros de um poço perfurado no campo de Sapinhoá foi, majoritariamente, descrito macroscopicamente por Carlos Emanoel Souza Cruz, e os demais membros da equipe da Universidade de Brasília realizaram viagens aos laboratórios da Universidade Federal do Rio de Janeiro (UFRJ) para colaborar na descrição e coleta de amostras. A descrição do testemunho foi feita a partir da classificação sugerida por Gomes *et al.* (2020) para descrição das fácies que compõem a BVF.

A ANP disponibilizou 100 lâminas polidas retiradas de plugs distribuídos em intervalos centimétricos a métricos que variavam de forma irregular ao longo de todo o testemunho. As lâminas haviam sido previamente impregnadas com resina azul para ressaltar os poros, e tingidas com alizarina S para uma melhor distinção entre os cristais de dolomita e de calcita. O sistema de descrição microscópica das amostras foi baseado nos parâmetros de textura, fábrica, composição e diagênese. A classificação seguiu o trabalho de Gomes *et al.* (2020).

Todas as lâminas foram descritas sob um microscópio modelo Axioscope Zeiss 5, software ZEISS Zen 3.4., no laboratório de Microscopia Ótica do Instituto de Geociências da Universidade de Brasília.

A partir da descrição microscópica, foram selecionadas 92 lâminas delgadas para uma quantificação automatizada por meio do microscópio eletrônico de varredura (MEV). Estas foram recobertas com cerca de 15 a 20μm de carbono para facilitar a

condução de elétrons de sua superfície durante a análise. As lâminas foram examinadas através da ferramenta QEMSCAN (Quantitative Evaluation of Minerals by Scanning Electron Microscopy), do laboratório QEMLab da Universidade de Brasília.

Esse equipamento coleta de dados por meio de detectores EDS (Energy Dispersive Spectrometry). Estes dados formam mapas minerais, imagens feitas pixel a pixel, a partir de dados elementares para obtenção de informações detalhadas das fases minerais. O equipamento utilizado foi o modelo Quanta FEI 650F, acoplado a um MEV com 2 detectores EDS de modelo XFlash da Bruker e feixe de tungstênio. As condições estabelecidas para as análises de cada lâmina foram 10 nA e tensão de 15 kV, tendo como resultado mapas de 10 μm de resolução, que levou cerca de seis horas para serem executadas. O mapa com as informações espaciais das fases minerais foi feito a partir da varredura pixel a pixel de áreas selecionadas de 4 cm² em cada uma das 92 lâminas. A quantificação modal e processamento da imagem foram realizadas pela versão 5.3 do software iDiscover do QEMSCAN. O parâmetro utilizado para gerar os dados de QEMSCAN foi a porcentagem de massa e Surface Area.

Para definir cada fase mineral, foi utilizada uma SIP (Species Identification Protocol), um banco de dados criado para se adequar aos carbonatos do pré-sal com base na literatura descrita e em dados adquiridos de espectros obtidos por meio de EDS. Cerca de 3.000 pontos de raio-X foram adquiridos pelo equipamento para cada espectro. A lista mineral engloba minerais stricto sensu e regras que possibilitam variações químicas dentre uma mesma fase mineral. Alguns minerais, como dawsonita e criolita, foram agrupados devido à limitação do equipamento em reconhecer alguns elementos, como flúor (F), por exemplo. Outra limitação do equipamento se dá no limite de detecção de argilas, pois essas fases se encontram em frações muito finas em relação a espessura do feixe do aparelho.

CAPÍTULO 4

ARTIGO

4   ARTIGO

Quantitative Mineralogy and its Application in the Barra Velha Superior Formation Carbonates from Santos Basin

4.1   Introduction

Exploration of ultra-deepwater petroleum provinces in the offshore basins presents a unique exploratory challenge in the last decades. The carbonate section of the pre-salt hydrocarbon reservoir has been the object of recent studies for being highly significant to the energy industry. Pre-salt is the sag-basin sedimentary sequence dated from the early Cretaceous (Karner and Gambôa, 2007). Several studies reviewed the genesis and the evolution of these carbonates and how they affect the composition and the distribution of the sedimentary system (Carminatti, DIAS and Wolff, 2009; Mohriak, Nemčok and Enciso, 2008; Terra et al., 2010; Wright, 2012; Herlinger, Zambonato and De Ros, 2017).

The most explored reservoirs in the Brazilian pre-salt are located in the Campos and Santos Basin. According to ANP (2021), the Sapinhoá field in Santos Basin is the third-largest producer within the core region of the pre-salt known as the Outer High of the Santos Basin.

The Cretaceous carbonates from the Barra Velha Formation were formerly interpreted as microbialites formed by microorganisms in marine systems (Moreira et al., 2007; Terra et al., 2010; Mercedes-martín et al., 2016). Later, abiotic precipitation in a lacustrine environment was suggested by Wright (2012), Wright and Barnett (2015), Herlinger, Zambonato and De Ros (2017), Lima and De Ros (2019) and Gomes et al. (2020). The Aptian facies were formed in alkali, silica, and magnesium-rich lakes composed of mud, spherulites and shrubs. Reworked facies generated by lake fluctuation and sedimentary processes over the *in situ* facies also take part in the sedimentary facies from BVF (GOMES et al., 2020; De Carvalho and Fernandes, 2021).

Lacustrine systems are dynamic and easily affected by tectonics, sedimentary input, temperature, hydrological and geochemical conditions. These variations influence the facies stacking patterns and lead to heterogeneous and complex deposits with no concrete analogs. As the textures and composition aspects of pre-salt carbonates are unusual, understanding their tectonic and stratigraphic context can contribute to

detangling the remanent questions about the pre-salt reservoirs related to the genesis of the carbonates, the environment where they were deposited as the absence of recent analogs for the depositional system (Mercedes-Martín et al., 2016; Herlinger, Zambonato and DE ROS,2017; Wright, 2022; Rebelo et al, 2023).

Intense carbonate reactivity altered the original components. Diagenetic alterations and hydrothermal fluids' percolation have modified structures and impacted permeability and porosity. These events led to processes like dissolution, cementation, and the replacement of minerals with new mineral phases within the facies (Chafetz, 2013; Herlinger, Zambonato and De Ros, 2017; Lima and De Ros, 2019; Gomes et al., 2020). Understanding these alterations is vital for predicting reservoir quality.

The main point of this paper is to corroborate the characterization of the facies from the Upper Barra Velha Formation by detailing the mineralogy of one well in order to explain the processes that lead to the alteration of the original features. In addition to the mega-scale (km) seismic interpretation and petrophysics in the formation, quantitative mineralogical characterization and facies interpretation will provide an overview from the microscopic scale (nm) to present the processes that control the reservoir quality.

4.2   Geological Setting

The southern Atlantic opening results from the separation of South American and African plates and follows the deposition of a thick layer of evaporites in the early Cretaceous (Szatmari *et al.*, 1987). The South Atlantic Basin resulted from two phases of extension: the first one is related to tilted blocks from the continental crust; and the second corresponds to the post-rift and sag basins (Chaboureau, 2013).

In other studies, authors agree that the Atlantic opening started with an extension movement in the Hauterivian to Barremian in the pre-rift stage. Succeeded rifting phases happened during the Barremian-Aptian. This rifting system relates to the faulting and the accretion of sediments forming the basins (Unternehr *et al.*, 2010). The primary structural trend is SW-NE oriented as a reflection of the east-west opening movement with a secondary faulting pattern pointing to the SE-NW direction. The post-rift phase was marked by the Aptian-Albian break-up unconformity, marking the base of the flexural and continuous sag basin (Moreira *et al.*, 2007; Milani *et al.*, 2017; Chaboureau, 2013).

The Santos Basin covers about 350,000 km² down to three km of bathymetry on the southeastern coast of Brazil along the states of Rio de Janeiro, São Paulo, Paraná, and Santa Catarina. The basin is enclosed by the Campos Basin to the north, bordering the Cabo Frio high, and limited to the south by the Florianópolis fault that limits the Pelotas Basin (Moreira *et al.*, 2007), as illustrated in Figure 1.
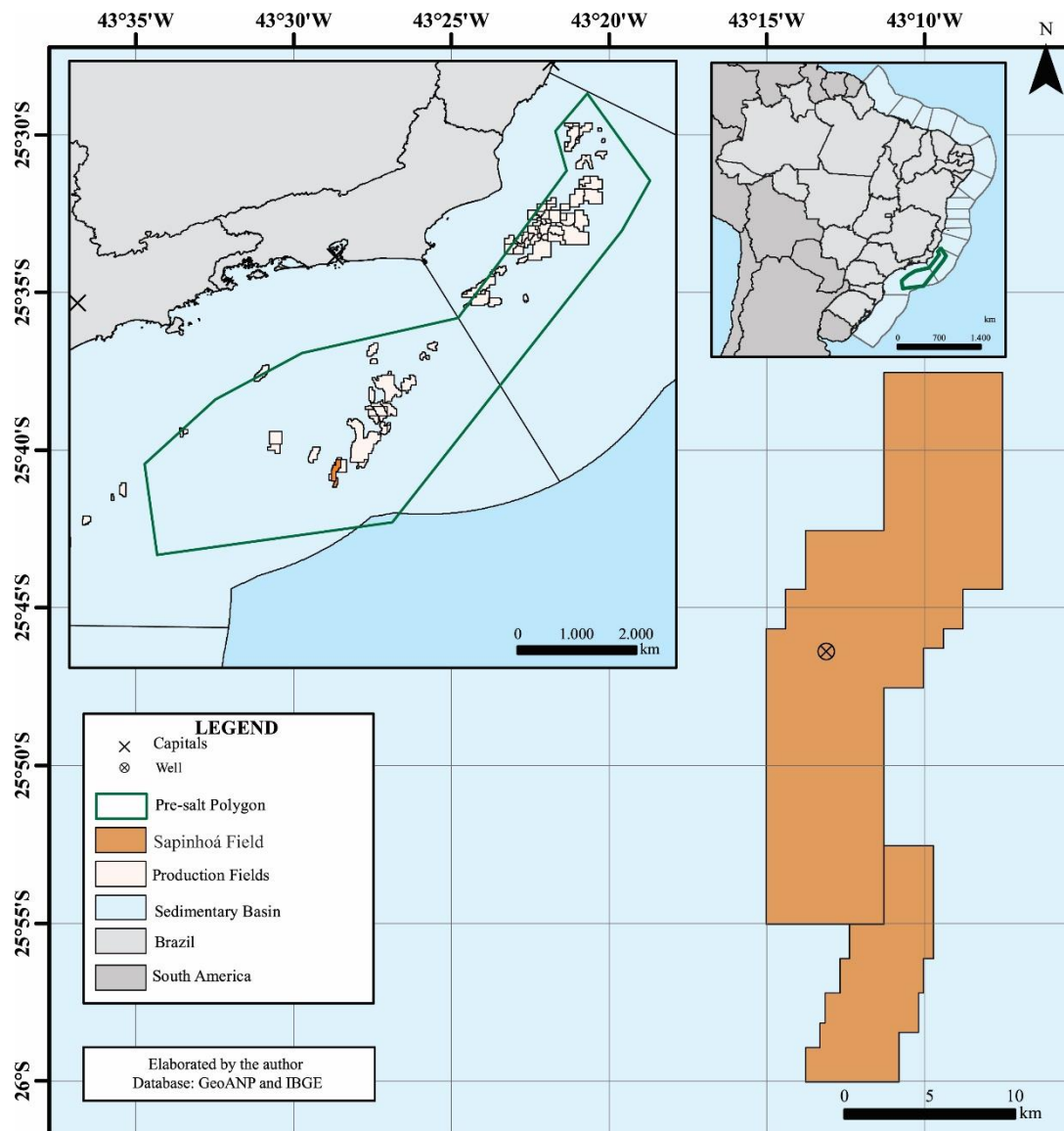
Figure 1 - Study area location (brown color) in the pre-salt polygon. (Prepared with data from GeoAnP and IBGE).

The study field is located on the wide intrabasinal Outer High (green polygon) in the central part of the Santos Basin. Gomes (2012) defines the Outer High as a positive feature, above its surrounding, where zones of deep crust and upper mantle exhumation

are side to side with transitional continental to oceanic material. This region is a key area of study, as mentioned by Almeida Carvalho *et al.* (2022).

Moreira *et al.* (2007) presented three major tectonostratigraphic super sequences to build up Santos Basin: rift, post-rift and drift. The rift phase started in the Heuterivian to early Aptian with a failed seafloor spreading and the formation of large faults as the result of former blocks tilting (Chang *et al.*, 1992; Mohriak, 2012). This phase is characterized by lithospheric extension, block tilting and the formation of grabens associated with intense magmatism that forms the basement of the basin, the tholeiitic basalts from Camboriú Formation. Source rocks from Piçarras Formation lay above that. These siliciclastic rocks are composed of alluvial sediments in proximal areas and talc-stevensitic shales from lacustrine distal regions. At the top of the rift phase, bioclastic carbonates and organic-matter-rich dark shales mark the Itapema Formation that was deposited during the local stage Jiquiá (Tosca *et al.*, 2015).

Later in the Aptian, the post-rift phase comprehends the local stage Alagoas. This stage is marked by a regional unconformity called Pre-Alagoas that consists of cycles of *in situ* carbonates and reworked facies from the Barra Velha Formation. The Intra-Alagoas Unconformity cuts the BVF and divides it into Lower and Upper Barra Velha Formation, the latter is the object of this study. The former is suggested to be the final stage of the syn-rift phase, while the latter encompasses the sag phase characterized by thermal subsidence followed by the deposition of a 2 km layer of evaporites from the Ariri Formation composed of halite and anhydrite that seals the reservoir. The Ariri Formation is placed on top of the Salt Base Unconformity (SBU) (Moreira *et al.*, 2007; Leite *et al.*, 2020).

Lastly, the drift phase includes siliciclastic rocks from marine platforms that comprise the groups Frade and Itamambuca. The sediments above the SBU comprise the post-salt marine sediments which have been deposited until the recent period (Milani *et al.*, 2007; Moreira *et al.*, 2007).

Upper BVF sediments were deposited above the Pre-Alagoas Unconformity, on top of the coquinas and at the end of the rift stage. The environment of deposition of the carbonates is still an issue. Moreira *et al.* (2007), Gomes *et al.* (2009) and Terra *et al.* (2010) suggest a transitional environment with marine influence where stromatolites and microorganisms build the carbonate accumulations.

Pietzsch *et al.* (2018) interpret the BVF carbonates as hydrothermal systems of

travertine-type deposits.

Wright and Barnett (2015), Pietzsch *et al.* (2018), Lima and De Ros (2019) and Gomes *et al.* (2020) agree that the sediments of the Barra Velha Formation were deposited in alkaline lakes and consider the activity of microorganisms related to marine incursions into the lacustrine system. These carbonates are organized in centimetric to metric cycles that comprise *in situ* facies such as mudstones, shrubstones, spherulitestones, and reworked facies (Wright and Barnett, 2015; Pietzsch *et al.*, 2018; Lima and De Ros, 2019; Gomes *et al.*, 2020).

The present study is based on the observation and analysis of one well from the Sapinhoá field in Santos Basin to interpret samples from the Upper Barra Velha Formation laid on the transitional boundary between the rift and the post-rift/sag phases.

Period	Stage	Local Stage	Formation		Basin Evolution
LOWER CRETACEOUS	APITIAN	Alagoas		Ariri	POST-RIFT
			Upper	Barra Velha	
			Lower	Barra Velha	
	BARREM.	Jiquiá		Itapema	RIFT
		Buracica		Piçarras	
		Aratu			
	HAUTER.			Camboriú	
		Rio da Serra			
PRECAMBRIAN				Basement	**LEGEND** ~~~ Unconformity

Figure 2 - Early Cretaceous simplified stratigraphic chart based on Moreira *et al.* (2007).

4.3   Dataset and Methodology

This article is part of the microscopic portion of a project at the University of Brasília (UnB) in partnership with Equinor. 3D seismic data, petrophysical data, and X-ray diffraction (XRD) data were also acquired from the ANP (National Petroleum Agency) to compose this work, which spans from a microscopic scale to a mega scale in upscaling.

3D seismic information was processed and interpreted by Cesar Atsushi Ushirobira. The well's spatial location was determined along with petrophysical data.

To understand and characterize the facies present in the reservoirs of the Upper Barra Velha Formation (BVF), the following steps were taken in this work: macroscopic and microscopic analyses using optical and scanning electron microscopes, which defined petrographic and faciological relationships.

A core sample of approximately 200 meters from a well drilled in the Sapinhoá field was mainly described macroscopically by Carlos Emanoel Souza Cruz, and other members of the University of Brasília team made trips to the laboratories of the Federal University of Rio de Janeiro (UFRJ) to assist in the description and collection of samples. The description of the core sample was based on the classification suggested by Gomes et al. (2020) for describing the facies that make up the BVF.

The ANP provided 100 polished thin sections from plugs distributed at irregular intervals ranging from centimeters to meters along the well core. The thin sections had been previously impregnated with blue resin to highlight the pores and stained with alizarin S to better distinguish between dolomite and calcite crystals. The microscopic sample description system was based on texture, fabric, composition, and diagenesis parameters. The classification followed the work of Gomes et al. (2020).

All thin sections were described under a Zeiss Axioscope 5 microscope, ZEISS Zen 3.4 software, in the Optical Microscopy Laboratory of the Institute of Geosciences at the University of Brasília.

From the microscopic description, 92 thin sections were selected for automated quantification using a scanning electron microscope (SEM). These sections were coated with approximately 15 to 20μm of carbon to facilitate electron conduction from their surface during analysis. The sections were examined using the QEMSCAN (Quantitative Evaluation of Minerals by Scanning Electron Microscopy) tool in the QEMLab

laboratory at the University of Brasília.

This equipment collects data through Energy Dispersive Spectrometry (EDS) detectors. These data form mineral maps pixel-by-pixel images based on elemental data to obtain detailed information about mineral phases. The equipment used was the Quanta FEI 650F model, coupled with an SEM with 2 Bruker XFlash EDS detectors and a tungsten beam. The conditions established for the analyses of each thin section were 10 nA and a voltage of 15 kV, resulting in 10 μm resolution maps, which took about six hours to execute. The map with spatial information of the mineral phases was created by pixel-by-pixel scanning of selected areas of 4 cm² on each of the 92 thin sections. Modal quantification and image processing were carried out using version 5.3 of the iDiscover software from QEMSCAN. The parameter used to generate QEMSCAN data was the percentage of mass and surface area.

A Species Identification Protocol (SIP) was used to define the assembly mineral phases. A database was created to suit pre-salt carbonates based on the described literature and data acquired from spectra obtained through EDS. Approximately 3,000 X-ray points were acquired by the equipment for each spectrum. The mineral list includes stricto sensu minerals and rules allowing chemical variations within the same mineral phase. Some minerals, such as dawsonite and cryolite, were grouped due to the equipment's limitation in recognizing certain elements, such as fluorine (F). Another limitation of the equipment is the detection limit of clays, as these phases are present in very fine fractions compared to the size of the device's beam.

4.4   Results

4.4.1   The Study Field

The field is located on a structural high aligned in the northeast-southwest direction for a 30 km extension approximately (Figure 3) and three to four km wide. It is bordered by normal faults that have probably been active since the rift stage. Some of them have also reached the evaporites of the Ariri formation. The image below illustrates the contact between the base of the salt and the top of the Barra Velha Formation in red and the contact between the Lowes and Upper BVF in green. In blue, the top of the "coquinas" from the Itapema formation. Frequent NE-SW faults, in pink, are present along the field, which possibly performed as conduct to fluids that affected the studied carbonates.

The image below represents the size of the well in comparison to seismic lines, in which each reflector reaches about 30 meters thick. The direction of deposition is mainly orthogonal to the section.
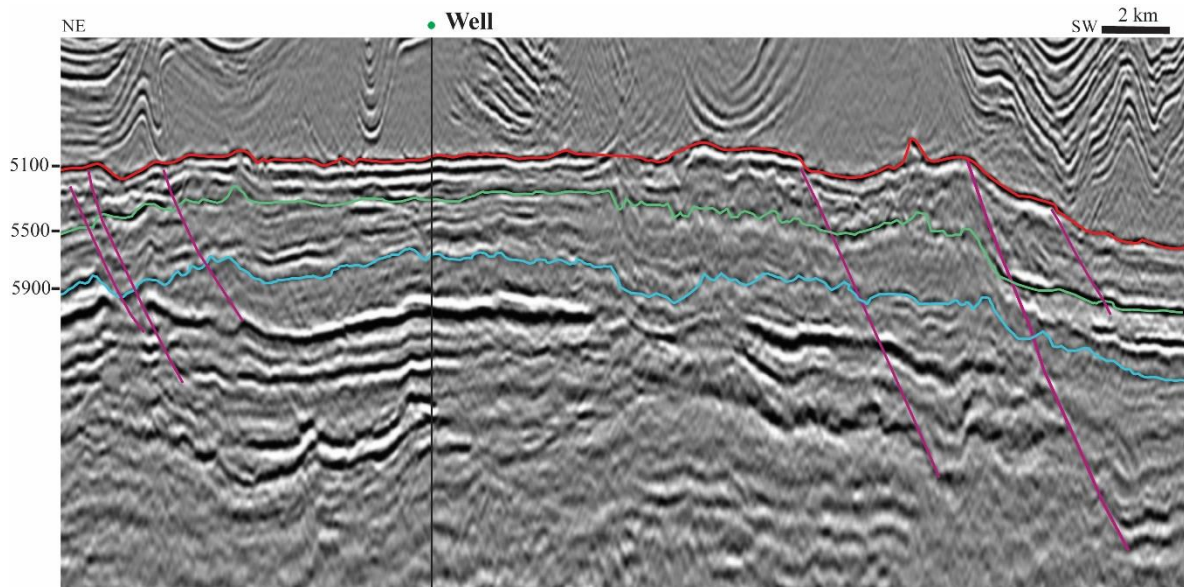
Figure 3 - Seismic cross section along the Sapinhoá field. The base of the salt unconformity is in red, intra-Aptian unconformity in green,and the pre-Aptian unconformity in blue. Faults reaching the reservoir rocks in pink.

4.4.2   Sedimentary Facies

Sedimentary facies equivalent to Barra Velha Formation have been analyzed in a series of recent works. Lima and De Ros (2019), Gomes *et al.* (2020) in Campos Basin, De Carvalho and Fernandes (2021) and Almeida Carvalho *et al.* (2020) in Santos Basin

have been moving towards an agreement regarding the description of the carbonates that form it. The BVF consists of *in situ* and reworked facies repeating in cycles. The major facies constituents recognized are calcite spherulites, calcite shrub-like particles and clay minerals. According to previous studies by Wright and Barnett (2015), Lima and De Ros (2019), Gomes *et al.* (2020), and Almeida Carvalho *et al.* (2022), the most frequent facies classified are mudstones, shrubstones, often classified as fascicular calcite crust, spherulitestones and grainstones.

Based on the classifications suggested by Gomes *et al.* (2020), the relative contributions of each constituent give the name to the rock, while the minor component gives a classifying adjective.

According to Gomes *et al.* (2020), the expected rocks were classified in contrast to Terra *et al.* (2010), who affirmed that the BVF originated under microbial influence formed by stromatolites, spherulites and mudstones. Wright and Barnett (2015) interpreted the BVF carbonates as comprising three cyclothems which vary from 0.75 m to 5 m. These successions are composed of three main facies: mudstones, spherulites and shrubstone.

Mg-rich clay laminations were interrupted and displaced by calcite spherulites during the early diagenesis stage (Wright and Barnett, 2015). The precipitation intensity and the disponibility of space lead to the formation of vertical structures such as shrubs (Wright and Barnett, 2014 and Lima *et al.*, 2020).

Reworked carbonate rocks such as grainstone, packstone and wackestone were also described along *well*. They formed due to the processes of fragmentation and transportation of the original components from the *in situ* facies. Fragmentation through the silicification caused the brecciation of any previously mentioned facies.

Figure 4 illustrates an 15.5 m section from the 200m lithologic log described core showing the coarsening-up cycles that repeat throughout the well. Although the *in situ* facies, such as shrubstones, are not detrital, they were considered granule-sized particles in the granulometric scale because they constitute individual carbonate elements with sizes ranging from a few millimeters to two centimeters in height. Therefore, they do not necessarily represent the level of energy acting during their formation.

Constituents vary vertically depending on the depositional process, if *in situ* or reworked facies, which intercalate regularly.
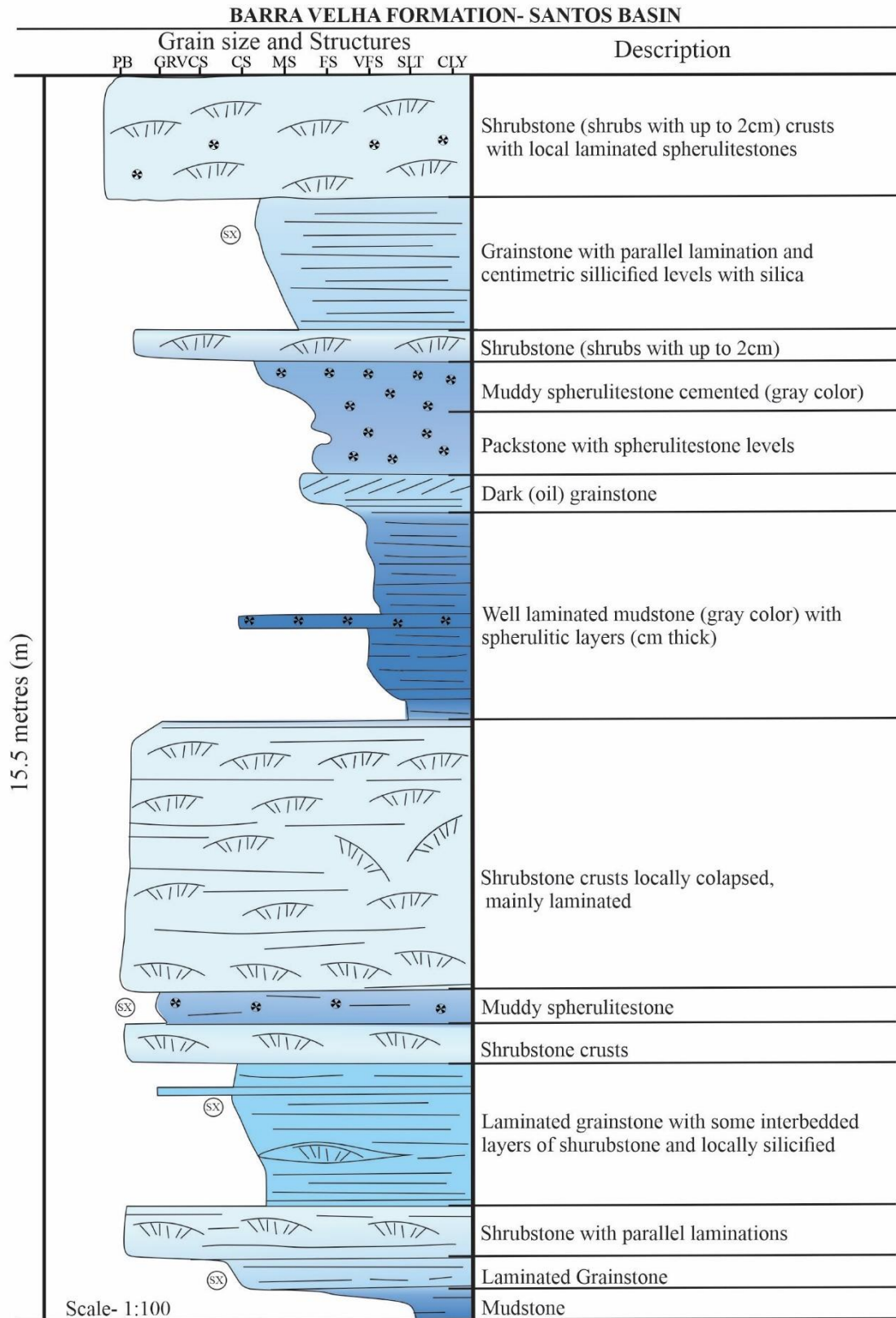
BARRA VELHA FORMATION- SANTOS BASIN

Figure 4 – Example of an interval of lithologic log from the well, presenting some coarsening-up cycles, with *in situ* and reworked sedimentary facies.

The main facies components are listed below:

Clay minerals are syn-depositional layers arranged in thin laminations on macroscopic specimens. On a microscopic level, it is frequently displaced by spherulites. They form brownish-green layers or aggregates and are rare on the well (Figure 7A), often appearing as relic components commonly replaced by rhombohedral dolomite or carried by dissolution opening porosity (Figure 13D). According to the DRX data provided by ANP for the well, the clay minerals within the well are illite, smectite and illite-smectite mixed layers (Table 1).

Table 1. Clay content along the well.

Well - Clay minerals content < 2µm (%)

Section of the well	Sample type	ILI	ISO	KAO
Top	CORE	54	46	-
	CORE	78	22	-
	CORE	0	-	-
	PLUG	0	0	0
	PLUG	56	44	-
	PLUG	31	59	10
	PLUG	28	68	4
Bottom	PLUG	28	68	4
ILI=Illite; ISO=Inter Illite-smectite; KAO=Kaolinite				

Spherulites (Sph) form spherical to sub-spherical masses with a circular outline built of calcite particles often replaced by dolomite, ranging from 0.2 to 2 mm (Figure 7). On the hand specimen, they look like light beige dots within the matrix. Spherulites are easily recognized for their repeatedly radial sweeping extinction under crossed polarized light forming a dark cross that rotates concurrently with the microscope stage angle. In some samples, silica replaces the center of spherulites (Figure 9E); and frequently, dolomite cement forms fringe around the particle (Figure 11H).

Shrubs often appear as millimetric crusts as local layers on the macroscopic level. On the microscopic level, it consists of a fascicular-optical fabric with lamellar twinning and brush extinction occurring under crossed polarized light. The shrub shape varies from rounded, 1:1 proportion when seen on basal or not well-developed particles, to an elongated fan form recurrently arranged with branches. These features range from 1 mm to 1.5 cm long and seem to be the evolution of a spherulite as shown in the Appendix, chemically formed from calcium carbonate precipitation on clay. Calcite shrub is often

replaced by dolomite (Figure 9B) and carved by dissolution micropores that appear along the growth structure (Figure 12B). Most particles analyzed are not connected due to vugs surrounding them. Both spherulites and shrubs compose reworked intraclasts.

Exceptionally, there are some rounded clay fragments 1 to 1.5 mm long with rounded edges on concave-convex grains contact with the spherulites and containing elongated prismatic laths of Na-rich minerals (dawsonite/cryolite, often replaced by pyrite) (Figure 11F).

4.4.2.1 *In situ* Facies

In situ components described above are present within the predominant *in situ* facies found in the Barra Velha Formation: mudstone, spherulitestone and shrubstone described below as they appear along the well.

Mudstone: Macroscopically, the samples present millimetric laminations built by alternating dark to light greenish-brown layers. On thin sections, fine-grained texture in which the components measure less than 60 µm characterized these laminated structures and comprised more than 90% of the sample. Muddy facies contain microcrystalline calcite, dolomite and clay minerals, and minor components oriented according to the laminations. Mudstones show low porosity, spread over 4% of the sample. Locally, mudstones present fractures (Figure 5D) and dissolution porosity (Figures 12C and 12D). Mixed mudstones present other components within the structure. Microcrystalline silica nodules and spherulites measuring 0.5 to 0.9 mm often displace the muddy layers. Pervasive silicification is frequent in mud facies. Silica fills the porosity with microcrystalline silica and quartz of 0.04 to 0.15 mm. When the content of silica, dolomite, calcite and particles is considerable, the facies receive a qualifier adjective related to the secondary components, such as dolomudstone or spherulitic mudstone. Apatite is present as grains measuring about 1 mm with anisotropic millimetric crystals cross cutting the framework. Additionally, fragments appear as long organic shapes that occur sparsely on muddy facies in well.
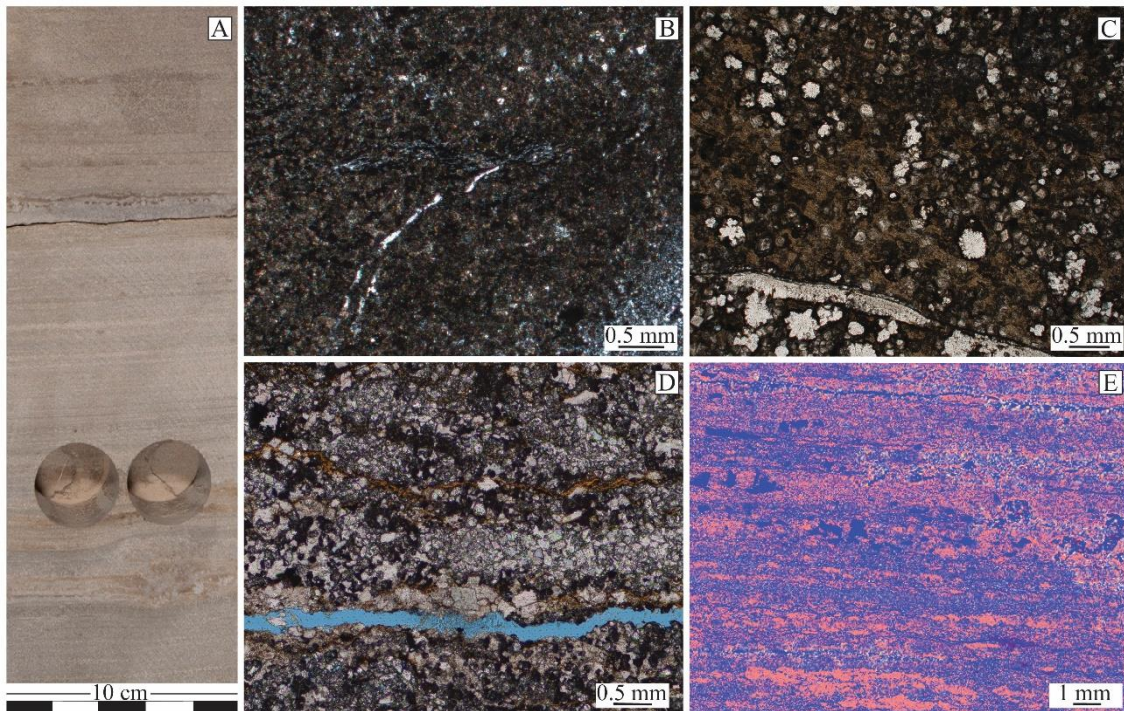
Figure 5 - Mudstone. A) Laminated mudstone in cores of the *well*; B) Photomicrography under crossed polarizer (XPL) of a mudstone replaced by pervasive macro and microcrystalline silica; C) Photomicrography under parallel polarizer (//PL) of partially dolomitized mudstone displaced by radial silica; D) Photomicrography under //PL of remaining clay with parallel lamination; fracture died in blue; E) QEMSCAN image of the previous sample (D) Secondary porosity, vugs and fractures (blue) and alternated lamination of dolomite (lilac), calcite (pink) and silica (beige).

Spherulitestone: Macroscopically, the spherulitestone has a light beige color, and the number of particles usually thickens towards the top of the well. Microscopically, these facies are massive. The predominant components are well-formed and well-sorted spherulites composed of calcite and commonly replaced by dolomite. Spherulites measure from 0.2 to 2.0 mm (Figure 6). The samples present rhombohedral dolomite measuring from 0.07 to 0.3 mm, with microcrystalline quartz frequently filling the interparticle porosity. Porosity shows uniform distribution covering 10 to 15% of the samples. Minor dissolution porosity within the spherulites is present, but interparticle pores and vugs are predominant. When there is a remaining clay matrix around the spherulites, the minor component is given as a qualifier adjective to the facies as muddy spherulitestone. The matrix in spherulitestones is often deformed, around the particles. The lamination encompasses the spherulites. The deformation of the matrix was replaced by "dolomite bridges" as Rebelo *et al. (2023) called.*
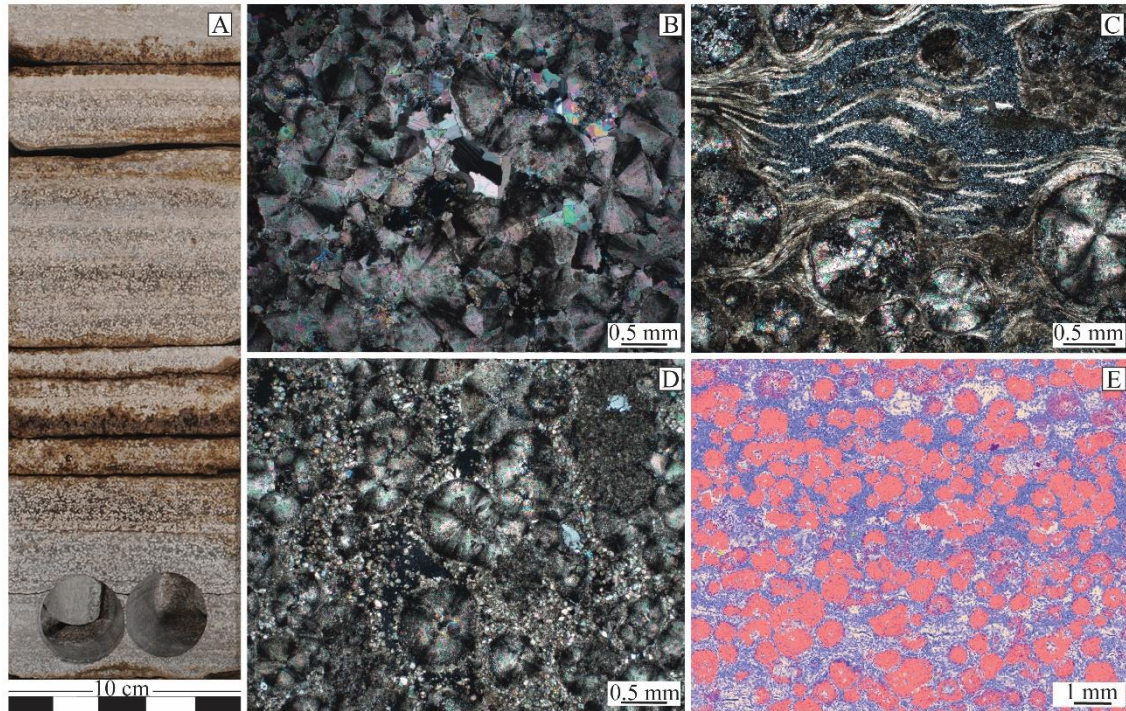
Figure 6 - Spherulitestone A) Spherulitestone in cores of the *well*; B) Photomicrography under crossed polarizer (XPL) of spherulites replaced by pervasive macrocrystalline silica; C) Photomicrography under XPL of partially silicified clay matrix being displaced by spherulites; D) Photomicrography under XPL of spherulites surrounded by dolomite rhombs filling vugular porosity; E) QEMSCAN image of a spherulitestone showing calcitic spherulites (pink) surrounded by matrix replaced by dolomite (lilac) and silica (beige), and barite (purple) is also filling porosity.

Shrubstone: Macroscopically, the shrubs form massive light beige millimetric to centimetric fan-shaped crusts growing in one direction, usually increasing towards the top of the well. On the microscopic scale, the shrubstone comprises elongated fan-shaped structures measuring 1.0 to 15 mm on longitudinal sections, and a radius up to 3 mm on the basal sections, forming a circular 1:1 ratio structure. The conical structures are usually oriented vertical to sub-vertical (Figure 7). The main mineral that forms the shrub is calcite, usually replaced by dolomite. Shrubs are often associated with minor spherulitic particles, which can add the qualifier spherulitic to the facies spherulitic shrubstone. Dissolution intraparticle porosity is common but less frequent than vugular interparticle pores counting as 20% of the thin section area. Intraparticle pores generated by the dissolution of the carbonates are less frequent than the vugular porosity. Silica and dolomite are the cement of these facies. Different types of dolomitization, such as microcrystalline and rhombohedral crystals of 0.07 to 0.3 mm, are found filling the pores. Microcrystalline and radial silica are distributed along the structures, probably related to

the original pores. Quartz measuring 0.2 to 1.5 mm and microcrystalline silica fill the vugs with millimetric blocky dolomite grains.
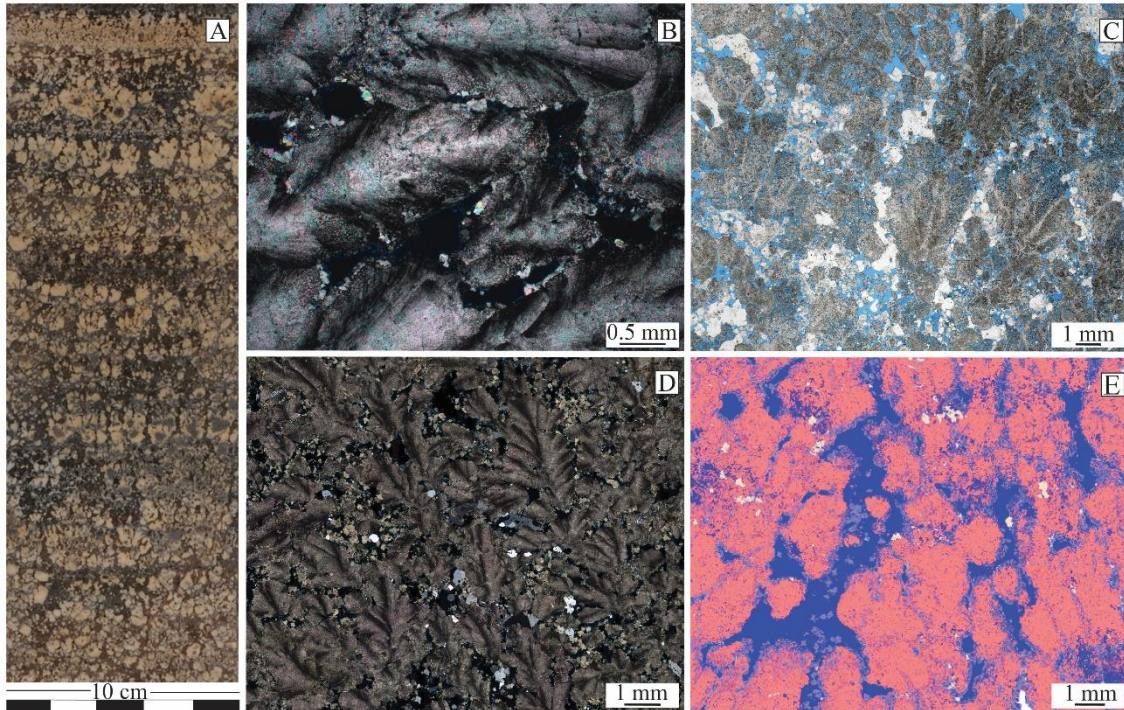
Figure 7 - Shrubstone A) Macroscopic scale upward distribution of shrubs in the well core; B) Photomicrography under XPL of shrubs with a dolomitic cement fringe; C) Photomicrography under //PL of shrubs oriented towards the top and silica filling the intraparticle pores; D) Photomicrography under XPL of oriented shrubs and silica filling the pores. E) QEMSCAN image of a shrubstone showing calcitic particles (pink) partially dolomitized on the borders (lilac) and few silica (beige) content filling the interparticle pores (blue).

4.4.2.2   Reworked Sedimentary Facies

Reworked facies represent particle-supported frameworks exhibiting modifications accrued during the diagenetic processes influenced by deposition conditions within the lacustrine environment, including the impact of tidal flow.

Intraclasts formed by fragments of spherulites and shrubs vary from fine to coarse-grained constituents composing massive and stratified facies. According to Dunham's (1962) and Gomes' (2020) descriptions, these facies are classified as wackestone, packstone, grainstone and rudstone, the former containing fine-grained material decreasing to the latter. Gomes (2020) proposes that the terminology should be used when 50% of the former components that compose the facies are reworked; otherwise, the *in situ* classification would be more suitable.

Wackestones are limited to less than 5% on *well*, mud-supported facies comprising more than 10% to 70% coarse material. Macroscopically, the facies are matrix-supported massive structures of fine-grained material disposed into millimetric to centimetric sub-planar to planar lamination. Microscopically, these facies present a finely laminated clay matrix often dolomitized and silicified. On average, 15 to 25% of the thin sections are particles from these facies formed by millimetric obliterated shrub and spherulite fragments, often stretched. Additionally, these facies present replacive rhombohedral dolomite and pervasive silica-filling dissolution porosity (Figure 8B).

Packstones are grain-supported facies with 70 to 90% of intraclast content. It comprises 13% of the analyzed samples. Macroscopically, they are medium-grained facies that present non-parallel to planar centimetric lamination, often silicified with rare fine-grained rich layers. Microscopically, packstones present sub-rounded to stretched particles that remain surrounded by dolomite rhombs and siliceous cement-filling dissolution porosity (Figures 8D and 8E).

Grainstones are about 20% of the described facies from the well. The rocks are grain-supported facies with less than 10% of fine-grained material. These facies comprise more than 90% of reworked constituents and their fragments. Shrubs and spherulites are often reworked. The size of the constituents is very variable, from 0.5 to 4.0 mm. It is noticeable that the sphericity of the spherulites is lower in reworked facies than in *in situ* facies, while their contacts evolve from long to concavo-convex and sutured (Figures 8A and 8C).
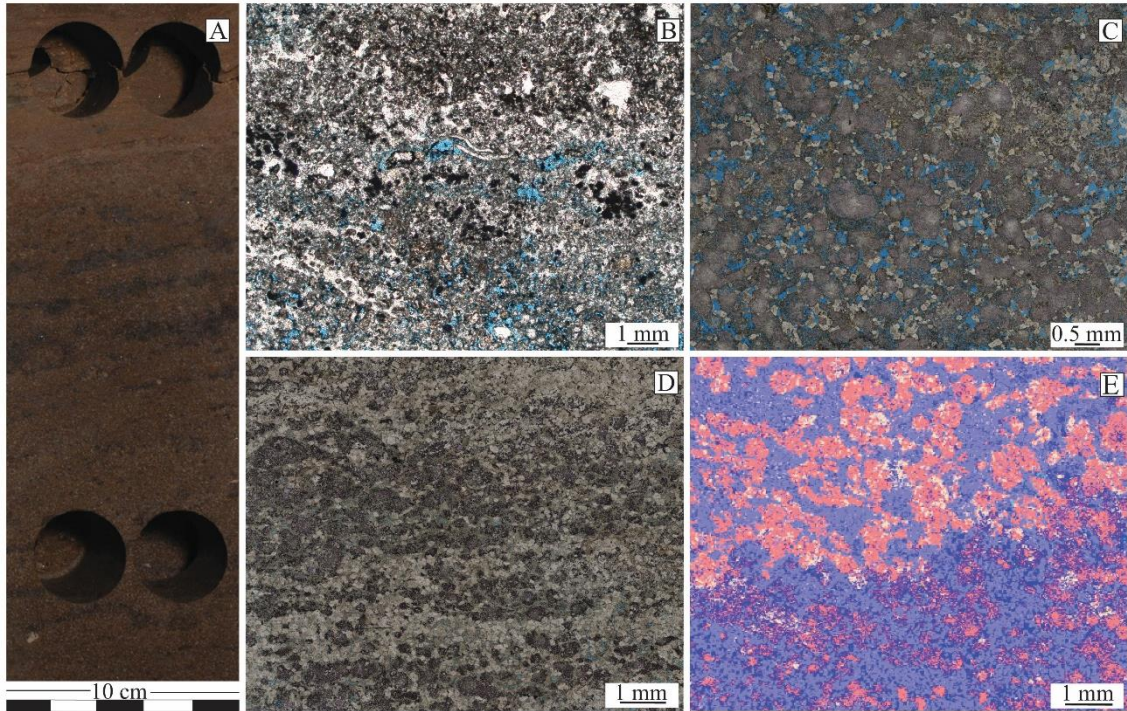
Figure 8 - Reworked Facies. A) Grainstone with cross stratification in core; B) Photomicrography under //PL of reworked and dissolved matrix dolomitized in a wackestone; C) Photomicrography under //PL of shrubs oriented and distorted particles and silica filling the intraparticle pores in a grainstone; D) Photomicrography under //PL of vertical-oriented particles and dolomitized matrix in a packstone. E) QEMSCAN image of a packstone showing calcitic particles (pink) partially dolomitized on the borders (lilac) and a few silica (beige) content filling the interparticle pores (blue).

4.4.2.3   Diagenesis of *In situ* and Reworked Sedimentary Facies

Lateral and vertical variations of several sedimentary and post-depositional diagenetic processes affected the permeability of the BVF, significantly enlarging and reducing porosity. These processes resulted in heterogeneous and non-continuous diagenetic processes along the sag phase of the pre-salt as mentioned by Herlinger, Zambonato and De Ros (2017), Lima and De Ros (2019), while studying Campos Basin, analogous to the Santos Basin, and later by Almeida *et al.* (2022), who studied the Santos Basin.

Neomorphism, cementation and replacement processes increase the complexity of the primary microstructures. Early diagenesis occurs at the surface or shallow depths, influenced by vadose and phreatic modifications. Along the well, the following products of diagenesis were observed:

Early diagenesis - evidence noticed in the studied thin sections marks the first stages of alterations processes that affected the BVF components. The replacement of

stevensite by dolomite and magnesite on fine-grained facies as mudstones (Figures 7A and 16A), dolomite frequently replaces the original structure in the spherulites and shrub (Figure 9B) on the coarser facies. Blocky dolomite is described as coarse grains of macrocrystalline dolomite ranging from 0.5 to 1 mm, forming a mosaic structure. Dolomite grains also build rims around shrub and spherulite structures, forming fringe cementation and frequently filling primary enlarged porosity (Figure 9C). Dedolomitization is marked by calcite grains ranging from 0.2 to 0.5 mm with concave-convex contact and noticeable lamellar twinning, forming a cement that occupies the original pores that were obliterated by blocky dolomite (Figure 9D). Microcrystalline silica is the most frequent siliceous phase, forming massive aggregates that fill intra and interparticle pores. It is common in both *in situ* and reworked facies. This type is more frequent to the top of the well, commonly associated with microporosity, as shown in Figure 10B. Microcrystalline silica precipitates, replacing the original calcite structure within shrubs and spherulites (Figure 9E). Different mechanical compaction levels are noticed as the burial pressure increases, and long contacts start appearing as concave-convex contacts (Figure 9F). Millimetric grain fracturing and deforming by mechanical compaction is common as well as the dissolution of the shrub and spherulite structures, resulting in a millimetric intraparticle porosity.
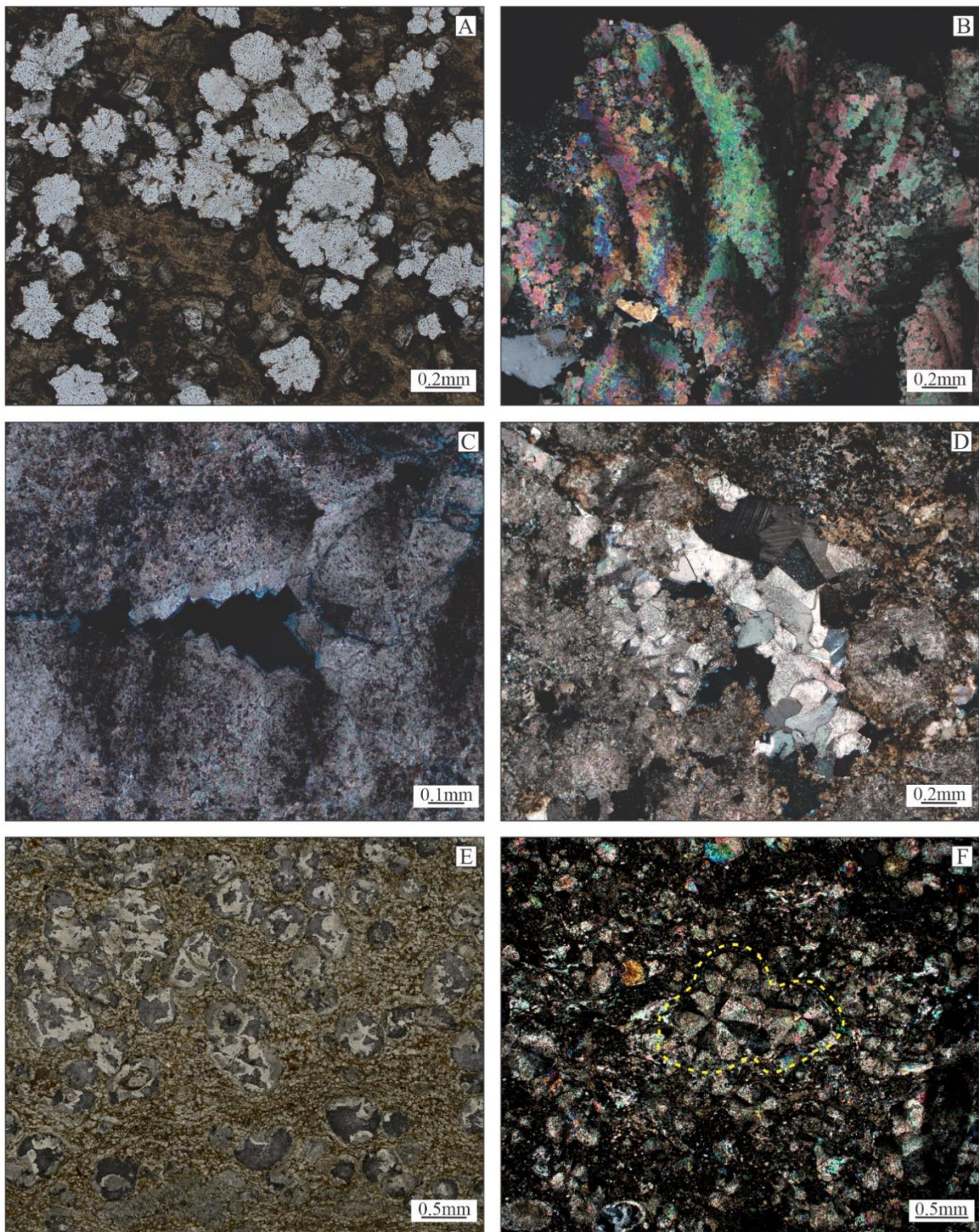
Figure 9 - (A) Stevensite replaced by magnesite and dolomite; (B) Replacive dolomite in the original shrub structure; (C) Block/Euhedral dolomite filling porosity (reduced porosity); (D) Dedolomitization calcite; (E) Replacive silica; (F) Mechanical compaction on spherulites circled in yellow.

De Carvalho (2021) mentions that late diagenesis encompasses chemical compaction (stylolitization), dissolution, fracturing, pervasive silicification, later dissolution, and later dolomitization as a possible effect of the hydrothermal fluid. Lima (2019) considers fracturing, chemical compaction and chalcedony replacement as mesodiagenetic features. After that, later dissolution is caused by hydrothermalism followed by dolomite precipitation and pervasive pore-filling macrocrystalline silica.

Burial diagenesis on the sections from the well appears as rare stylolite related to shrubs on two thin sections. The feature of chemical compaction crosscut a shrubstone section (Appendix 1 and Figure 10B) and mechanical fracturing of shrub particles occurs in a few samples (Figure 10A), lastly, precipitated radial chalcedony appears filling the framework.
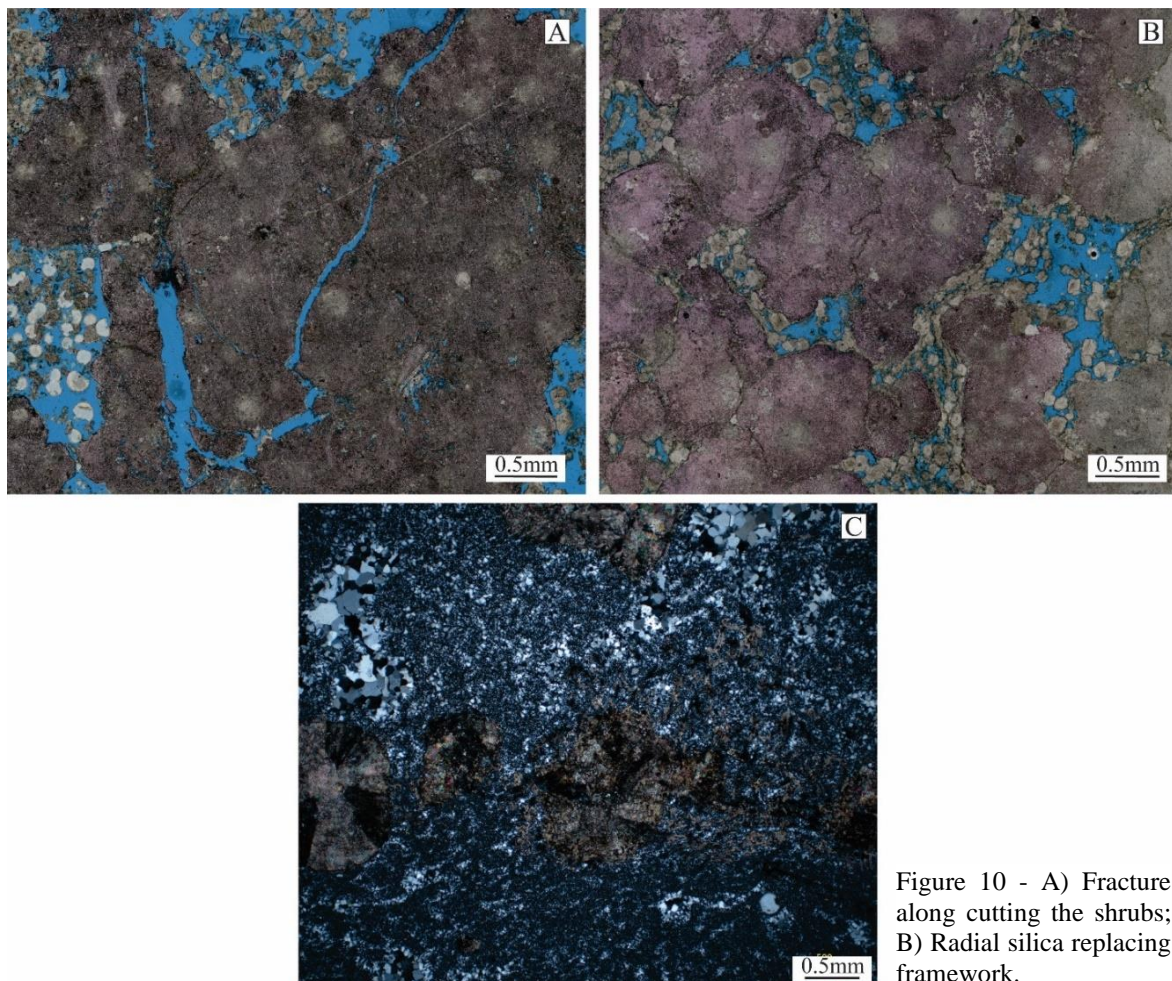
Figure 10 - A) Fracture along cutting the shrubs; B) Radial silica replacing framework.

This microscopic-sized silica developed into fibro-radial structures measuring around 0.3 mm with rounded habits that often resemble the extinction of spherulite under

crossed polarizers. It is most frequent in *in situ* facies and occurs predominantly at the bottom of the well, filling secondary macro-pores. (Figure 10C).

4.4.2.4 Hydrothermal Events on *In situ* and Reworked Sedimentary Facies

Geothermal gradient triggered by magmatic heating is common in the extensional tectonic regime as the continental margin rift. Pressurized water flows ascend through faults and structures below 5 km depth that conduct the fluid to the basin. Davies *et al.* (2006) proposed that fault, fractures, and discontinuities conduct hydrothermal ascending fluids.

Hydrothermal solutions are understood as hot fluids with a temperature at least 5 degrees above the host rock, may be the cause of metasomatism due to the presence of CO_2 and H_2S in their composition (Machel *et al.*, 2002).

The input of CO_2 from hydrothermal activity resulted in the dissolution of Mg-clays, leading to a silica and magnesium-rich environment and the posterior precipitation of dolomite and silica phases (Herlinger, Zambonato and De Ros, 2017).

The common mineral paragenetic phases associated with burial diagenesis or hydrothermal conditions that altered the original composition of the studied wells are carbonates as rhombohedral dolomite (described by other authors as saddle dolomite). Saddle dolomite is a common mesodiagenetic mineral in carbonates, but it is not a diagnostic feature of hydrothermal activity (Herlinger, Zambonato and De Ros, 2017).

Rare undulose extinction was described on a limited number of thin sections, the term "saddle" was not adopted in the present work, disregarding the curved shape of the dolomite rhombs.

Enlargement pores and vugs were observed in the facies (Figure 11A). Silica precipitated and filled the pores as macrocrystalline quartz. Coarse crystalline silica forms cement as subhedral grains measuring from 0.3 to 1 mm that fill pores and fractures; it is the least abundant siliceous type and is more frequent from the middle level to the bottom of well (Figure 11B). In Figure 11C, it is possible to notice the core crystalline silica enclosing the dolomite rhomb. Further, the presence of sulfate, sulfide and other low-temperature alteration minerals listed below can be related to the variation of the hydrothermal fluids.

Barite crystals measuring less than 0.2 mm fill pores and replace diagenetic

constituents as dolomite. It appears as a subhedral to anhedral mineral, anisotropic under crossed polarizers (Figure 11D). The sulfate often replaces the diagenetic constituents of the former clay laminations. On the other hand, fluorite was only recognized in the automated mineralogy analysis.

Pore-filling residual pyrite of 0.01 to 0.03 mm fills vugular porosity or replaces primary constituents such as dolomite and quartz. Sulfide occurs as subhedral crystals opaque under transmitted light and light yellow under reflected light (Figure 11E), and bright gray on the SEM image (Figure 11H and 14B).

Dawsonite ($NaAlCO_3(OH)_2$) is the most abundant accessory mineral. It frequently fills porosity with low-relief acicular crystals, often forming rosettes of 0.2 millimeters (Figure 11F). Dawsonite is usually related to the spherulitic and shrubby levels and is rarely associated with illite and pyrite.
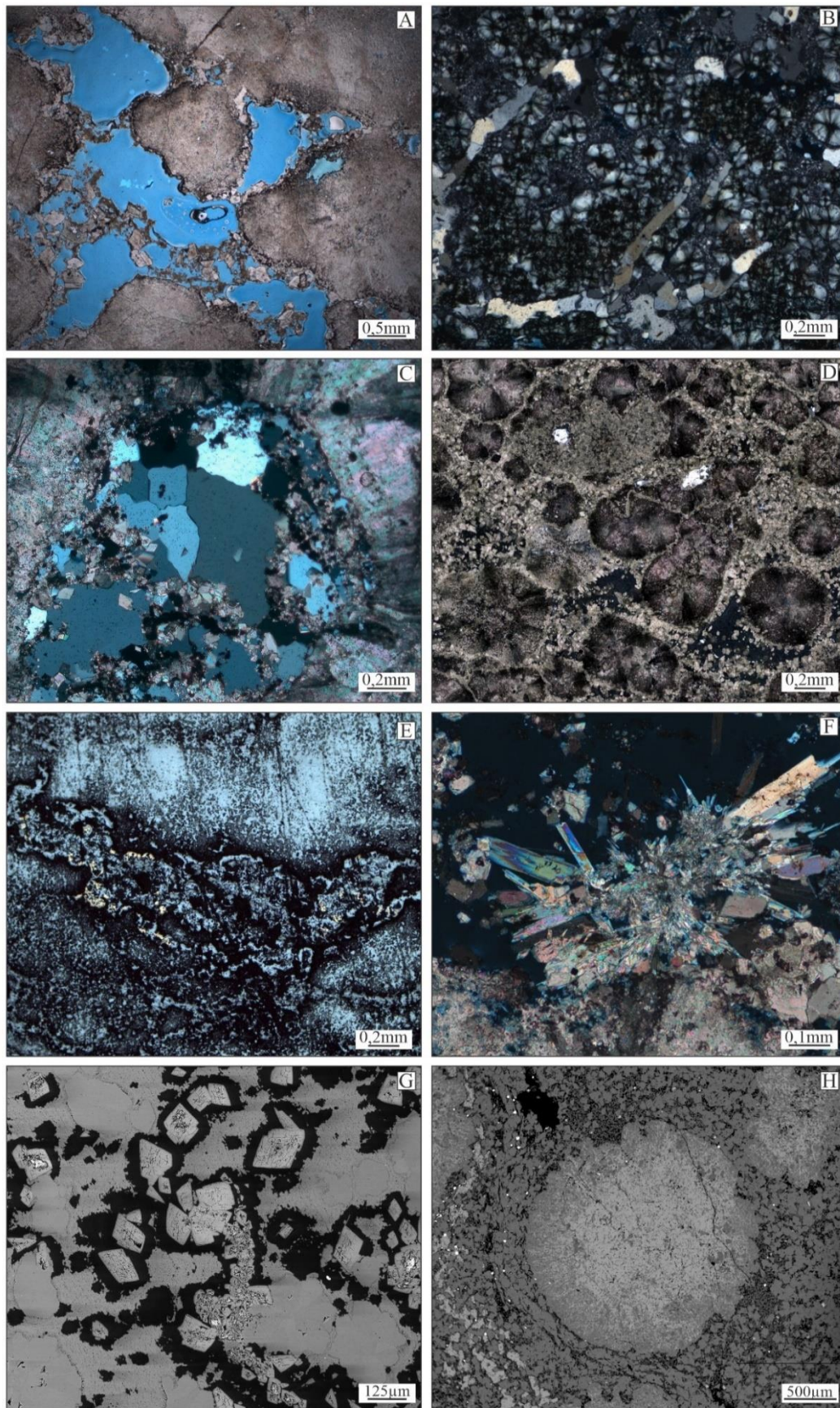
Figure 11 - A) Secondary porosity (vugs) in shrubstone; B) Precipitated macrocristallyne silica; C) Microcrystalline silica enveloping dolomite rhomb; D) Apatite and dolomite rhombs filling vugular/fenestral porosity; E) Pyrite thin filling porosity in reflected light; (F) Dawsonite filling porosity; G) SEM/EDS dolomite rhombs and pervasive silica; H) Dolomite replacing calcite on spherulites and dolomite rhombs filling secondary porosity.

Porosity in carbonate rocks is classified into primary, formed during sediment deposition, and secondary porosity, which develops after deposition and depends on the depositional environment and the diagenesis. The size, shape, compaction and sorting of the grains directly influence the porosity (Tucker *et al.*, 2017).

High porosity can be related to the enlargement of pores and the connection among vacant spaces. In oil and gas exploration, the porosity of carbonate rocks is an essential factor in determining reservoir quality as it controls permeability.

Vugular porosity is frequent around the structures and particle fragments that compose intraclastic facies, varying in size from cm to metric scale cavities, formed by the chemical action of dissolution during mesodiagenesis or hydrothermal activity (Figure 12A, E, and F). When vugular porosity is associated with interparticle porosity, permeability is higher, generating better reservoir conditions. Among the grain-supported rocks, shrubstones and grainstones present the best permeability, as shown in the plot below (Figure 15).

The partial dissolution of intraclasts generates secondary intraparticle micropores. It is occasionally seen in rocks with some preserved intraparticle porosity as shrubstones (Figure 12B).

In Figure 15, mudstones and packstones, fine-grained to matrix-supported facies, express lower permeability. Interlamination micropores and fractures measuring less than 0.5 mm were generated by matrix dissolution commonly occurring repeatedly, subparallel to the lamination (Figure 12C and D). In Figure 12D, the siliceous nodule seems to be previously formed, implying that the fracturing and dissolution happened after it settled.

The spherulitestones may have good porosity and permeability when interparticle primary porosity or matrix dissolution is still preserved. Nonetheless, the presence of replacive silica and dolomite reduces their permeability.
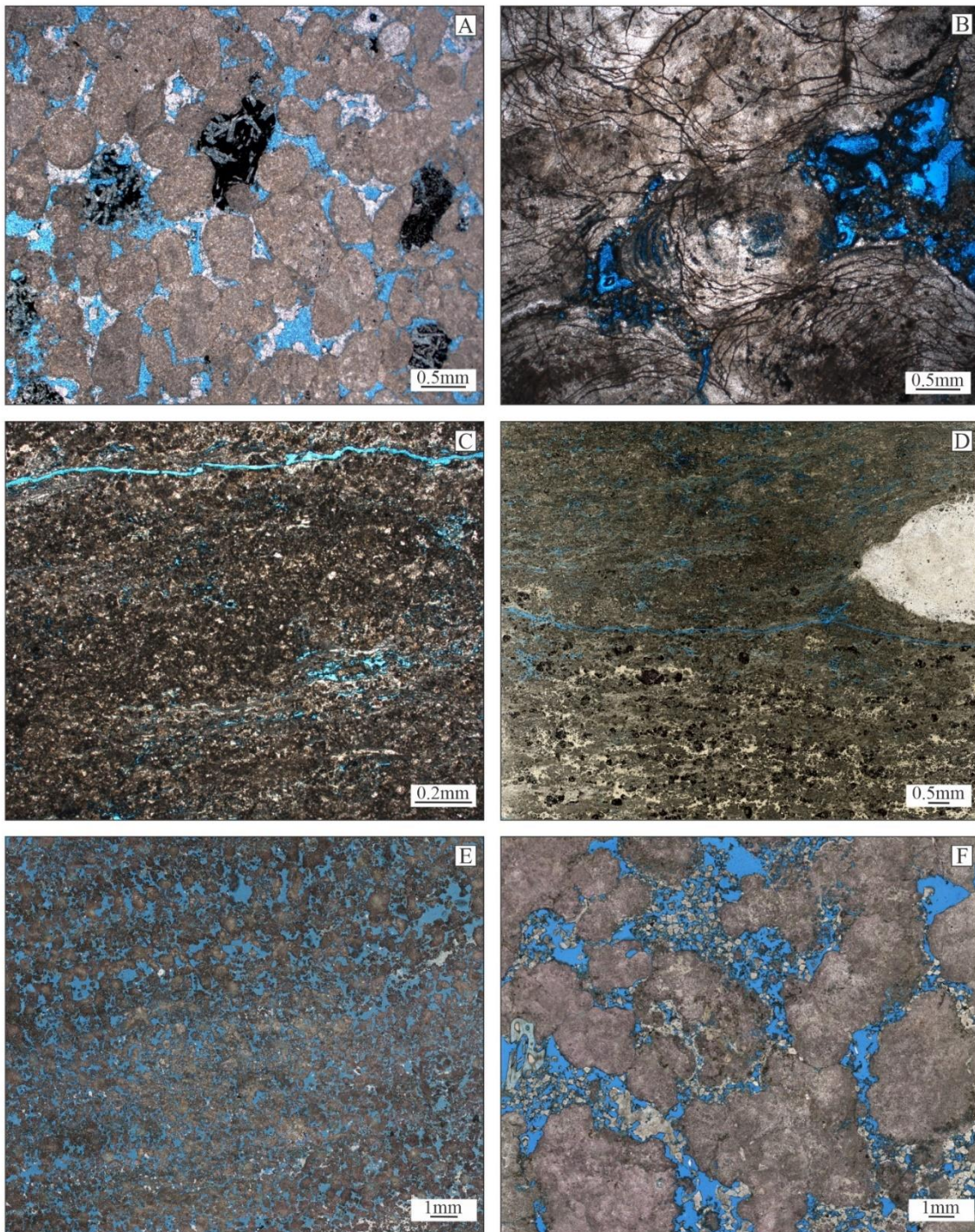
Figure 12 - A) Enlarged primary porosity; B) Intraparticle porosity within the shrub structure and vugular porosity around it; C) Dissolution porosity and fracture on clay-rich facies; D and E) Dissolution and fenestral porosity; F) Vugular porosity.

4.4.2.5   Reservoir quality

The qualitative description of reservoirs is determined by the permeability values. Based on Rider (1996), facies with permeability below 10 mD characterize a poor-quality reservoir and from 11 to 15 mD, a fair reservoir. Moderate-quality reservoirs comprise rocks with permeability varying from 15 to 50 mD, good quality reservoirs, from 50 to 250 mD and very good quality reservoirs, from 250-1000 mD. Lastly, excellent quality reservoirs show permeability values above 1000 mD.

Spherulitestone, breccia, chert and packstone are considered low-quality reservoirs because they sit below the 10 mD mark; wackestone and rudstones are moderate, whereas grainstones and shrubstone are considered very good to excellent reservoirs.

The cross plot below presents absolute permeability and total porosity in all sedimentary carbonate facies in the well core. Figure 13 shows that the *in situ* facies of shrubstones and the reworked facies of grainstones are the two best reservoir facies in the Upper Barra Velha Formation. Due to matrix dissolution, rudstones are also good reservoirs but are rare on this well chert and breccia facies.
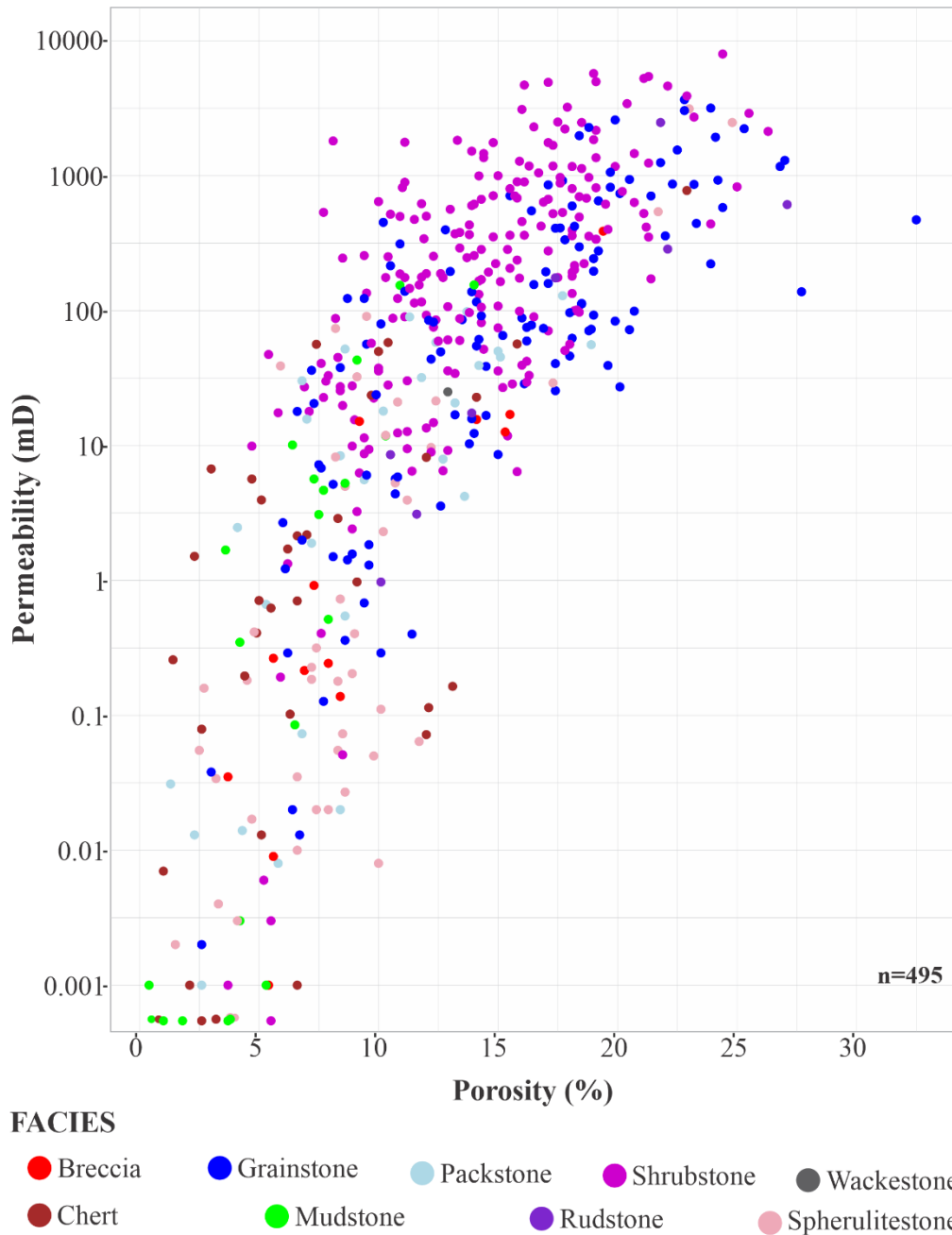
Figure 13 - Cross plot of absolute permeability and total porosity in all sedimentary carbonate facies present in cores of the well. The *in situ* shrubstones and the reworked grainstones are the two best reservoir facies in the Upper Barra Velha Formation. Rudstones are also good reservoirs but are not so frequent in the study field.

4.4.2.6   Vertical Mineral Distribution

Mineralogy measurements were obtained via QEMSCAN on thin sections of carbonate rocks from well. Modal mineralogy based on paragenetic assembly resulted

in the distribution of main minerals and accessory minerals associated with the pores (see appendix). The measurements were based on the surface area using an estimation of the average surface area and the volume ratio across all the particles present in the thin section present on a millimetric mineral map distribution, as shown below (Figure 14).
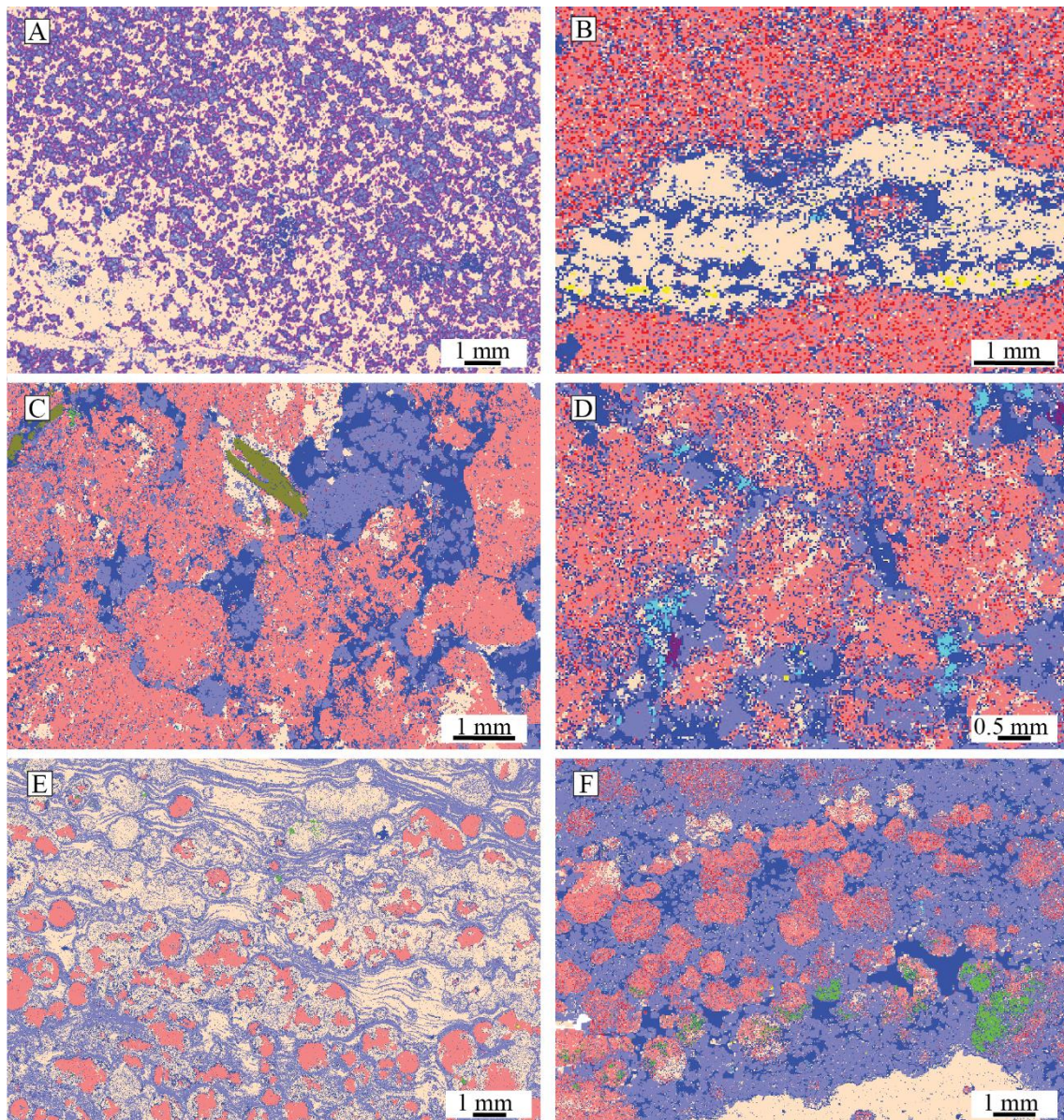
Figure 14 - Modal map of phases generated by QEMSCAN. calcite in pink (B, C, D, E, F), dolomite in lilac (A, B, C, D, E and F), quartz in light yellow (A, B, C, D, E and F), pores in blue, apatite in brownish green (C), fluorite in bright green (E and F), Na-rich minerals in cyan (D) and barite in purple (D).

The graphs for main minerals (calcite, dolomite and quartz) and accessory minerals (apatite, barite, fluorite, dawsonite/cryolite, gypsum/anhydrite and pyrite) were made after normalizing the data acquired from the surface area according to the

following equations:

First, the depth resolution is 10 m. For the sake of total mineralogy quantification per sample, the pores were disregarded, and the main minerals were separated from the accessory minerals. Therefore, the sum of each of these groups is considered 100%.

Mineral Normalized* = 100%

The average per decameter was calculated,

Σ Mineral $\times \frac{Normalized}{n}$, where n is the number of thin sections per decameter

* Main or accessory minerals.

4.4.2.7   Main Minerals

Dolomite (CaMg (CO$_3$)$_2$) is the most abundant mineral in the well. Although the percentage of dolomite remains stable at around 35 to 60% of the bulk composition, there is a trend for it to increase in the deeper facies. However, it is also enlarged on the superior quarter of the graph. Framework and cement dolomite are distributed up to 75.8% of the thin section surface. The dolomite content tends to be inversely proportional to the calcite content. In addition, it is noticeable that the lower silica content corresponds to the higher dolomite levels on the well.

Calcite (CaCO$_3$) concentration is lower than the dolomite of the well. The distribution of the carbonate tends to reduce due to the dolomitization of the later carbonate. *In situ* structures, such as spherulites and shrubs, are formed by calcite precipitation. The lowest quantity of calcite is located on the bottom portion of the well, and it is noticeably thickening at a mid-depth, where it reaches the highest concentration and decreases one more time as it reaches the top of the well. There is no clear relationship between the Mg-rich calcite and calcite, and the former appears at the maximum occurrence of 10% while the latter reaches up to 75% of the surface area of some samples. It is noticeable the inverse relationship of calcite (Mg-bearing and non-Mg calcite) with the silica through the well.

Quartz (SiO$_2$) is the least abundant of the main minerals. Besides the sharp decrease of content in the third quarter (top to bottom), silica concentration tends to increase towards the extremities of the well. In some samples, the quartz content covers an area of 2.2% at its minimum and 98% at the maximum of the thin section. This is probably related to the sampling method. As silica is the main product of the diagenetic

process, it relates to the lowering levels of the other two main components. It often appears to replace calcite and dolomite and fills inter and intraparticle pores as micro, macrocrystalline and radial forms. Silicification can be very pervasive and intense, generating portions of chert along the well.

Figure 15. Main minerals quantified distributed along the well.

Calcite, in pink, represents basically primary minerals. The others, dolomite in lilac and silica in yellow, are related to early and burial diagenesis.

The image below reveals the distribution of the main replacement minerals in their different forms observed under the optical microscope from the thin sections along the well and its position in contrast with the gamma-ray log. The highest peaks may be related to the intercalation of the muddy sections, forming a zig-zag pattern that indicates the cyclicity of facies. These muddy facies were not observed in the analyzed well, although the geometry and matrix texture remain on the samples, the clay minerals were already replaced by the new mineral phases.

They manifest ubiquitously across all facies constituting the well, encompassing fine and coarse-grained samples. Their presence persists, often in reduced proportions, even when calcite remains.

Dolomite macrocrystalline cementing samples are as rare and sparse as radial silica. In contrast, dissolution dolomite frequently replaces the calcitic structures (Figure 15). Replacive, macro and microcrystalline silica occur simultaneously at the top of the well core (Figure 16). Silicification occur as discontinuous masses not necessarily related to dolomitization.
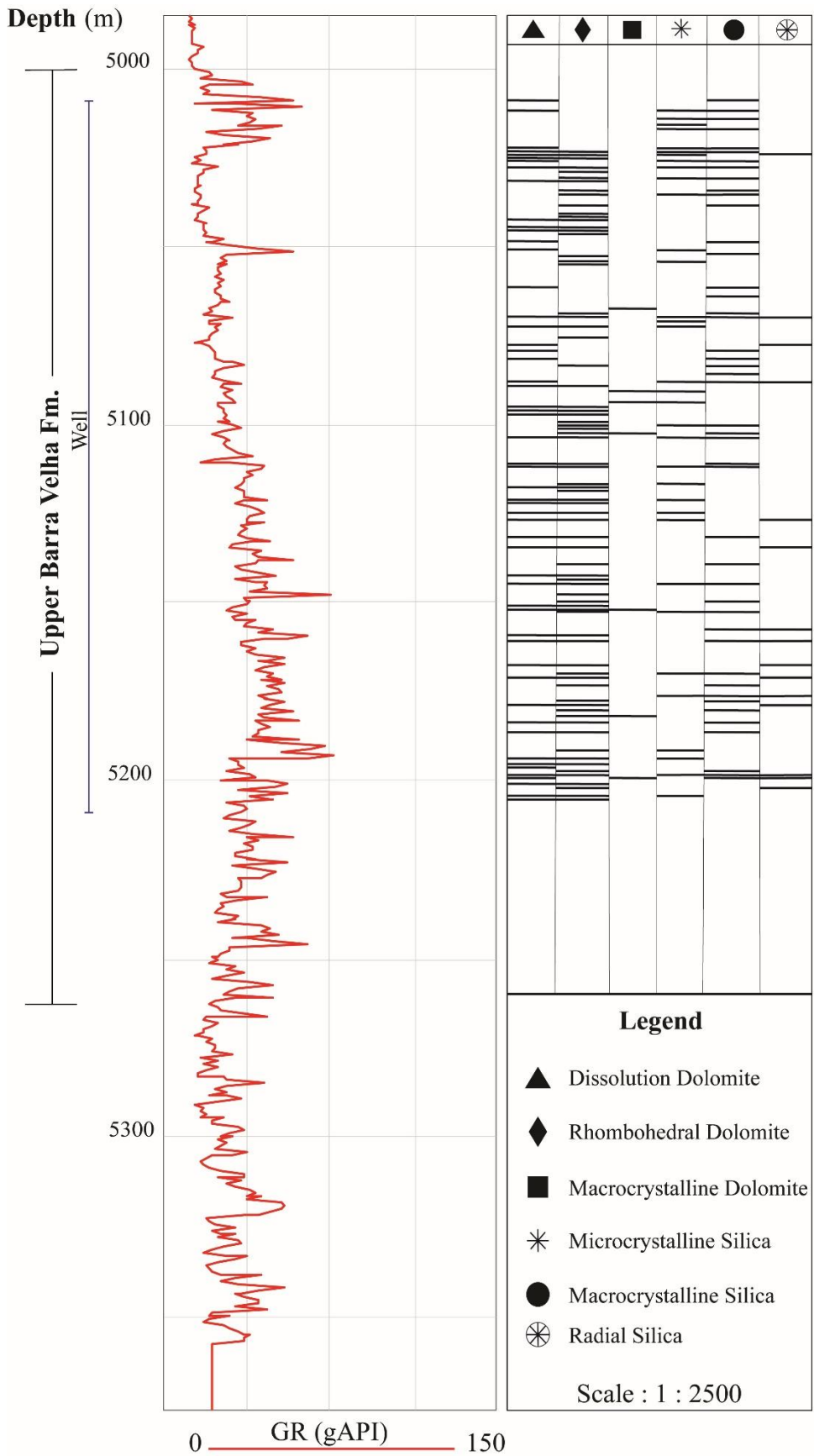
Figure 16. Replacement minerals, result of dolomitization and silicification disposed along the well in contrast with the gamma-ray from the well.

4.4.2.8 Accessory Minerals

The accessory minerals do not exceed 3% of the sample, so they were separated and normalized so that we can quantify them more clearly. Accessory minerals precipitated during a replacement process related to the dissolution of primary minerals.

Apatite ($Ca_5(PO_4)$)) is rare on the well thin sections yet is present on the shallower portion of the well. The highest concentration is located at the mid-point of the superior quarter. The apatite content appears at 5.3% on the surface area of the thin sections. It does not have a straight correlation to other minerals as it is possibly related to the remains of organisms, as shown on some shrubstone samples and a mudstone section (Figure 14C).

Barite ($BaSO_4$) is the most abundant accessory mineral, reaching 8.5% on thin sections. It is regularly distributed along the well, the predominant accessory mineral, as shown on the graph. The mineral replaces the carbonate minerals and rare siliceous phases. It is noticeable that the barite peak is around the mid-point on the superior quarter, below the apatite peak. The mineral fills secondary pores below at greater depths, as observed on thin sections (Figure 14D).

Gypsum ($CaS0_4.2H_2O$) and **anhydrite ($CaSO4$)** rarely occur at the top of the well.

Fluorite (CaF_2) is the least abundant accessory mineral. It fills pores and is precipitated along the vugs around carbonate structures. It is incipient, with less than 6% of the accessory minerals. It is concentrated on shallow levels, especially around the upper mid-depth. Fluorite fills voids, possibly related to halite ($NaCl$) presence at the top of the well. (Figure 14F).

Cryolite (Na_3AlF_6) and **dawsonite ($NaAlCO_3(OH)_2$)** needles occur, filling the pores on thin sections with an acicular habit. The distribution of these Na minerals is predominant at the bottom of the well and has the highest peak at the highest depths. It is highly noticeable in the inferior quarter. It is scarce or absent towards the top of the well. The maximum occurrence along the thin sections reaches up to 6.8% of the section surface map on the thin section (Figure 14D).

Pyrite (FeS_2) is the second most frequent accessory mineral in the samples analyzed. The precipitation of pyrite has cyclicity; it oscillates from the bottom to the top of the well. The maximum concentration abruptly occurs around the third quarter, followed by an absence of the sulfide occurring again in a smaller amount at the middle

of the well, between a large concentration of the mineral at the top part of the third quarter of the well and the uppermost section of the well core. On the thin section, the maximum content is about 2.2% of the section's surface area, often showing as a subhedral opaque mineral under an optic microscope. The sulfide content does not occur in the presence of barite (Figure 14B).

Figure 17. Accesory minerals distribuited along the well.

4.5   Discussion

The field is settled in an elongated horst approximately 30 km long and three km wide, as shown on the seismic section. The last tectonic event affected the sub-salt layers and even the evaporites of the Ariri Formation. However, it is possible that the horst structure was already present before the deposition of the Barra Velha carbonates because faults were repeatedly reactivated.

Considering the rift and sag stages, the Itapema Formation was already sitting above this structural high, where the deposition of sediments from the Lower Barra Velha Formation had started. This structural situation has provided a shallower water lake level on the higher position, a suitable place for crusts and grainstone facies genetation, and a deeper water lake level in the lower position, around the high block, a suitable place for the deposition of the fine-grained facies. Tectonic activity is a significant factor in shaping a lake's geometry and altering its hydrodynamics as mentioned by Rebelo *et al*. (2023)

Wright *et al.* (2022) stressed that seismic geometries are not usually associated with lacustrine carbonate studies. The same authors mention there is no exact recent analogue system that presents large and differentiated platforms, although the existence of lacustrine carbonate build-ups can be associated with coarser-grained facies as *in situ* shrubs surrounded by grainstones within these mound-like features (Wright and Barnett *et al.*, 2017). These features described by the authors are located close to faults and were formed at 400 m depth, often exposed (Barnett *et al.*, 2018). Wright (2022) adds that these features could be stratigraphic, not topographic, so they would appear on seismic sections but developed by sediment stacking.

The most frequent reworked facies on this work are grainstones. The common placement of reworked facies on the structural high region suggests a deposition process associated with shallow water conditions as Barnett *et al.* (2021) explained. The varying degrees of reworking, grain selection, rounding, and changes in grain composition, support the interpretation of an energetic littoral zone influenced by wave activity where wave action removed mud from the coarse-grained facies (Rebelo *et al*., 2023).

As mentioned by Wright and Barnett (2015), Silva and Pereira (2017), Pietzsch (2018) and Almeida (2022), the predominant depositional setting seems to be an alkaline lacustrine environment, where water depths range from deep to shallow, with exposure

of the substrate favoring the development of shrubstone crusts, as a result of alternation from humid to an arid climate. Replacive phases point to arid and more acidic conditions, but fluctuations frequently alter the facies deposition cycles. There is a tendency for shallowing upward trend due to the fluctuation of the lake's chemistry and level.

Owen *et al.* (2018) mention that the run-off, direct precipitation, and groundwater from hot springs are commonly associated with rifting. Mercedes-Martín *et al.* (2019) add that changes in climate, like evaporation and precipitation, affect the balance of the solutes in the water.

The conditions on this vast lake changed rapidly and locally within the basin. Jones and Galan (1988), Tosca and Wright (2016), and Lima and De Ros (2019) mention the factors that control the formation of Mg-rich clays and their dissolution as the alkalinity, pCO_2, and salinity of the system. Chemical pH above 10, low pCO_2, and high concentration of Si and Mg resulted in clay precipitation, as shown in only a few depths according to the XRD data provided by ANP. Less dry periods and the improvement of pCO2 could be a result of hydrothermal activity. Lima *et al.* (2019) mention that they would influence the precipitation of the calcite structures, enhancing the dissolution of the Mg-clay when the pH was below 8. The high cyclicity promoted by local chemical changes in the water, expressed by the replacement of clay by dolomite, follows the base formula:

$Mg_3Si_4O_{10}$ (stevensite) $+ 2.8Ca^{+2} + 7.6CO_2 + 15.6H_2O \rightarrow 2.9CaMg (CO_3)_2$ (dolomite) $+ 4H_4SiO_4 + 5.6H^+$
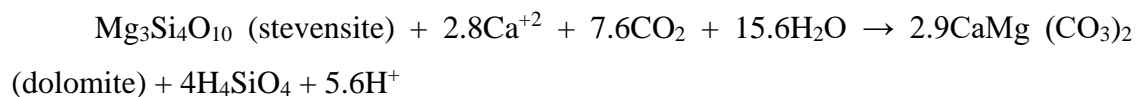
The concentration of hydrogen ions drops the initial pH of the lake.

The depositional facies are divided into two groups regarding the chemical background above.

The reworked facies comprise most of the rocks described on the well. The most abundant is the intraclast facies of grainstone, less than a quarter of the samples are composed of packstone and wackestone. The *in situ* facies most described are shrubstones and spherulitestones. Almost no evidence of terrigenous remains on facies from the Upper Barra Velha Formation, as observed on the well from the Sapinhoá Field. Clay minerals were rarely observed on the thin section except for illite agglomerates.

Diagenesis significantly impacted the BVF facies and camouflaged the original constituents after post-depositional processes in different intensities. Dissolution is recurrent in the samples described. On the other hand, compaction features are scarce on

the well. Moreover, recrystallization, cementation, dolomitization and silicification were intense and modified the characteristics of the original facies, generating different interactions with porosity.

The transition from muddy facies to spherulitstones occurred gradually as spherulites precipitated and developed within the matrix during early diagenesis (Lima and De Ros, 2019; Rebelo *et al*, 2023.

Lima *et al.* (2019) relate the following structures that formed during eodiagenetic processes: spherulites, framboidal pyrite, replacive dolomite and magnesite, and stevensite dissolution. The authors mention the original calcite component of the shrub and spherulite structures being replaced by dolomite and silica. Later, these features were affected by physical compaction. The evidence of dissolution follows these processes as early burial stage in the mesodiagenetic phase. On the other hand, De Carvalho *et al.* (2021) suggest weathering as the first effective shallow burial process, followed by dissolution and matrix precipitation, physical compaction and dolomitization. The dedolomitization process happened at the end of the eodiagenesis to mesodiagenesis stage.

Girard *et al.* (2017) state that it is well established that rift systems can be the locus of elevated geothermal gradients, leading to high temperatures in shallow burial depths. The author adds that volcanic activity is common in these systems and may induce hydrothermalism.

Lima *et al.* (2019) mention the precipitation of hydrothermal phases like saddle dolomite, calcite, zeolite, Sr-barite, celestine, pyrite, chalcopyrite, galena, sphalerite and bitumen filling the framework and fractures, and replacing pre-existing constituents. Within the samples studied, possible hydrothermal phases and paragenetic assembly were described on optical microscopy, mapped, and quantified on QEMSCAN as cement filling secondary pores, and replacing pre-existing components. The distribution of these phases on the Barra Velha carbonate rocks considers pyrite, barite, fluorite and dawsonite. The mineral assemblage points to low-temperature hydrothermal alteration products, as Deer *et al.* (1997) supported, as the hydrothermal mineral suite is present on the studied well but not so expressive compared to the wells described by the authors. Hydrothermalism in the Santos Basin is associated with igneous intrusions, which are not homogeneously distributed laterally or vertically on the basin, rather than in other fields where hydrothermalism was more intensely present than in Field 1.

Coveney (1971) mentions sodium brines as a suggestive environment to precipitate dawsonite and questions it as a daughter mineral attributed to hydrothermal activity. Zhao (2018) concludes that elevated CO_2 concentrations in magmatic-induced flux were favorable for dawsonite cementation.

Hydrothermal alterations' influence is interpreted as a localized process affecting the carbonate facies. The origin of the mineralogy mentioned above could result from burial diagenesis, as Almeida *et al.* (2022) mentioned.

Machel *et al.* (2002) mention that not all saddle dolomite has a hydrothermal origin. Dolomite can precipitate in different diagenetic environments ranging from the surface of the burial depth. The shallow-marine environments with regular seawater salinity that registered fossil and ripple marks present saddle dolomite that has survived the replacement process.

Although dolomite rhombs were described and saddle dolomite are often used as a guide-mineral to hydrothermalism by authors as Lima *et al.* (2019), the term "saddle" was not adopted in the present work. In addition, other mineral phases were interpreted as direct evidence of a possible hydrothermal alteration of the clay and carbonates related to the presence of dawsonite (carbonate), cryolite (aluminofluoride), sulfide as pyrite, sulfate as barite, and fluorite.

Among the sulfides and the sulfates related to vents, barite is an unique phase because it requires an specific ration between the hydrothermal fluid and the surrounding water to precipitate. Due to the sulfate low solubility, barite preserves the conditions during the precipitations and can be used as an indicator of former conditions (Jamieson *et al.*, 2016).

Hydrothermal fluids were possibly responsible for the dissolution of the original minerals and the cause of the enlargement pores, creating larger openings and vugs in the facies (Figure 11A). The dissolution of components during the process led to silica precipitation as macrocrystalline quartz.

The organic-shaped apatite particles delineated on the QEMSCAN image can corroborate the seawater incursion related to an alternative explanation of the presence of saddle dolomite in carbonate facies.

Trombetta and De Ros (2023) mention that saddle dolomite precipitates at similar temperatures to the oil window (60 to 150 ºC) and confirm that it is not necessarily evidence of hydrothermalism, because it may be associated with burial/mesodiagetic

precipitation from supersaturated solutions.

Diagenesis and hydrothermalism processes generally produce secondary porosities and reduce permeability as cementing obstructs the pores. Therefore, it is not a limiting factor. It is noticeable from the permeability plot that the reservoir quality is controlled essentially by the original sedimentary facies, especially when the framework is built up from coarser material as shrubs in shrubstones and fragments in grainstones.

4.6   Conclusion

The integrated analysis of the mineralogy composition of the sedimentary facies and diagenetic features of the BVF from the study field from the Santos Basin contributes to understanding the depositional settings of primary constituents and the post-depositional processes that affected them.

- Samples of coarse-grained rocks showed a direct relation with better reservoir quality. *In situ* and reworked facies are distributed similarly along the well. The most frequent facies are shrubstones and grainstones, which are considered excellent-quality reservoirs;

- The Upper Barra Velha Formation's recurrent lithological variation indicates frequent climate and water conditions changes;

- Mg-clays are almost absent and rarely preserved, which may indicate diagenetic alterations affected the Upper Barra Velha carbonates, replacing them with dolomite, silica, and secondary components;

- Dolomitization and silicification are the most relevant diagenetic processes in the BVF, replacing Mg-clays and modifying porosity;

- The ratio of silica and dolomite is possibly in evidence in the gamma-ray well logs and seismic section, showing a break in the reflectors;;

- Dissolution is associated with diagenesis and fluid percolation and it is an essential process for secondary porosity generation, enlarging primary porosity;

- Dissolution and replacement are the most relevant recurrent processes throughout the well, alternating between them, opening and obstructing pores;

- Precipitation of rhombohedral dolomite, dawsonite, cryolite, barite and fluorite are possible products of hydrothermal alteration, suggesting a subtle effect of hydrothermal pulses into the BVF carbonates;

- Although diagenesis and hydrothermalism affect the permeability of the original facies, permeability is controlled by the facies.

Acknowledgements

4.7 References

Almeida, C.A.M. *et al.* (2022). Facies and diagenesis distribution in an Aptian pre-salt carbonate reservoir of the Santos Basin, offshore Brazil: A comprehensive quantitative approach. Marine and Petroleum Geology, p. 105708.

ANP. Boletim da Produção de Petróleo e Gás Natural, Junho, 2021. http:// https://www.gov.br/anp/pt-br/centrais-de-conteudo/publicacoes/boletins-anp/boletim-mensal-da-producao-de-petroleo-e-gas-natural. Access: August 2021.

Barnett, A. J. *et al.* (2018). Origin and significance of thick carbonate grainstone packages in nonmarine successions: A case study from the Barra Velha formation, Santos Basin, Brazil. Adapted from poster presentation given in 2018. AAPG Annual Convention & Exhibition.

Carminatti, M., Dias, J.; Wolff, B. (2009). From turbidites to carbonates: breaking paradigms in deep waters. In: Offshore Technology Conference. OnePetro.

Chang, H. K. *et al.* (1992). Tectonics and stratigraphy of the East Brazil Rift system: an overview. Tectonophysics, v. 213, n. 1-2, p. 97-138.

Chaboureau, A. *et al.* (2013). Paleogeographic evolution of the central segment of

the South Atlantic during Early Cretaceous times: Paleotopographic and geodynamic implications. Tectonophysics, v. 604, p. 191-223.

Chafetz, H. S. (2013). Porosity in bacterially induced carbonates: Focus on micropores. AAPG Bulletin, [s. l.], v. 97, n. 11.

Coveney, R. M.; Kelly, W. C. (1971). Dawsonite as a daughter mineral in hydrothermal fluid inclusions. Contributions to Mineralogy and Petrology, v. 32, p. 334-342.

Davies, G. R.; Smith, L. B. (2006). Structurally controlled hydrothermal dolomite reservoir facies: An overview. AAPG bulletin, v. 90, n. 11, p. 1641-1690.

Da Silva, S.F.C.R.; Pereira, E. (2017). Tectono-stratigraphic evolution of Lapa field pre-salt section, Santos Basin (SE Brazilian continental margin). Journal of Sedimentary Environments, v. 2, n. 2, p. 133-148.

De Carvalho, M.D.; Fernandes, F.L. (2021) Chapter 5: Pre-Salt Depositional System: Sedimentology, Diagenesis, and Reservoir Quality of the Barra Velha Formation, as a Result of the Santos Basin Tectono-Stratigraphic Development. In: memoir 124: The supergiant lower Cretaceous pre-salt petroleum systems of the Santos Basin, Brazil. [S. l.]: AAPG. p. 121–154.

Deer, William A.; Howie, Robert A.; Zussman, J., ed. (1997) Rock-forming minerals: single-chain silicates, Volume 2.

Folk, R. L. (1959). Practical petrographic classification of limestones. AAPG bulletin, v. 43, n. 1, p. 1-38.

Folk, R. L. (1962). Spectral subdivision of limestone types.

Girard, J.; Miguel, San Miguel, G. (2017). Evidence of high temperature hydrothermal regimes in the pre-salt series, Kwanza Basin, offshore Angola. In: AAPG Annual Convention and Exhibition.

Gomes, P. O. *et al.* (2009). The outer high of the Santos Basin, Southern São Paulo Plateau, Brazil: pre-salt exploration outbreak, paleogeographic setting, and evolution of the syn-rift structures. In: AAPG International Conference and Exhibition. p. 15-18.

Gomes, P. O. *et al.* (2012). Tectonic evolution of the outer high of Santos Basin, Southern São Paulo Plateau, Brazil, and implications for hydrocarbon exploration.

Gomes, J. P. *et al.* (2020). Facies classification and patterns of lacustrine carbonate deposition of the Barra Velha Formation, Santos Basin, Brazilian Pre-salt. Marine and Petroleum Geology, v. 113, p. 104176.

Herlinger J. R. Ronaldo; Zambonato, E. E.; De Ros, L. F. (2017). Influence of diagenesis on the quality of Lower Cretaceous pre-salt lacustrine carbonate reservoirs from northern Campos Basin, offshore Brazil. Journal of Sedimentary Research, v. 87, n. 12, p. 1285-1313.

Jones, B. F.; Galan, E.; Bailey, S. W. (1988). Hydrous phyllosilicates (exclusive of micas). Sepiolite and Palygorskite, Reviews in Mineralogy, v. 19, p. 631-674.

Karner, G. D.; Gambôa, L. A. P. (2007). Timing and origin of the South Atlantic pre-salt sag basins and their capping evaporites. Geological Society, London, Special Publications, v. 285, n. 1, p. 15-35.

Leite, C.O.N.; Silva, C.M.A.; De Ros, L.F. (2020). Depositional and diagenetic processes in the pre-salt rift section of a Santos Basin area, SE Brazil. Journal of Sedimentary Research, v. 90, n. 6, p. 584-608.

Lima, B.E.M.; De Ros, L.F. (2019). Deposition, diagenetic and hydrothermal processes in the Aptian Pre-Salt lacustrine carbonate reservoirs of the northern Campos Basin, offshore Brazil. Sedimentary Geology, v. 383, p. 55-81.

Machel, Hans G.; Lonnee, Jeff. (2002). Hydrothermal dolomite—A product of poor definition and imagination. Sedimentary geology, v. 152, n. 3-4, p. 163-171.

Mercedes-Martín, Ramon *et al.* (2016). Growing spherulitic calcite grains in saline, hyperalkaline lakes: experimental evaluation of the effects of Mg-clays and organic acids. Sedimentary Geology, v. 335, p. 93-102.

Mercedes-Martín, Ramon *et al.* (2019). The hydrochemical evolution of alkaline volcanic lakes: a model to understand the South Atlantic Pre-salt mineral assemblages. Earth-Science Reviews, v. 198, p. 102938.

Milani, E. J. *et al.* (2007). Bacias sedimentares brasileiras: cartas estratigráficas. Boletim de Geociencias da Petrobras, v. 15, n. 2, p. 183-205.

Mohriak, W.; Nemčok, M.; Enciso, G. (2008). South Atlantic divergent margin evolution: rift-border uplift and salt tectonics in the basins of SE Brazil. Geological Society, London, Special Publications, v. 294, n. 1, p. 365-398.

Mohriak, W. U.; Szatmari, P.; Anjos, S. (2012). Salt: geology and tectonics of selected Brazilian basins in their global context. Geological Society, London, Special Publications, v. 363, n. 1, p. 131-158.

Moreira, J. L. P., Madeira, C. V., Gil, J.A. Machado, M. A. P. (2007). Bacia de Santos. Boletim de Geociencias da Petrobras, v. 15, n. 2, p. 531-549.

Owen, R. B.; Renaut, R. W.; Lowenstein, T. K., (2018). Spatial and temporal geochemical variability in lacustrine sedimentation in the East African Rift System: Evidence from the Kenya Rift and regional analyses. Sedimentology, v. 65, n. 5, p. 1697-1730.

Pietzsch, R., Tedeschi, L. R., Neto, J. V. Q., Figueiredo, M. F., Vasquez, J. C., Souza, R, S., (2018). Palaeohydrology of the Lower Cretaceous pre-salt lacustrine system, from rift to post-rift phase, Santos Basin, Brazil. Palaeogeography, Palaeoclimatology, Palaeoecology, v. 507, p. 60-80.

Rebelo, T. B., Batezelli, A., Mattos, N. H., & Leite, E. P. (2023). Sedimentary processes and paleoenvironment reconstruction of the Barra Velha formation, Santos Basin, Brazilian pre-salt. Marine and Petroleum Geology, 150, 106141.

Rider, M.H. (1996). The Geological Interpretation of Well Logs. Gulf Publishing Company. Well logging. p.280.

Rigoti, Caesar Augusto. Evolução tectônica da Bacia de Santos com ênfase na geometria crustal: Interpretação integrada de dados de sísmica de reflexão e refração, gravimetria e magnetometria. 2015. 135 f. Dissertação (Mestrado em Análise de Bacias;Tectônia, Petrologia e Recursos Minerais) - Universidade do Estado do Rio de Janeiro, Rio de Janeiro, 2015.

Szatmari, Peter *et al.* (1987). Evolução tectônica damargem equatorial brasileira. Revista brasileira de Geociências, v. 17, n. 2, p. 180-188.

Terra, G. J. S. *et al.* (2010). Classificação de rochas carbonáticas aplicável às bacias sedimentares brasileiras. Boletim de Geociências da Petrobras, v. 18, n. 1, p. 9-29.

Tosca, N. J. 2015. Geochemical pathways to Mg-clay formation. In: Pozo, M. & Gala´n, E. (eds) Magnesian Clays: Characterization, Origins and Applications. AIPEA (Association Internationale pour l'Etude des Argiles), Special Publications, 2, 283–329.

Tosca, N. J.; Wright, V. P. (2016). Diagenetic pathways linked to labile Mg-clays in lacustrine carbonate reservoirs: a model for the origin of secondary porosity in the Cretaceous pre-salt Barra Velha Formation, offshore Brazil. Geological Society, London, Special Publications, v. 435, n. 1, p. 33-46.

Trombetta, M. C.; De Ros, L. F. (2023). Depositional and diagenetic conditions during early South Atlantic opening: Evidence from the upper aptian Oiteirinhos Member, Muribeca Formation, Sergipe-Alagoas Basin, NE Brazil. Journal of South

American Earth Sciences, p. 104366.

Tucker, M. E.; Dias-Brito, D. (2017)Petrologia sedimentar carbonática: iniciação com base no registro geológico do Brasil. Rio Claro: UNESP–IGCE-UNESPetro, Obra, v. 3, p. p208.

Unternehr, P., Péron-Pinvidic, G. Manatschal, G. and Sutra, E. (2010). Hyper-extended crust in the South Atlantic: in search of a model. Petroleum Geoscience.

Wright, V. P. (2012). Lacustrine carbonates in rift settings: the interaction of volcanic and microbial processes on carbonate deposition. In: Garland, J., Neilson, J. E., Laubach, S. E. & Whidden, K. J. (eds) Advances in Carbonate Exploration and Reservoir Analysis. Geological Society, London, Special Publications, 370, 39–47

Wright, V. P.; Barnett, A. J. (2014) Cyclicity and carbonate-silicate gel interactions in Cretaceous alkaline lakes. AAPG Annu. Conv. Ehibition, v. 51011, p. 18.

Wright, V. P.; Barnett, A. J. (2015). An abiotic model for the development of textures in some South Atlantic early Cretaceous lacustrine carbonates. Geological Society, London, Special Publications, v. 418, n. 1, p. 209-219.

Wright, V. P.; Barnett, A. J. (2017). Critically evaluating the current depositional models for the pre-salt Barra Velha Formation, offshore Brazil. AAPG Search and Discovery, Article, v. 51439.

Wright, V. P. (2022). The mantle, CO2 and the giant Aptian chemogenic lacustrine carbonate factory of the South Atlantic: Some carbonates are made, not born. Sedimentology, v. 69, n. 1, p. 47-73.

Zhao, S., Liu, L.; Liu, N. (2018). Petrographic and stable isotopic evidence of CO_2-induced alterations in sandstones in the Lishui sag, East China Sea Basin, China. Applied Geochemistry, v. 90, p. 115-128.

CAPÍTULO 5
APPENDIX

5   APPENDIX

Mosaics built from photomicrographs in parallel (left) and crossed (right) polarizers. The top image shows stylolite crossing the section. The lower image presents a shrub that has developed from spherulite elements.
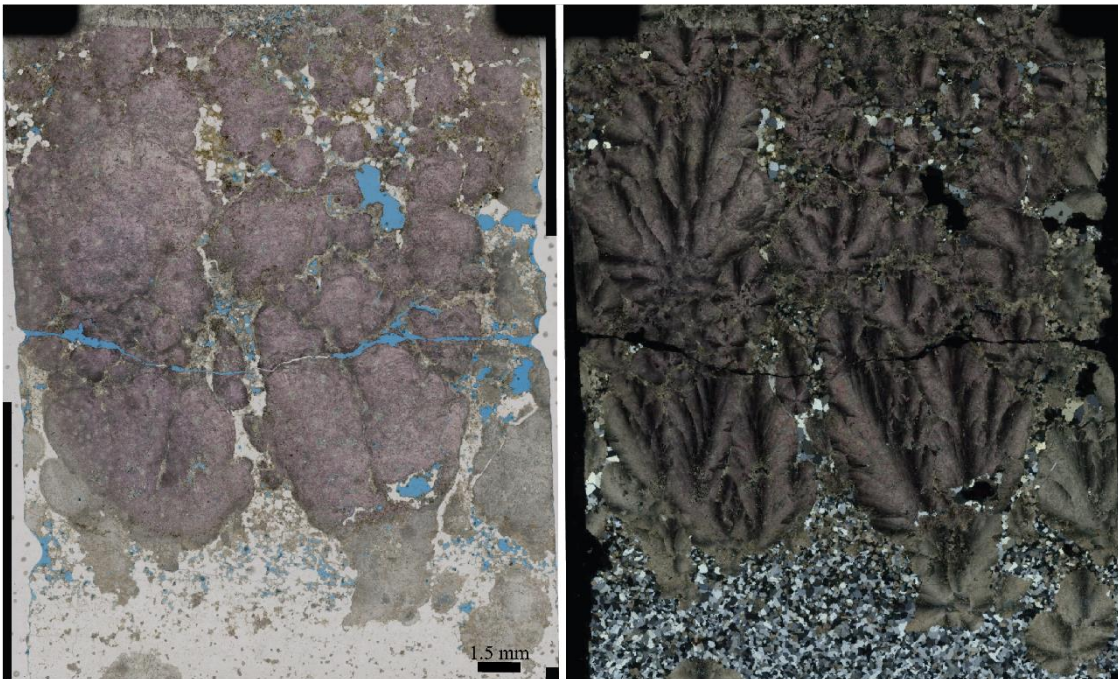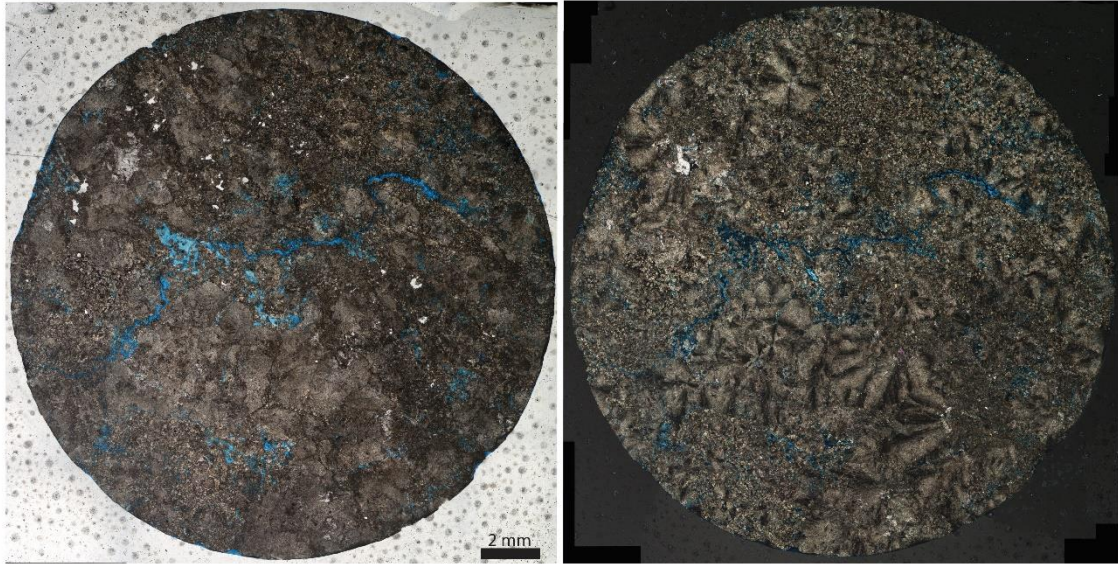
Few modal mineralogical maps show texture and mineral phases along the well. The samples presented below were used to quantify the graphs presented above. The phase maps are arranged from the top to the bottom of the well core. Each image represents 4cm² of a thin section mapped by QEMSCAN according to the following facies list.
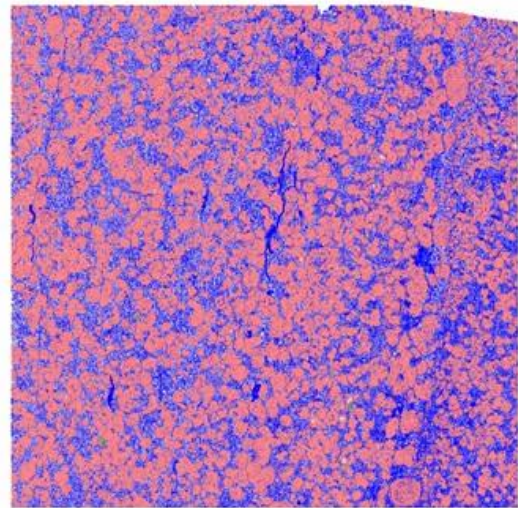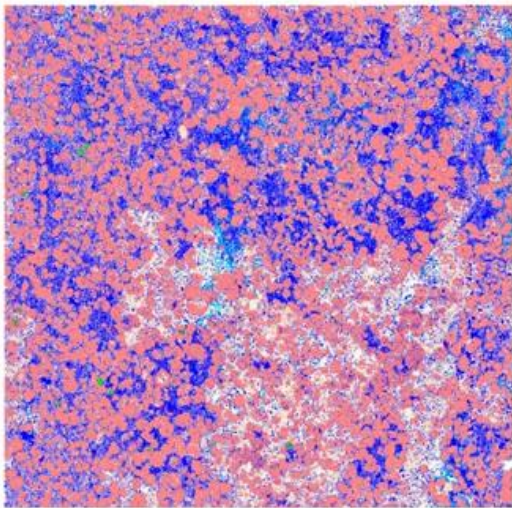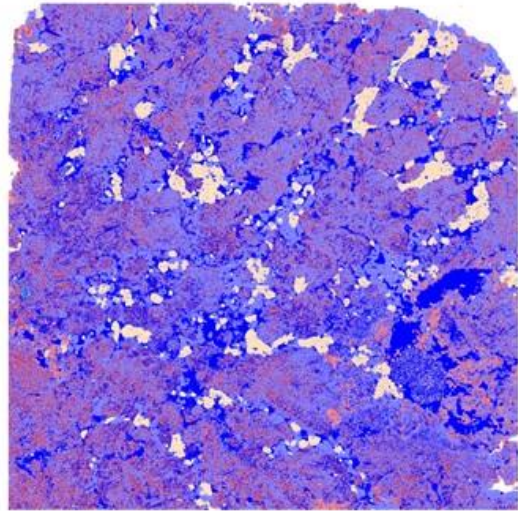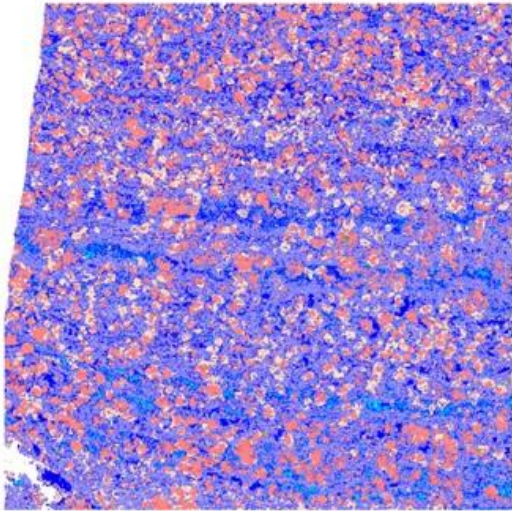
Legend to the QEMSCAN images:
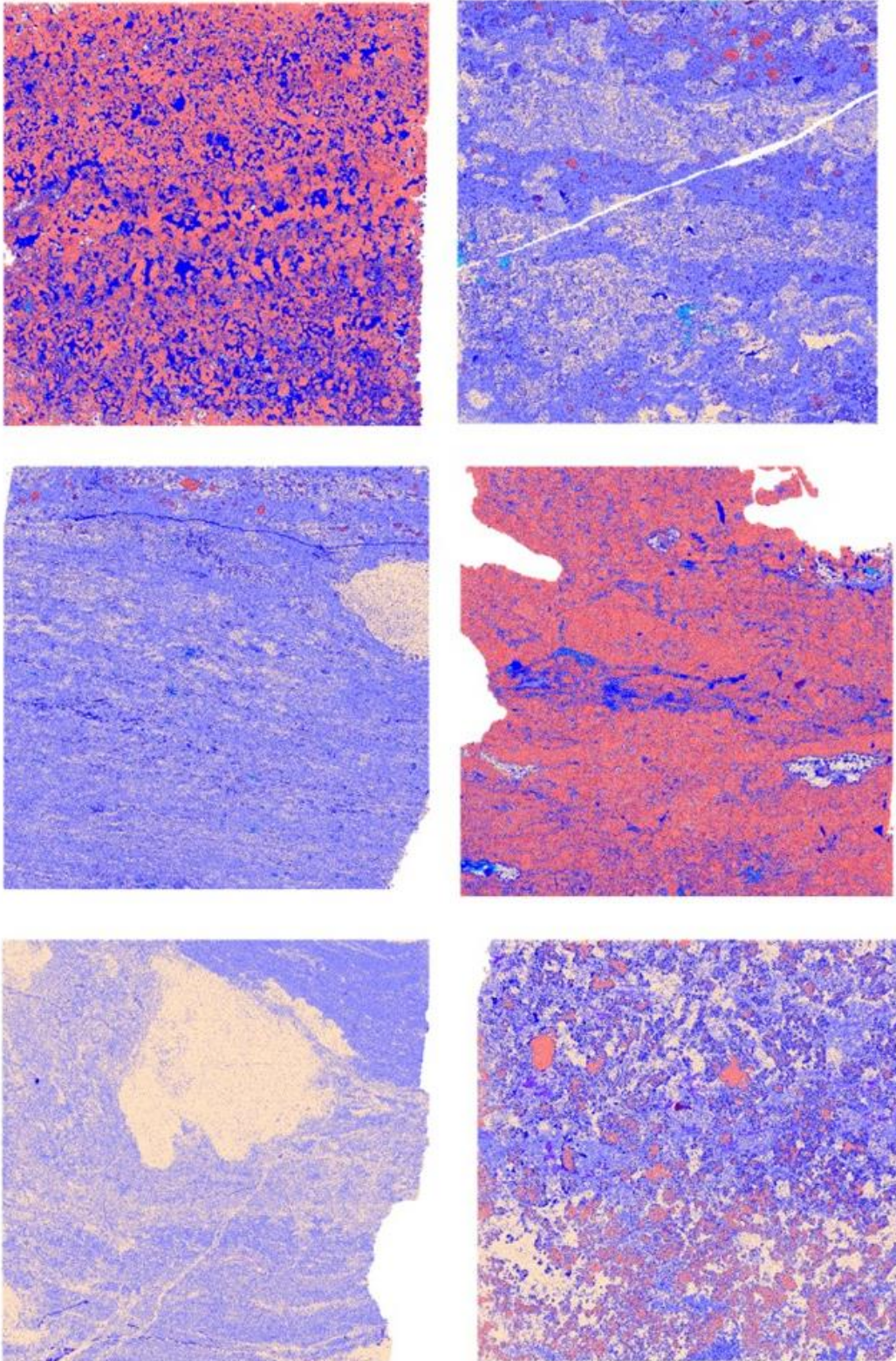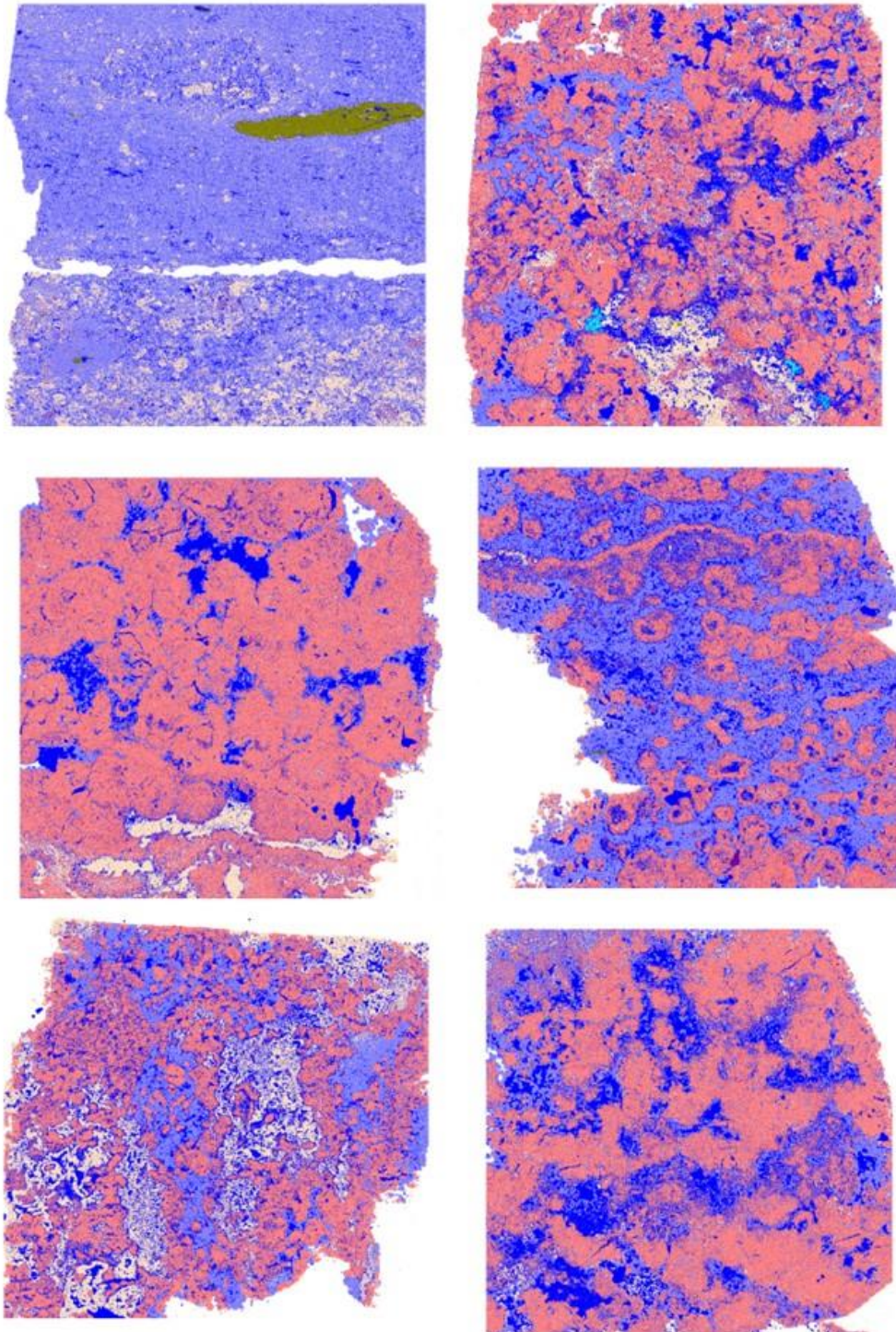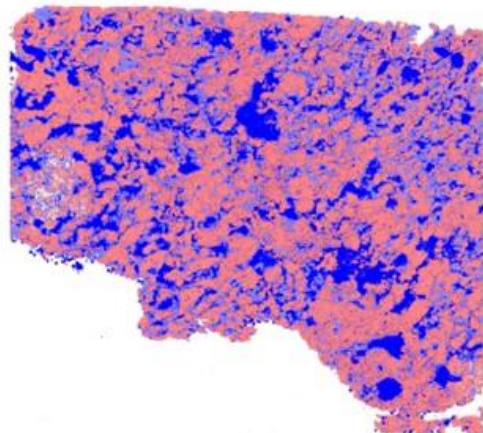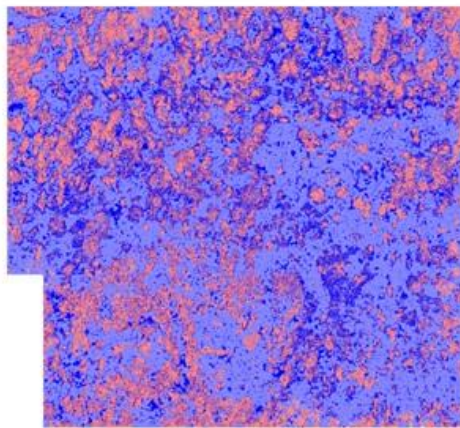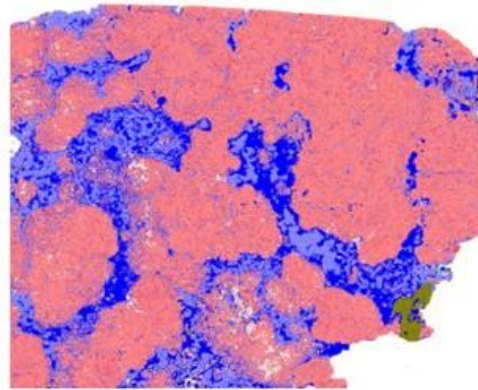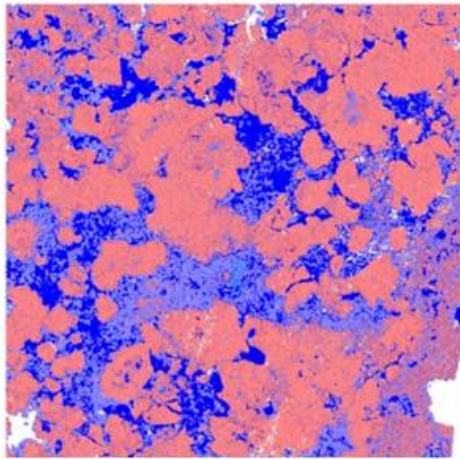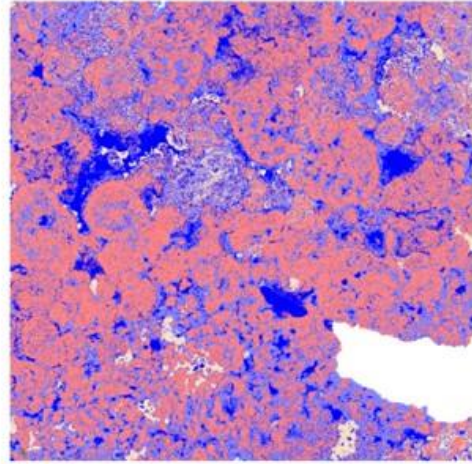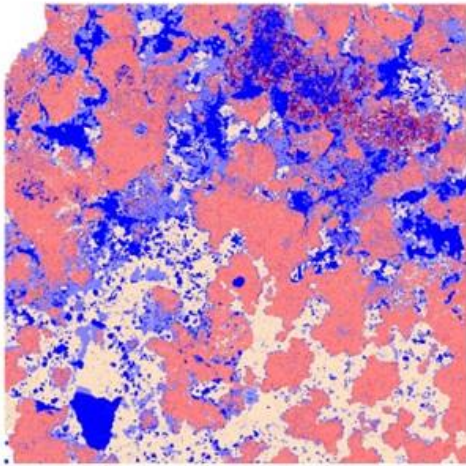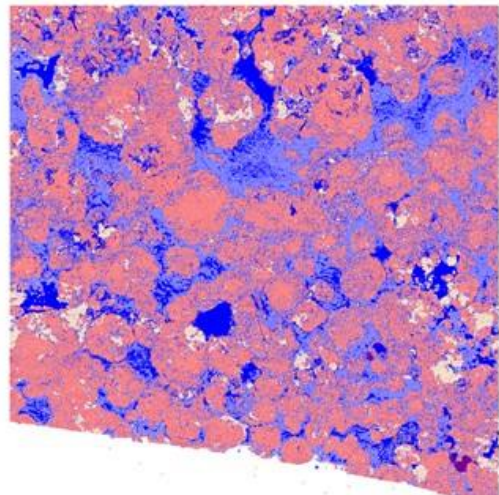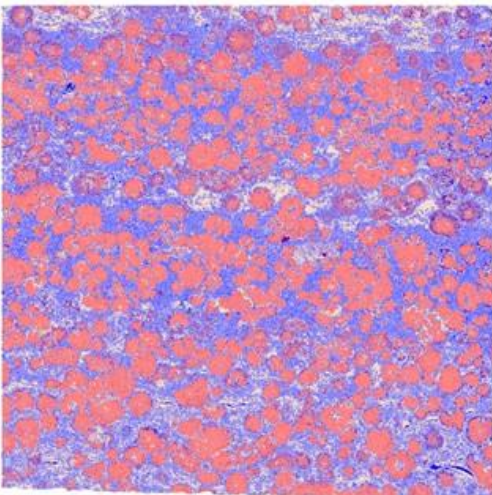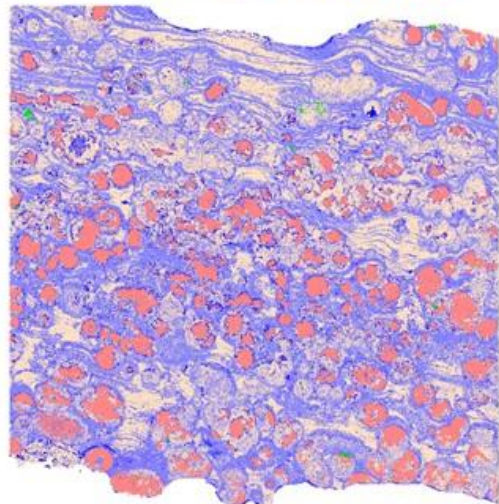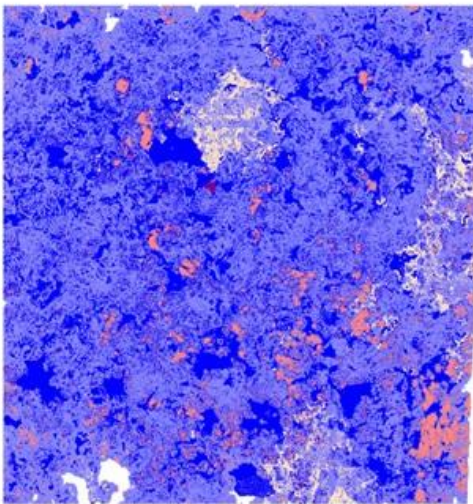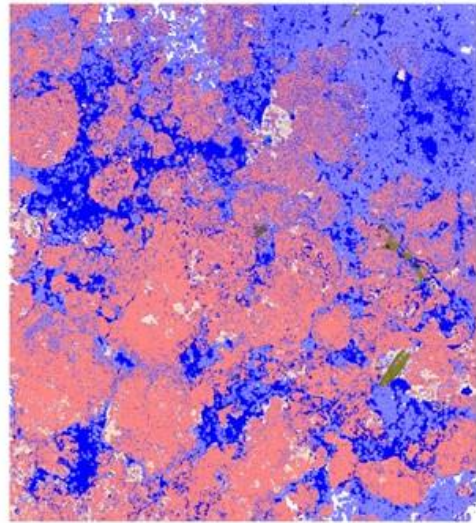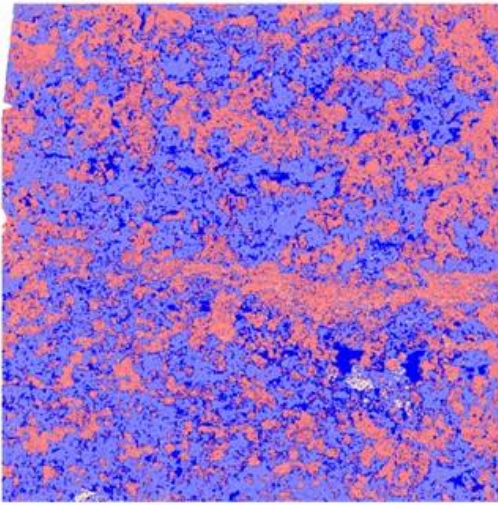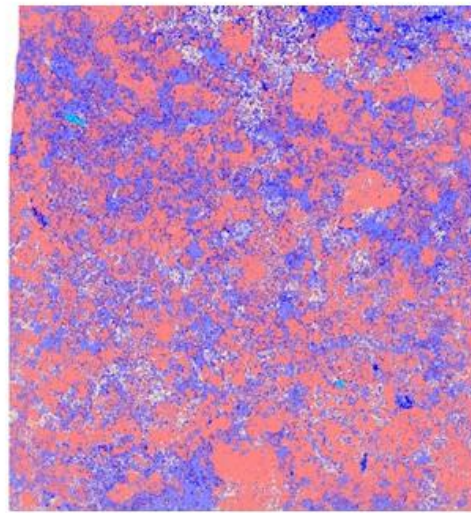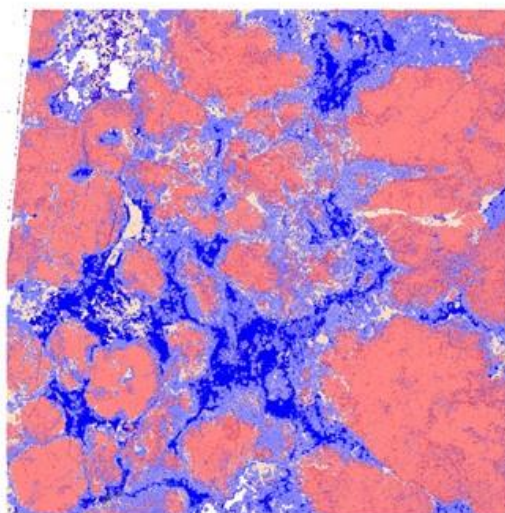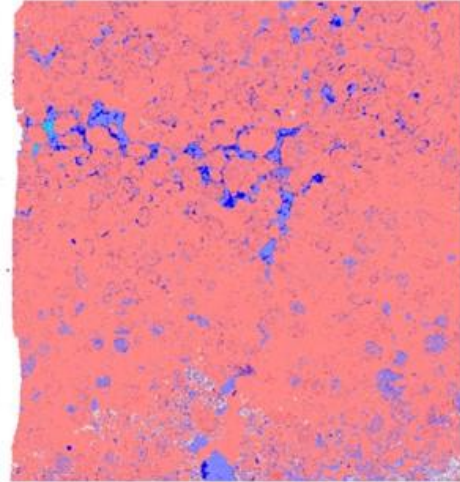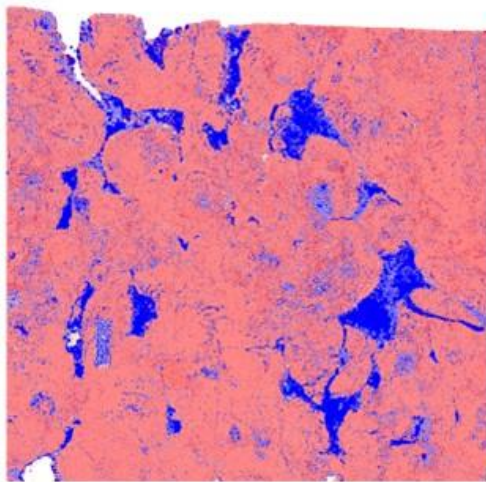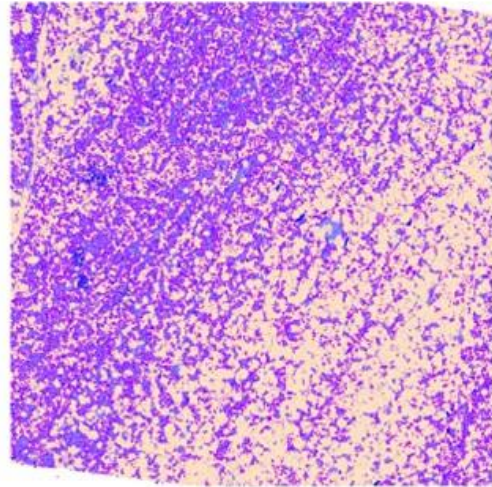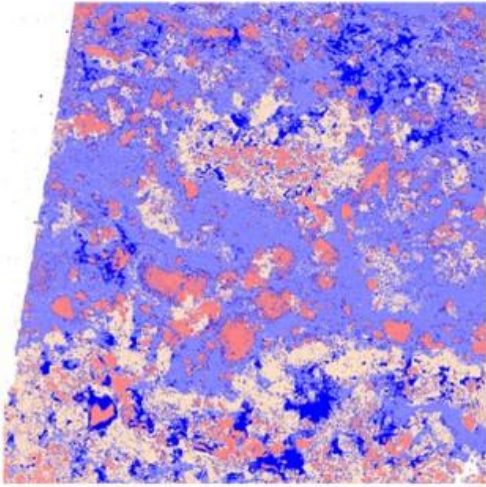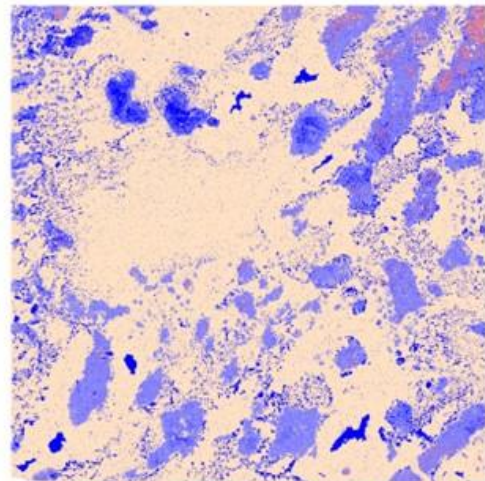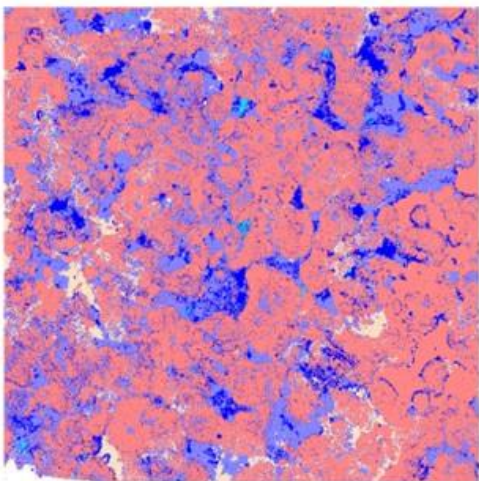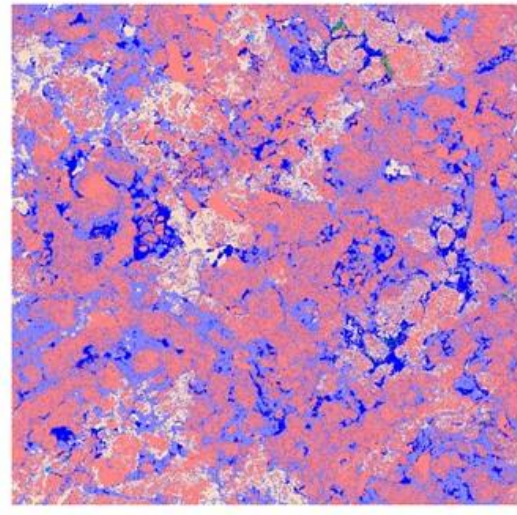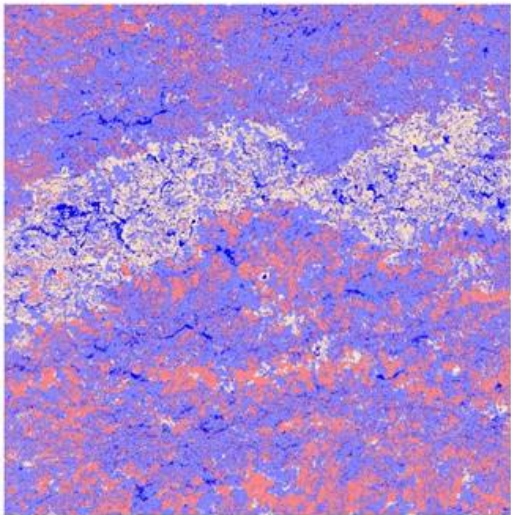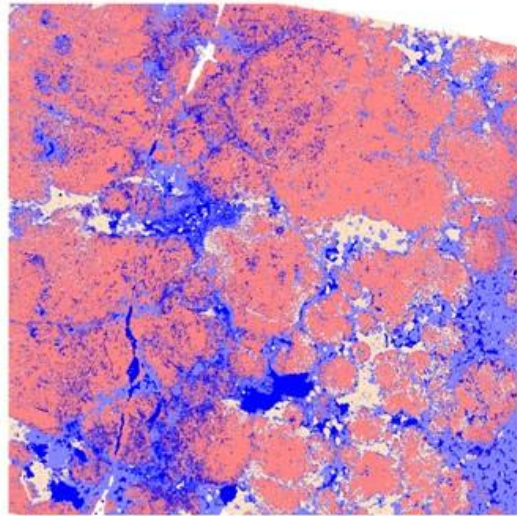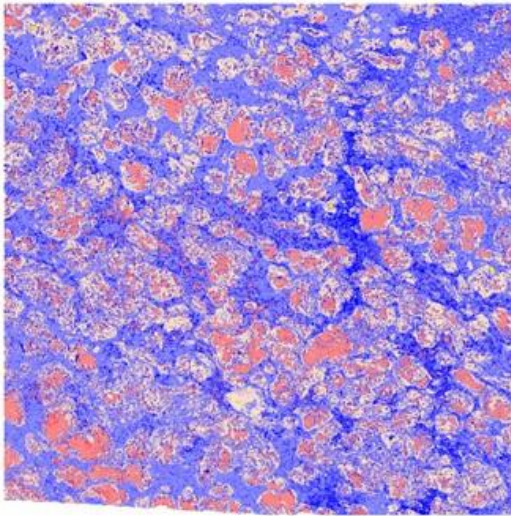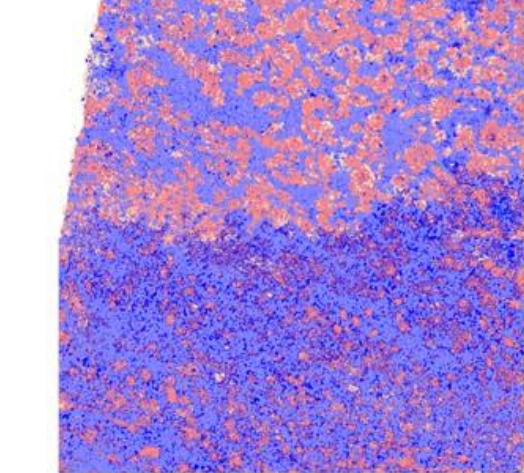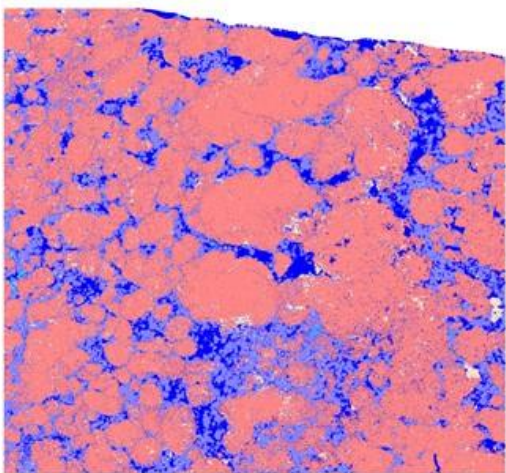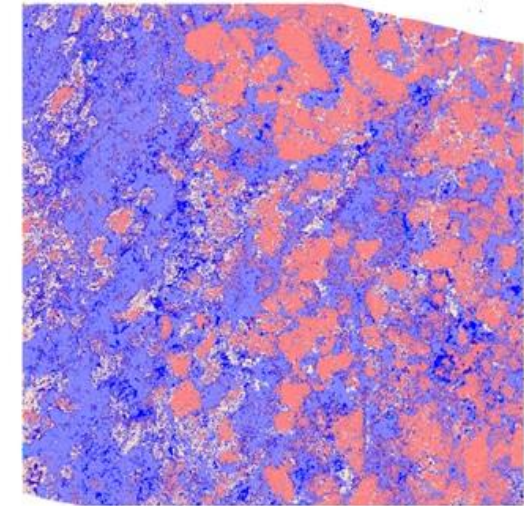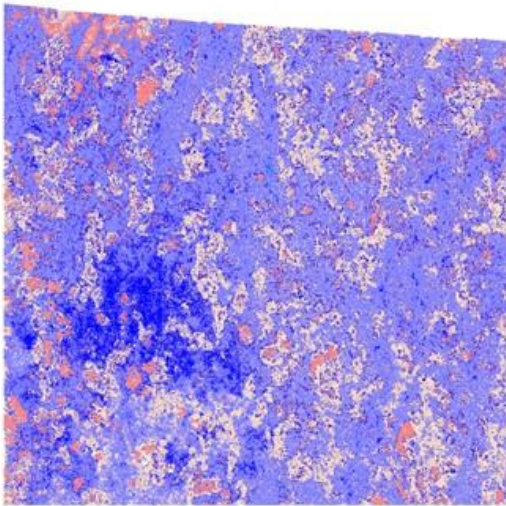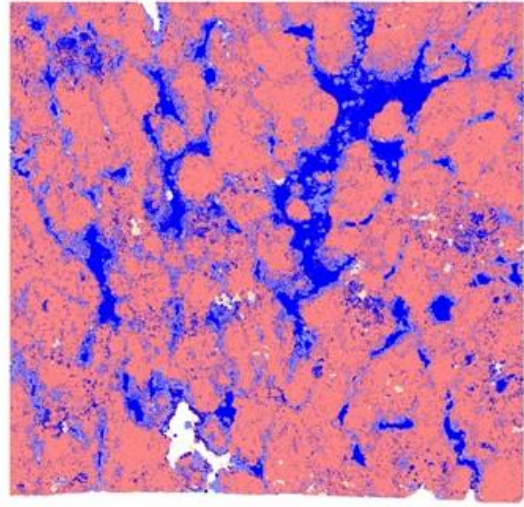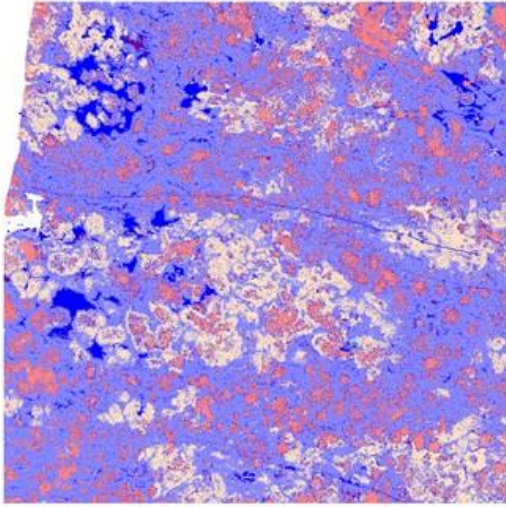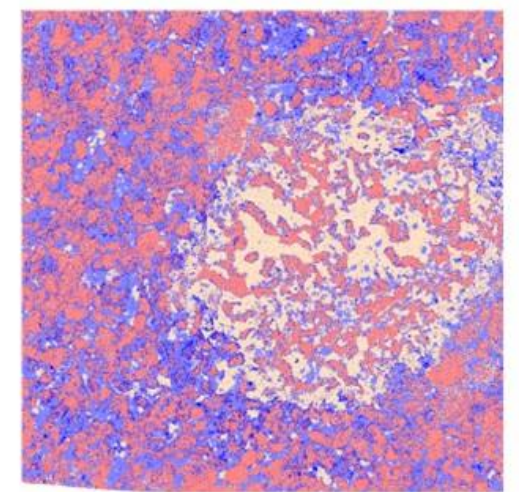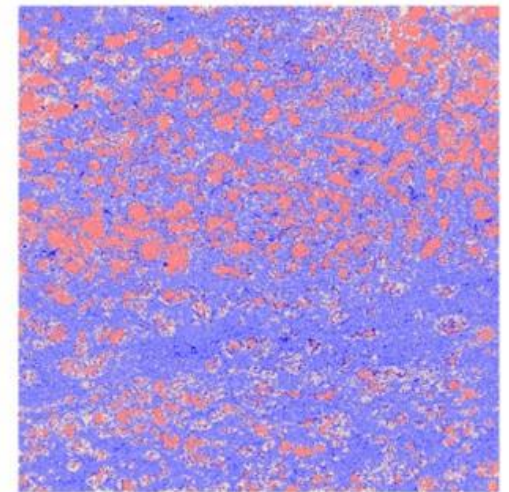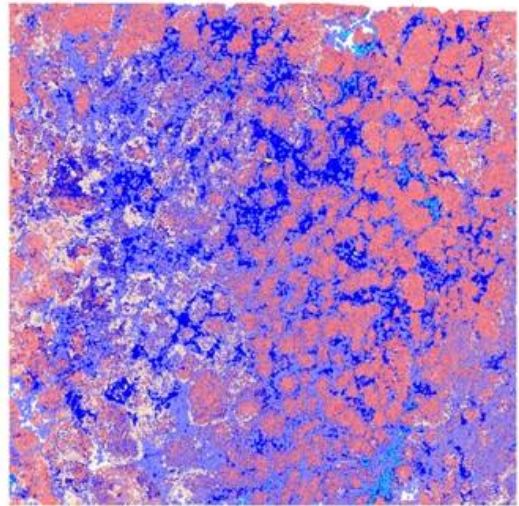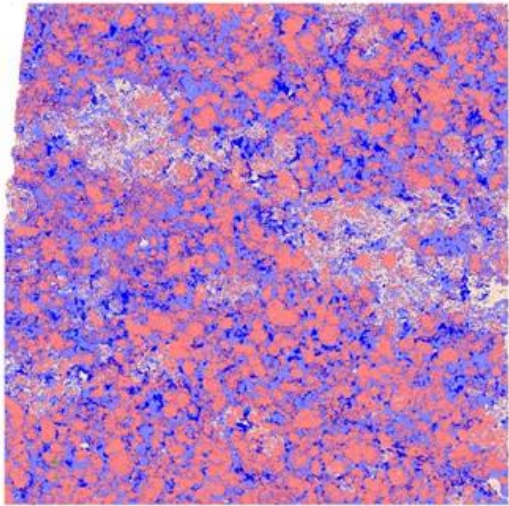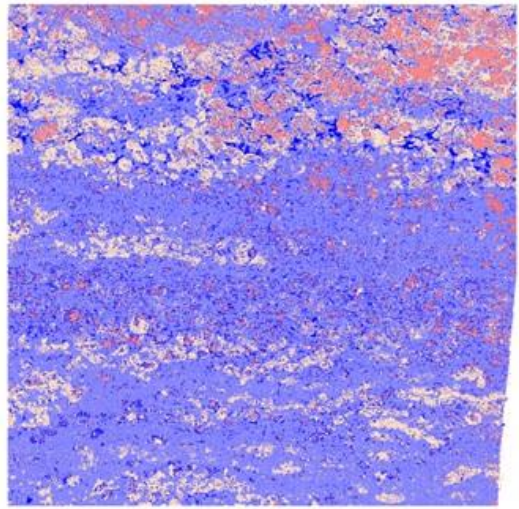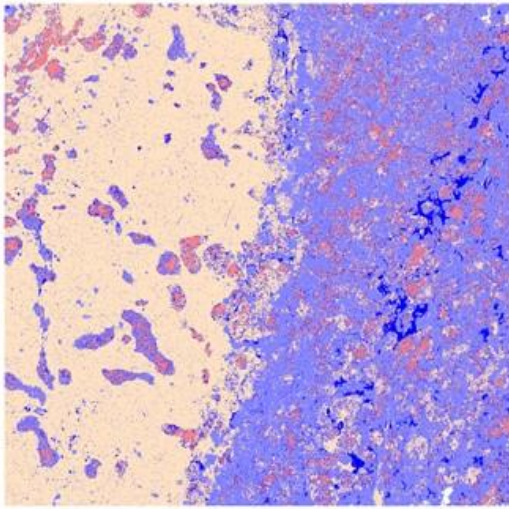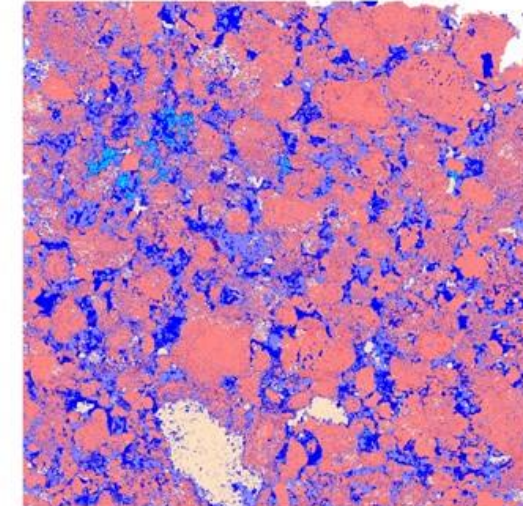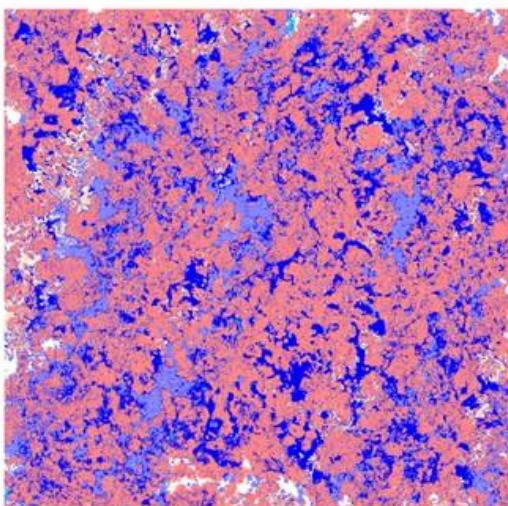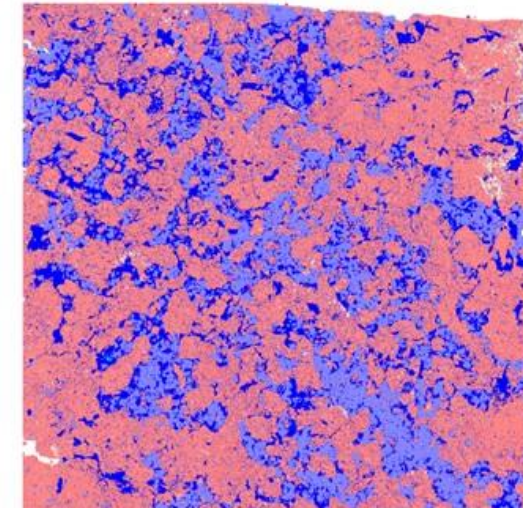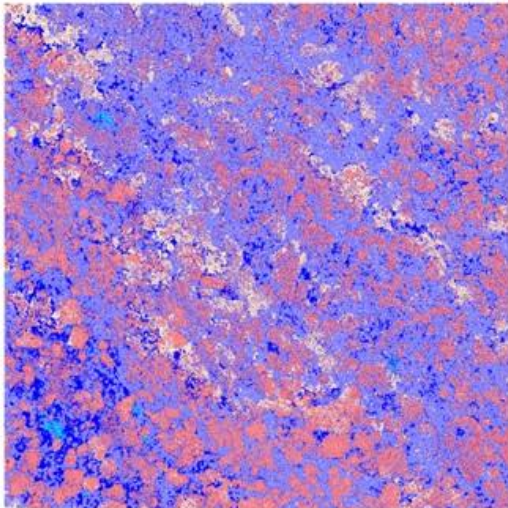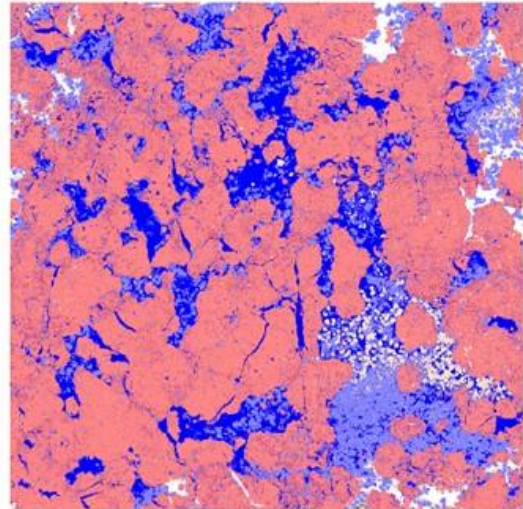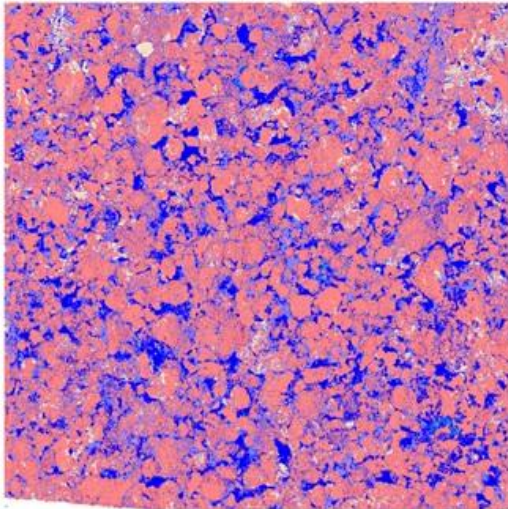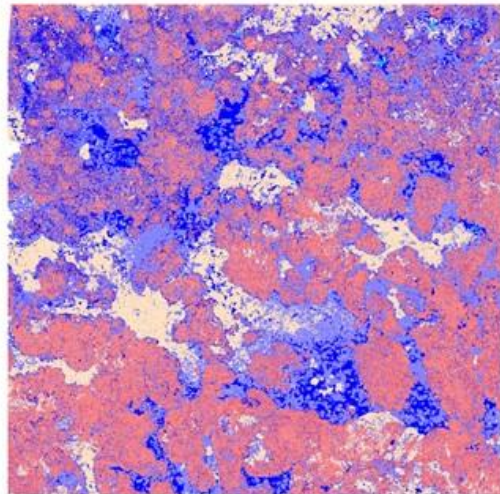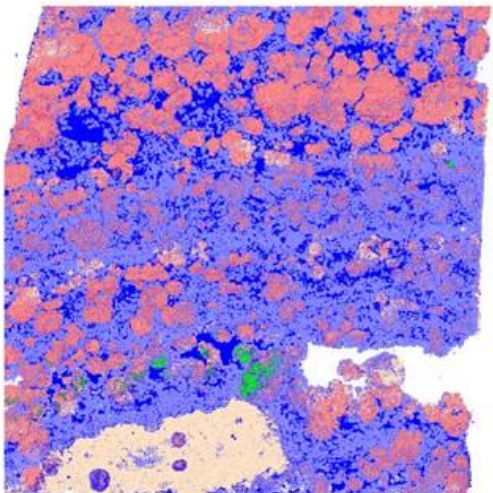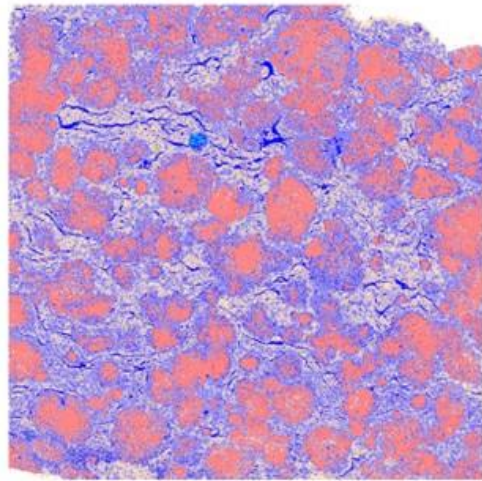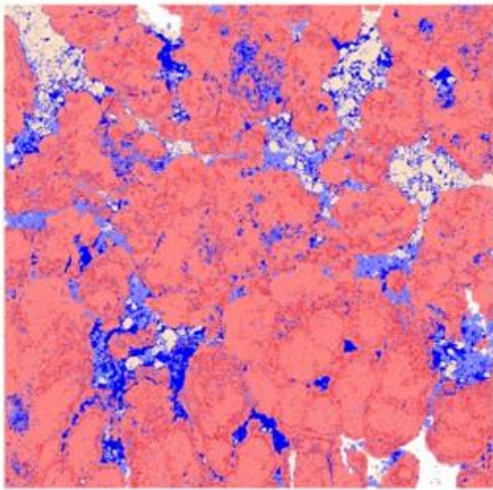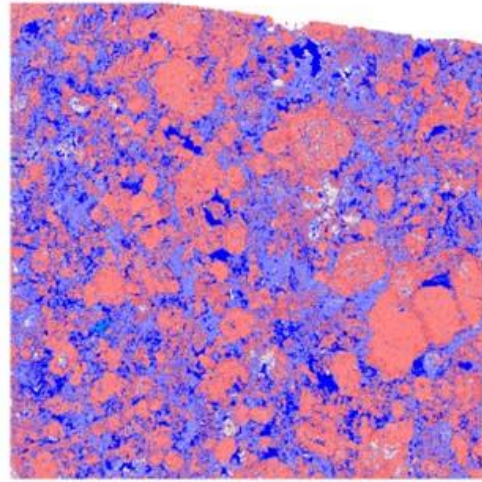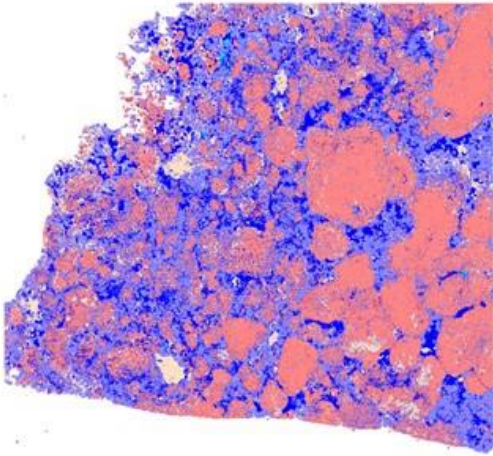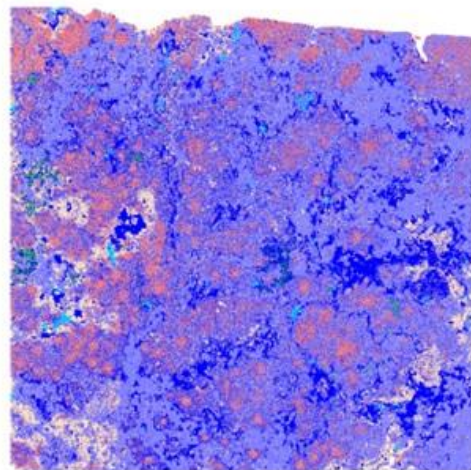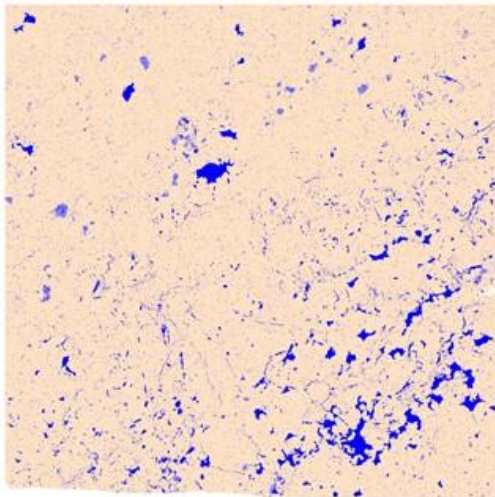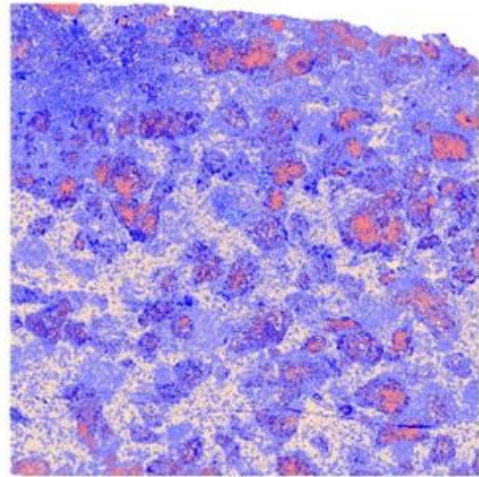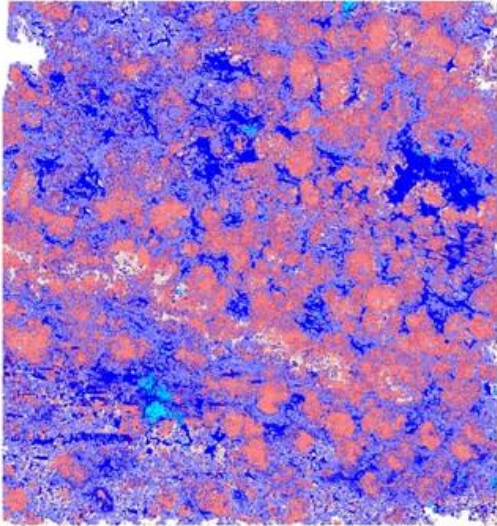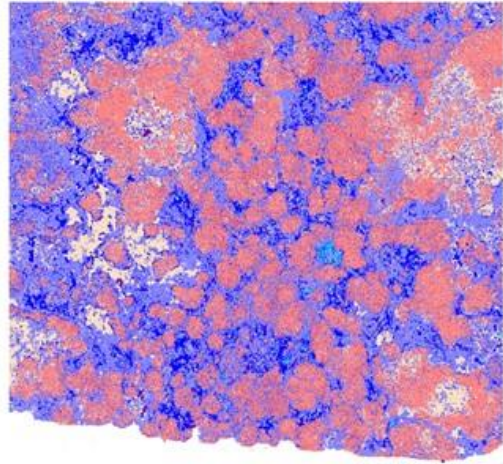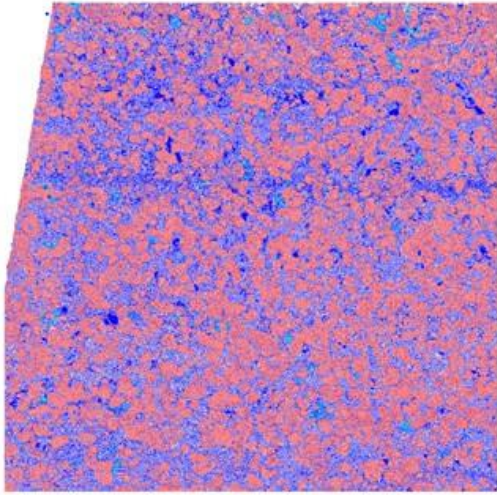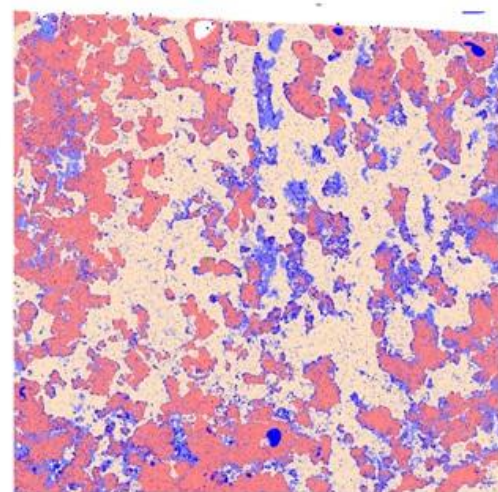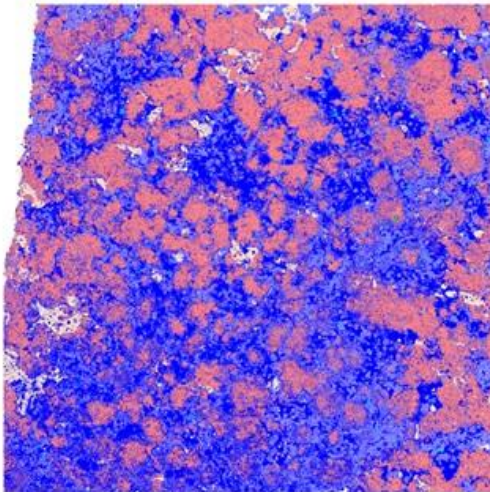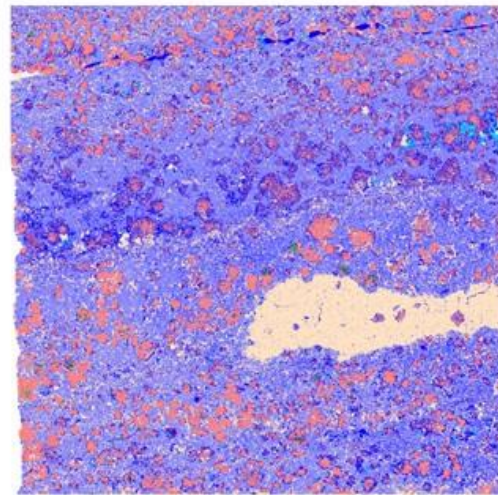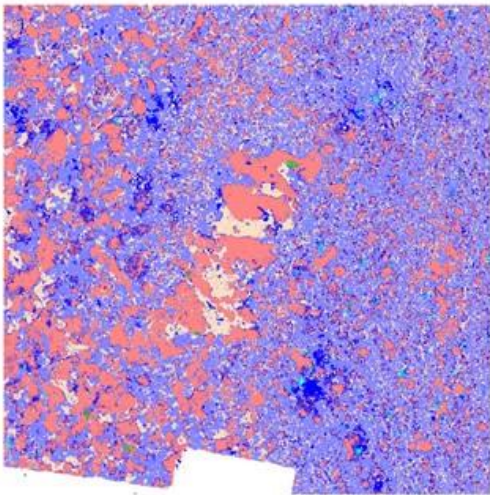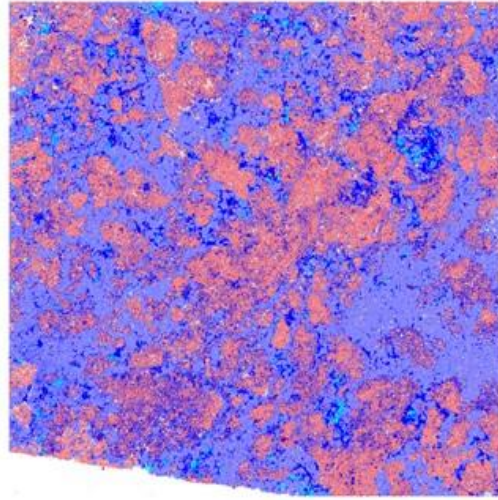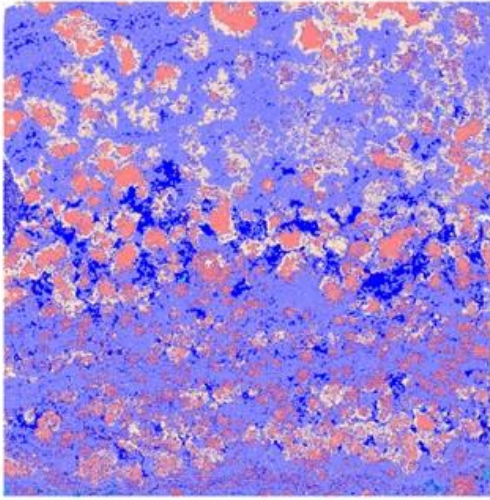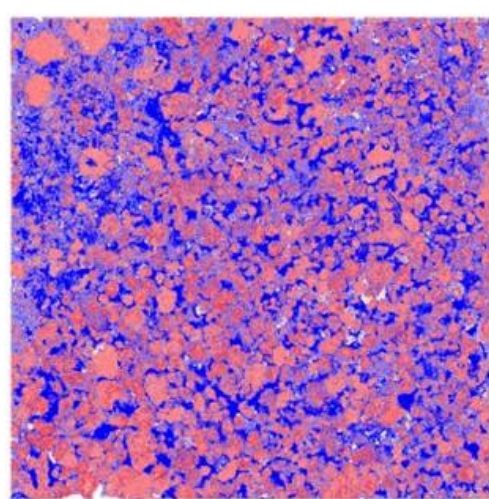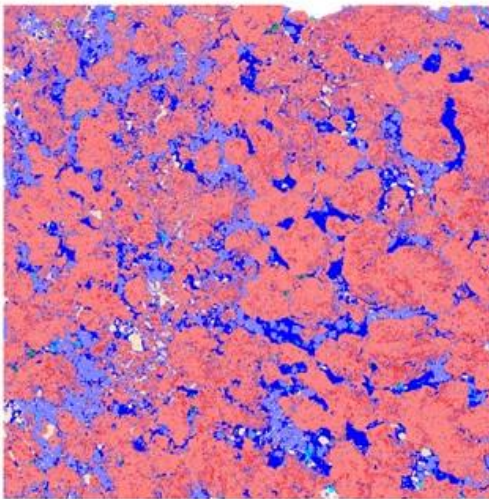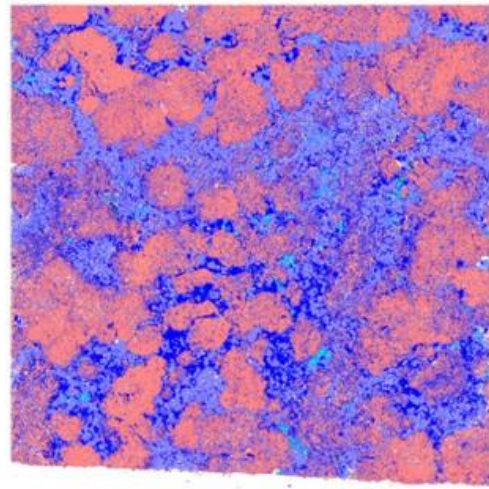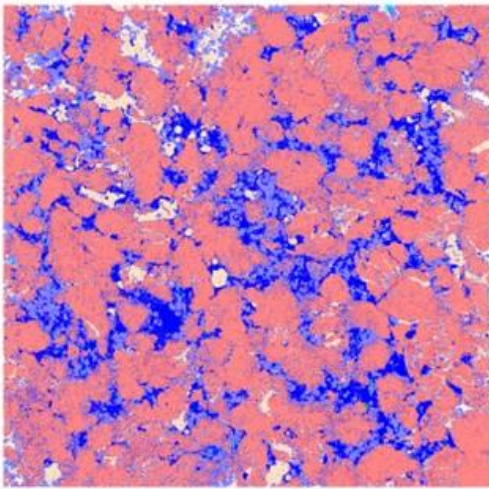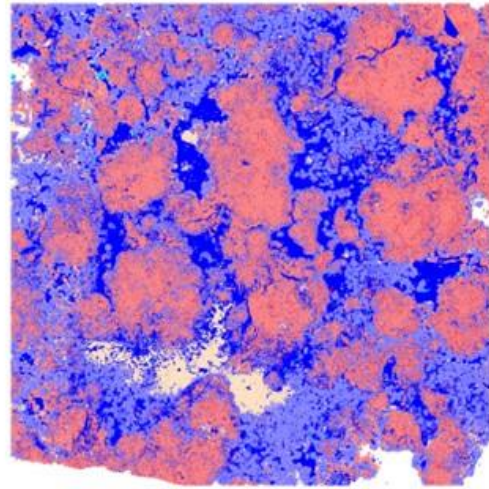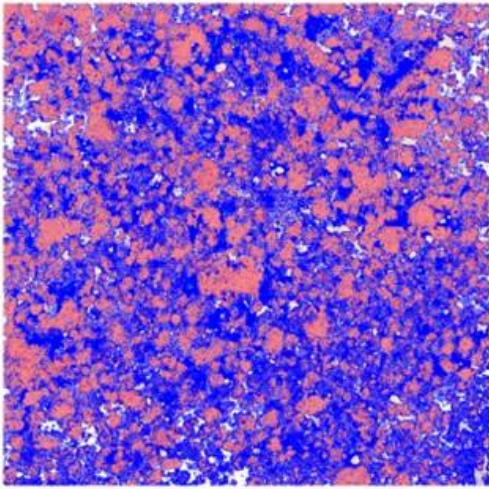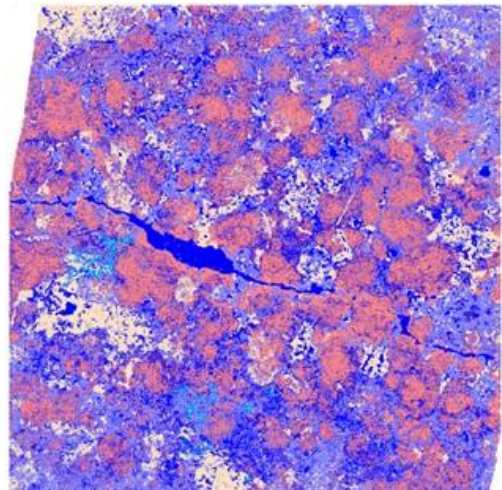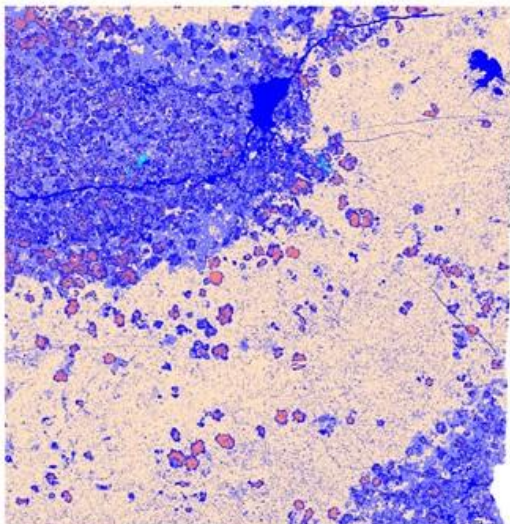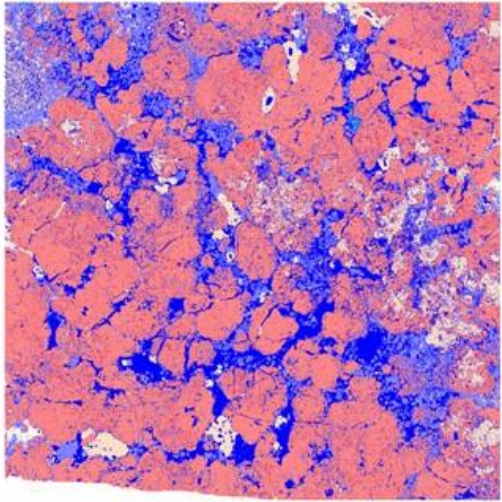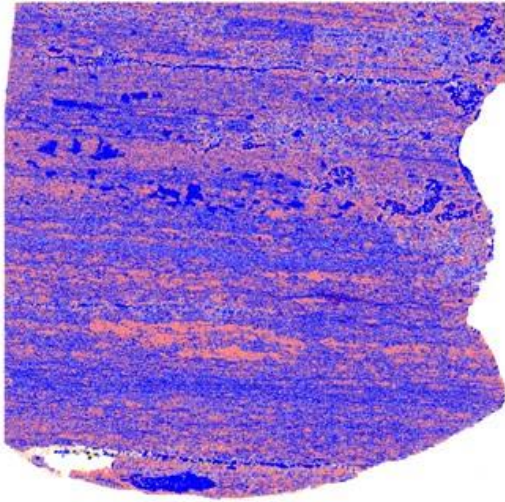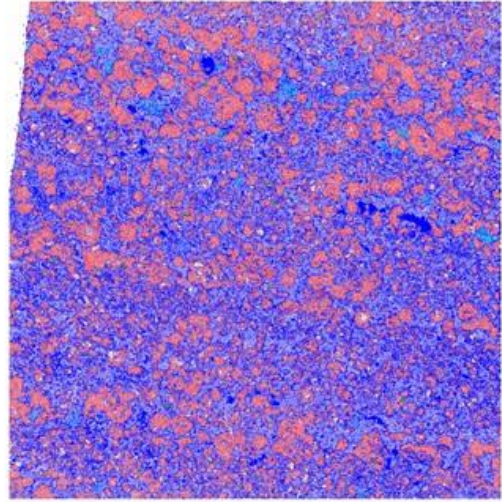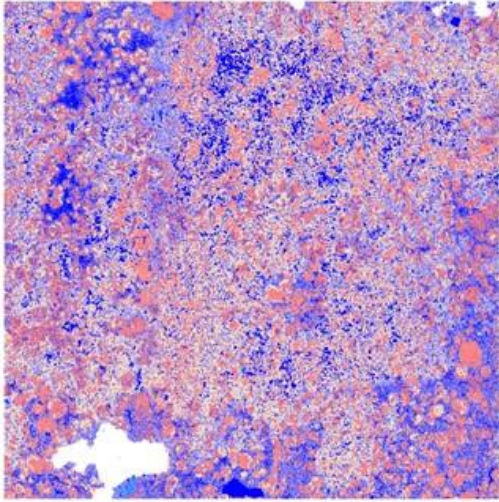
REFERÊNCIAS BIBLIOGRÁFICAS

As referências utilizadas foram citadas no capítulo 4, seção 4.7, deste trabalho. Além destas supracitadas, foi utilizada a bibliografia a seguir:

Buckley, J. P.; Bosence, D.; Elders, Chris. (2015). Tectonic setting and stratigraphic architecture of an Early Cretaceous lacustrine carbonate platform, Sugar Loaf High, Santos Basin, Brazil. Special Publications, v. 418, n. 1, p. 175-191.

Chang, Hung Kiang *et al.* (2008). Sistemas petrolíferos e modelos de acumulação de hidrocarbonetos na Bacia de Santos. Brazilian Journal of Geology, v. 38, n. 2, p. 29-46.

Contreras, Jorham *et al.* (2010). Seismic stratigraphy and subsidence analysis of the southern Brazilian margin (Campos, Santos and Pelotas basins). Marine and Petroleum Geology, v. 27, n. 9, p. 1952-1980.

Dunham, Robert J. (1962) Classification of carbonate rocks according to depositional textures. American Association of petroleum Geologists. Memoir, v-1. p.108-121.

Embry, A F.; Klovan, J. E. (1971). A late Devonian reef tract on northeastern Banks Island, NWT. Bulletin of Canadian petroleum geology, v. 19, n. 4, p. 730-781.

Farias, Felipe *et al.* (2000). Evaporitic carbonates in the pre-salt of Santos Basin–Genesis and tectonic implications. Marine and Petroleum Geology, v. 105, p. 251-272, 2019.

Guardado, L. R. *et al.* (2000). Petroleum System of the Campos Basin. Petroleum systems of South Atlantic margins: AAPG Memoir 73. Brazil. p. 317-324.

Jamieson, J. W., Hannington, M. D., Tivey, M. K., Hansteen, T., Williamson, N. M. B., Stewart, M., & Langer, J. (2016). Precipitation and growth of barite within hydrothermal vent deposits from the Endeavour Segment, Juan de Fuca Ridge. Geochimica et Cosmochimica Acta, 173, 64-85.

Karner, Garry D.; Driscoll, Neal W. (1999). Tectonic and stratigraphic development of the West African and eastern Brazilian Margins: insights from quantitative basin modelling. Geological Society, London, Special Publications, v. 153, n. 1, p. 11-40.

Kusznir, N. J.; Ziegler, P. A. (1992). The mechanics of continental extension and

sedimentary basin formation: a simple-shear/pure-shear flexural cantilever model. Tectonophysics, v. 215, n. 1-2, p. 117-131.

Lavier, Luc L.; Manatschal, G. (2006) A mechanism to thin the continental lithosphere at magma-poor margins. Nature, v. 440, n. 7082, p. 324-328.

Mercedes-Martín, R. *et al.* (2022). Effects of salinity, organic acids and alkalinity on the growth of calcite spherulites: Implications for evaporitic lacustrine sedimentation. The Depositional Record, v. 8, n. 1, p. 143-164.

Morais, J. M. (2013). Petróleo em águas profundas: uma história tecnológica da Petrobras na exploração e produção offshore. Ipea.

Moulin, M.; Rabineau, M.; Daniel, A.; Patriat, M. (2013). Kinematic of the Santos-Namibe basins. Geological society London Special Publucations.

Thiede, D. S.; Vasconcelos, P. M. (2010). Paraná flood basalts: rapid extrusion hypothesis confirmed by new 40Ar/39Ar results. Geology, v. 38, n. 8, p. 747-750.

Tosca, N. J.; Masterson, A. L (2014). Chemical controls on incipient Mg-silicate crystallization at 25 C: Implications for early and late diagenesis. Clay Minerals, v. 49, n. 2, p. 165-194.

Tucker, M.E., and Wright V.P. (1990). Carbonate Sedimentology. Blackwell Scientific Publications, Oxford, London, Edinburgh, Boston, Melbourne, 0. 482.

White, R., Mckenzie, D. (1989). Magmatism at rift zones: the generation of volcanic continental margins and flood basalts. Journal of Geophysical Research: Solid Earth, v. 94, n. B6, p. 7685-7729.